

DNA 1240H-2

HANDBOOK  
OF  
UNDERWATER NUCLEAR EXPLOSIONS (U)  
VOLUME 2 - PART 2

March 1972

Published for:  
Defense Nuclear Agency  
Washington, D. C. 20305  
Under Contract DASA 01-70-C-0035

Published by:  
DASIAC  
(DoD Nuclear Information and Analysis Center)  
General Electric Company-TEMPO  
Santa Barbara, California 93102

This work was supported by the Defense Nuclear Agency  
under NWER Subtask DC 001-01.

DECLASSIFIED BY ACTING CHIEF ISC M  
SIGNATURE John F. Bibby E.

Copy no. 9 of 175  
Total no. of pages 646

810



CONTENTS

CHAPTER	TITLE	PAGE
VOLUME 2 – PART 1		
11	INTRODUCTION	11-1
12	UNDERWATER EFFECTS ON SURFACE SHIPS	12-1
13	AIRBLAST EFFECTS ON SURFACE SHIPS	13-1
14	SURFACE SHIP STRUCTURAL RESPONSE AND DAMAGE DEVELOPMENT: THE EFFECTS OF SURFACE WAVES	14-1
15	SURFACE SHIP EQUIPMENT DAMAGE FROM UNDERWATER PHENOMENA	15-1
VOLUME 2 – PART 2		
16	THE EFFECTS OF AIR BLAST ON SURFACE SHIP EQUIPMENT	16-1
17	THE INTERACTION OF SURFACE SHIPS WITH THE THERMAL AND RADIOLOGICAL ENVIRONMENT	17-1
18	SURFACE SHIP PERSONNEL CASUALTIES: EFFECTS OF UNDERWATER SHOCK ON PERSONNEL	18-1
19	SUBMARINE HULL RESPONSES AND DAMAGE DEVELOPMENT	19-1
20	SUBMARINE EQUIPMENT	20-1
21	UNDERWATER SHOCK EFFECTS ON SUBMARINE PERSONNEL	21-1
22	NAVAL MINE SWEEPING WITH NUCLEAR EXPLOSIONS	22-1



CHAPTER 17

THE INTERACTION OF SURFACE SHIPS  
WITH THE THERMAL AND RADIOLOGICAL ENVIRONMENT

by

R. W. Shnider

U. S. Naval Radiological Defense Laboratory  
San Francisco, California

[Originally published as USNRDL-475]

20 January 1964

Abstract

This chapter considers the interaction of surface ships with the thermal and nuclear radiation fields resulting from water-surface and underwater bursts, but does not include effects on personnel. Two classes of interaction are considered: (1) interaction of the ship with radiations, involving shielding against thermal, neutron, and gamma-radiations; (2) interaction of the ship with material particles, involving deposition of radioactivity on the ship's weather surfaces, or ingress of activity within the weather envelope via ventilation or combustion air. The classes of radiation considered include (a) thermal, (b) fireball-plume-cloud, (c) transit, (d) deposit, (e) radiation from contaminated water, (f) radiation from contaminated ventilation or combustion air. Available weapons-test data are given for shipboard radiation levels due to each class, along with current theoretical methods for assessing the radiation fields at various shipboard locations.



[REDACTED]

BEST AVAILABLE COPY

[REDACTED]

## CONTENTS

ABSTRACT	17-i
ILLUSTRATIONS	17-vi
TABLES	17-vii
SYMBOLS	17-viii
SECTION 17.1 — PURPOSE AND SCOPE	17-1
17.1.1 Introduction	17-1
17.1.2 Description of the Effects of Nuclear Surface and Underwater Bursts	17-1
17.1.3 Scope	17-2
SECTION 17.2 — THERMAL RADIATION	17-4
17.2.1 Introduction	17-4
17.2.2 Free-Field Data	17-6
17.2.3 Criteria for Assessing Thermal Effects on Materials	17-9
17.2.4 Summary	17-12
SECTION 17.3 — FREE-FIELD DATA NECESSARY FOR ASSESSMENT OF NUCLEAR RADIATION EFFECTS	17-13
17.3.1 General Introduction	17-13
17.3.2 Measurement of Nuclear Radiation	17-13
17.3.3 Contributions to Nuclear-Radiation Exposure	17-14
17.3.4 Sources of Weapons-Test Data	17-16
17.3.5 Summary	17-18

SECTION 17.4 — FIREBALL-PLUME-CLOUD RADIATION	17-20
17.4.1 Introduction	17-20
17.4.2 Factors Affecting the Interaction of F.P.C. Radiation with a Target Ship	17-21
17.4.3 Field-Test Fireball-Plume-Cloud Radiation Data and Estimates of Free-Field Fireball-Plume-Cloud Radiation Dose	17-23
17.4.4 Effect of Geometry on the Interaction of F.P.C. Gamma Radiation with a Target Ship	17-26
17.4.5 Effects of F.P.C. Radiation on Shipboard Electronic Equipment	17-31
17.4.6 Summary	17-32
SECTION 17.5 — TRANSIT RADIATION	17-34
17.5.1 Introduction	17-34
17.5.2 Weapons-Test Data for Unshielded Shipboard Locations	17-35
17.5.3 Weapons-Test Data for Shielded Locations	17-38
17.5.4 Theoretical Calculations of Transit Radiation for Unshielded Locations	17-39
17.5.5 Theoretical Calculations for Shielded Locations	17-55
17.5.6 Effect of Geometry at Unshielded Locations	17-62
17.5.7 Effects of Transit Radiation on Electronic Equipment	17-68
17.5.8 Summary	17-68
SECTION 17.6 — DEPOSIT RADIATION	17-70
17.6.1 Introduction	17-70
17.6.2 Weapons-Test Data for Unshielded Locations	17-71
17.6.3 Weapons-Test Data for Shielded Locations	17-75
17.6.4 Theoretical Calculations for Unshielded Locations	17-77
17.6.5 Theoretical Calculations for Shielded Locations	17-81
17.6.6 Simulant Experiments	17-85
17.6.7 Summary	17-85

SECTION 17.7 – RADIATIONS FROM CONTAMINATED WATER	17-90
17.7.1 General Introduction	17-90
17.7.2 Mechanisms of Water Contamination	17-90
17.7.3 Water-Contamination Data	17-91
17.7.4 Shipboard Dose-Rate Data from Contaminated Water	17-99
17.7.5 Summary	17-103
SECTION 17.8 – CONTAMINATION INGRESS	17-105
17.8.1 Introduction	17-105
17.8.2 Theoretical Investigations	17-105
17.8.3 Weapons-Test Data	17-107
17.8.4 Summary	17-111
REFERENCES	17-113

ILLUSTRATIONS

FIGURE	TITLE	PAGE
17-1	Idealized Thermal Pulse	17-5
17-2	Surface Burst Radiant Exposures Normalized to 1 KT versus Range	17-7
17-3	Delivery Time of Effective Thermal Energy versus Yield, Water Surface Bursts	17-10
17-4	Neutron Dose Normalized to 1 KT versus Distance	17-25
17-5	F.P.C. Gamma Dose versus Range for 1-MT Surface Bursts	17-27
17-6	Yield versus Multiplying Factor for F.P.C. Gamma Dose, Surface Bursts	17-28
17-7	Peak F.P.C. Gamma Dose Rate versus Distance, Shots Wahoo and Umbrella	17-29
17-8	F.P.C. Gamma Dose versus Distance, Shots Wahoo and Umbrella	17-30
17-9	Classification of Underwater Burst Depths	17-43
17-10	Base Surge Geometry	17-45
17-11	Effective Mean Free Path as a Function of Time after Fission	17-51
17-12	Minimal Shielding (1t) Calculations, USS RANGER, Airborne Activity 70 Seconds after Fission	17-63
17-13	Expected Shielding (2t) Calculations, USS RANGER, Airborne Activity 70 Seconds after Fission	17-64
17-14	Minimal Shielding (1t) Calculations, USS RANGER, Airborne Activity 1.12 Hours after Fission	17-65
17-15	Expected Shielding (2t) Calculations, USS RANGER, Airborne Activity 1.12 Hours after Fission	17-66
17-16	Schematic Cross-Section Through COWPENS (AVT) at Two Frames	17-86



## TABLES

TABLE	TITLE	PAGE
17-1	Approximate Thermal Criteria for Destruction of Some Topside Combustibles	17-11
17-2	Water Shots for which Nuclear-Radiation Data are Available	17-17
17-3	Scaled Base Surge Data	17-48
17-4	Fraction of Fission Products, $\beta$ , Assigned to Base Surge	17-52
17-5	Experimental and Computed Shielding Factors for COWPENS (AVT)	17-87
17-6	Dose Rate and Dose Data for Shot Navajo	17-101
17-7	Dose Data from DD-593 for Shot Umbrella	17-102
17-8	Compartments in which It is Estimated That Radiation Fields were Caused by Ingress of Radioactive Contaminants	17-109
17-9	Estimates of Portion of External Gamma Dose Due to Ingress of Contaminant, DD-592, Shot Umbrella	17-110

LIST OF SYMBOLS

$A_{\max}$	Maximum radius of bubble produced by the burst
B	Dose buildup factor
$B_i$	Infinite-medium dose buildup factor
C	Correction factor applied to bring calculated dose rates into agreement with observed rates
D	Distance from surface zero, in cm
D	Total transit dose
$D_{\max}$	Maximum diameter of water column
$E_i$	Source energy
$E(t)$	Energy emission rate of fission products
$E_\gamma$	Gamma ray energy
I	Energy flux density
$J_o$	Volume source density in Mev/cm <sup>3</sup> -sec.
N	Ratio of dose rate
P	Point of measurement
Q	Radiant explosive
R	Polar coordinate

R	Base surge radius
$R_{sc}$	Scaled radius
S	Distance from axis of cone
SF	Ship shielding factor
$\bar{T}$	Atmospheric transmissivity
V	Base surge volume
X	Distance
Y	Weapon yield, in kilotons
Z	Height of base surge
d	Dose rate from airborne activity at any time after burst
d	Depth of burst
$d_o$	Dose rate corrected for decay to reference time of 1 hour
$f_i$	Fraction of $d_o$ due to source energy
h	Distance below contaminated flight deck
t	Time
$t_f$	Final arrival of activity, in hours
$t_i$	Initial arrival of activity, in hours
$t_m$	Time to final maximum
$t_{sc}$	Scaled time
u	Velocity

[REDACTED]

DNA 1240H-2

- $\alpha$  Interior angle between each face of the surge and base, or water surface
- $\phi$  Fraction of total fission-product activity in the base surge
- $\mu_A$  Energy absorption coefficient
- $\mu_j, \mu_i$  Linear total absorption coefficient for medium
- $\theta$  Polar coordinate

[REDACTED]

CHAPTER 17  
THE INTERACTION OF SURFACE SHIPS WITH THE  
THERMAL AND RADIOLOGICAL ENVIRONMENT

17.1 PURPOSE AND SCOPE

17.1.1 Introduction

Knowledge of the interaction of naval ships with the radiation fields resulting from nuclear water-surface or underwater bursts is important in determining the effects of these fields on the personnel aboard the ships. This chapter will discuss the nature of the thermal and radiological effects resulting from nuclear water-surface or underwater bursts in terms of the modification of the radiation fields by surface ships, including physical interaction with the ship's structure, up to the point where injury of the crew is involved. Effects on ships' personnel will be considered in Chapter 18. Means of predicting thermal and radiological effects include theoretical calculations and scaling techniques employing data from nuclear tests. It should be noted that only a few underwater bursts and no true water-surface bursts over deep water have occurred; thus data pertinent to the effects of such bursts are limited. A brief qualitative description of the general phenomenology involved, is given next as background for the rest of the chapter.

17.1.2 Description of the Effects of Nuclear Surface and Underwater Bursts

When a nuclear weapon is detonated, a large amount of energy is liberated in a very small period of time within a limited quantity of matter. This liberated energy manifests itself in the form of a shock wave, thermal radiation, and nuclear radiation. Extremely high temperatures are produced by the tremendous amount of energy created, and a glowing mass of hot gases called the fireball is formed. A large amount of thermal radiation is emitted by this fireball within the first few seconds after a detonation, and the fireball of a surface burst tends to rise at the rate of several hundred feet per second.

For a water-surface burst, a large quantity of water is vaporized by the high temperatures, carried up under the fireball into a cloud, and mixed with the fission products that are formed by the detonation. Nuclear radiations are emitted during the first minute after a detonation by the fireball, stem, and cloud. As the water vapor cools and condenses back to droplets, these droplets fall to the surface as

fallout (or "rainout") particles, emitting nuclear radiations due to the admixed fission products.

In the case of an underwater burst, a bubble is formed due to the dissociation and vaporization of the water by the energy of detonation. The gases and steam in the bubble are initially confined within a volume similar to that of the original charge, whereas under normal conditions they would require a much greater volume. Since the bubble is at a high initial pressure, it expands and breaks through the water surface on its first expansion, if the burst depth is less than the bubble radius at maximum expansion. For a deep burst, the bubble may go through several expansions, contractions, and upward migrations until it reaches the surface. When the bubble of a shallow burst breaks through the surface, a hollow column of water will be thrown up into the air; plumes of water will be thrown up by deeper bursts. The water will mix with the fission products initially contained in the bubble, and on return to the surface will form a contaminated base surge, or aerosol, that emits gamma radiations. This base surge at first expands radially, but ultimately moves with the wind until it evaporates, disperses, or settles out.

### 17.1.3 Scope

Two classes of interaction of surface ships with radiation fields are considered: (1) interaction of a ship with radiations, involving thermal, neutron, and gamma radiations; (2) interaction with material particles, involving either the deposition of radioactivity on the ship's weather surfaces, or ingress of activity into the weather envelope via combustion-air and ventilation-air intakes or other openings. The radiation fields are due to six classes of radiation: (1) thermal, (2) fireball-plume-cloud, (3) transit, (4) deposit, (5) radiation from contaminated water, (6) radiation from contaminated air within the ship.

The discussion of thermal radiation, in 17.2, includes the free-field data required to predict damage, the protection from thermal exposure due to shielding by the ship's structure and gear, and the criteria needed to estimate the effects of thermal radiation on combustibles that may be located topside.

The assessment of nuclear-radiation effects requires an understanding of the different radiations that emanate from the various radioactive sources resulting from a detonation. Thus, 17.3 discusses the categories into which radiations have been divided, some general characteristics of the various radiations, and sources of weapons test data. The two main categories are fireball-plume-cloud radiations and residual radiations.

Discussion in 17.4 of the interaction of a ship's structure and gear with fireball-plume-cloud radiation includes discussion of the factors affecting such radiation, a summary of available experimental information,

and current methods of predicting free-field effects.

The remaining four classes of radiation fall into the category of residual radiations. In 17.5, current knowledge of the effects of transit radiation from airborne sources is summarized, and available methods of predicting transit radiation aboard ship are discussed. In 17.6, radiation from activity deposited on ships' weather surfaces is discussed. Weapons-test data are summarized and methods of predicting deposit radiation effects aboard ship are presented. Radiation aboard ship from water contaminated by a nuclear burst is discussed in 17.7. The discussion includes available weapons-test data and theoretical calculations, and indicates that negligible radiation from waterborne sources would penetrate combatant ships later than 1 hour after burst. Section 17.8 summarizes effects of radiation from contaminated air within a ship including available weapons-test data.

## 17.2 THERMAL RADIATION

### 17.2.1 Introduction

#### General Characteristics of Thermal Radiation

Immediately after it forms, the fireball of a nuclear detonation starts to emit the infrared, ultraviolet, and visible light known as thermal radiation. This emission occurs in two pulses, shown in idealized form in Figure 17-1. During the first pulse of extremely short duration (0.1 sec or less), temperatures in the fireball are very high, and energy emission rapidly rises to a maximum and rapidly declines to a minimum. The second pulse may last for several seconds, temperatures are lower, and there is a less rapid rise in energy emission to the second or final maximum, followed by a comparatively slow decline to zero. Since temperatures during the first pulse are very high, most of the emitted radiation is in the ultraviolet region, which is attenuated rapidly in air. Furthermore, only about 1% of the total thermal radiation appears in the first pulse because it has such a short duration and because the radiating area is still relatively small. Thus, the radiant exposure from the first pulse, at some distance from the burst is insignificant. During the second pulse, most of the radiation falls in the infrared and visible regions, and can cause fires to start when combustible materials are directly exposed to the fireball at sufficiently close range.

The thermal radiation from nearly all underwater bursts will be absorbed through vaporization and dissociation of the water, and thus is of no concern as a weapons effect. However, thermal radiation from surface or extremely shallow underwater bursts is of concern, although such radiation can affect only the exposed topside personnel and materiel of a surface ship. Any opaque object along the fireball-to-target line of sight will furnish full protection from thermal radiation; thus, topside personnel or materiel in the shadow of the ship's superstructure or topside gear would be shielded from thermal radiation. Such radiation probably will not start shipboard fires, since normally there is insufficient combustible materiel topside on combatant ships to sustain fire. (However, cargo ships may carry combustible deck loads, and in special wartime conditions, even combatant ships might have combustibles topside.) The most probable thermal-radiation effects are incapacitating flash burns or flash blindness among topside personnel directly exposed to the fireball of surface bursts, topics which will be considered in detail in Chapter 18.

#### Topics Considered

The free-field data and criteria necessary for assessing thermal-radiation damage, and the procedure for evaluating topside thermal exposures



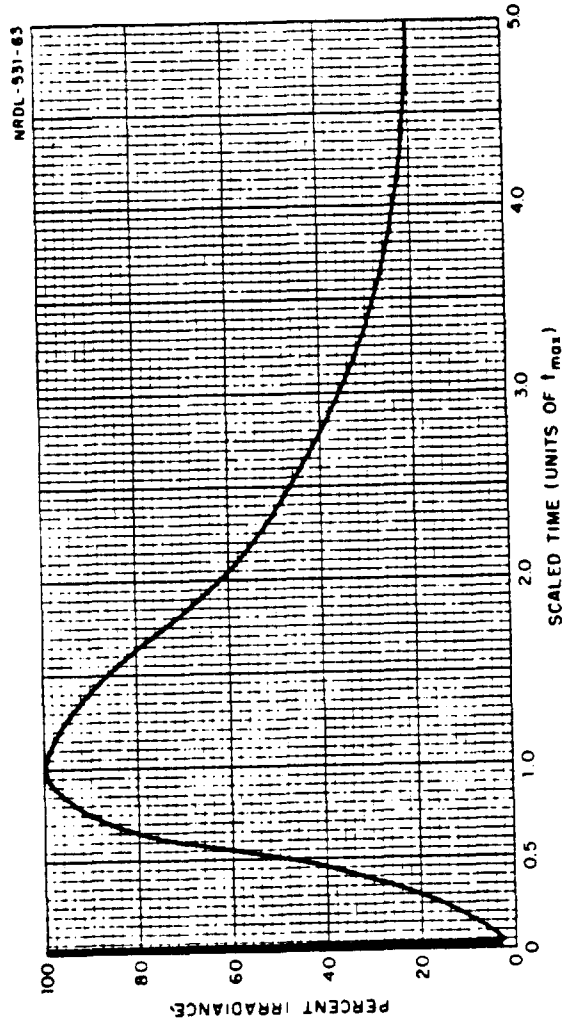


Figure 17-1. Idealized thermal pulse.

are discussed in 17.2.2 and 17.2.3, along with the reliability of topside radiant-exposure predictions.

#### 17.2.2 Free-Field Data

Experimental findings have established that the free-field data required to assess the damage produced by thermal radiation are given by two quantities---the radiant exposure, or the amount of incident thermal energy per unit area of the target, and the rate at which this energy is delivered. The total amount of incident thermal energy delivered to a target, measured in  $\text{cal/cm}^2$ , varies directly with the amount of thermal energy emitted at the fireball. The amount of emitted energy increases linearly with increasing weapon yield, attenuates with distance from the energy source, and varies with atmospheric conditions. The rate at which the energy is delivered is determined by the duration of the thermal pulse, which lengthens with increasing yield. As a result, thermal energy from large-yield weapons is delivered more slowly than that from small-yield weapons. The significance of the delivery rate lies in the fact that since a target rapidly dissipates the heat it receives, it will not overheat if the delivery rate is sufficiently slow. Thus, for a given amount of thermal energy per unit target area, damage to a target will be greater when the energy is delivered so rapidly that little heat loss can occur during delivery, than when the energy is delivered more slowly. For instance, the fireball of a 1-KT detonation can deliver  $4 \text{ cal/cm}^2$  in less than 1 second, resulting in an incapacitating burn on bare skin. A  $4 \text{ cal/cm}^2$  radiant exposure from a 10 MT burst, which is delivered at a slower rate (it will take more than 30 sec), may cause no more than a 1st-degree burn on the same bare skin.

#### Radiant Exposures

The ranges from surface zero at which water-surface detonations of various yields will cause specified radiant exposures have been estimated through analysis of data taken at weapons tests.<sup>1</sup> This analysis is summarized in the lower curve of Figure 17-2, Radiant Exposure Normalized to 1 KT vs Range. From this curve, at any given range, values of the radiant exposure from any yield can be scaled for the atmospheric conditions prevailing during weapons tests at the Pacific Proving Grounds, where visibility was only about 10 miles. The upper curve of the figure was fitted to data obtained at land-surface bursts in Nevada, including data for tower surface-intersecting shots. Visibility was excellent and atmospheric transmission was high during these tests. Since water-surface bursts may occur in regions such as the North Pacific, where visibility and atmospheric transmission are generally higher than they were in the test area, the Nevada curve is included and represents upper limiting values of radiant exposures from surface bursts. Data points to which both curves were fitted are indicated on the plots.

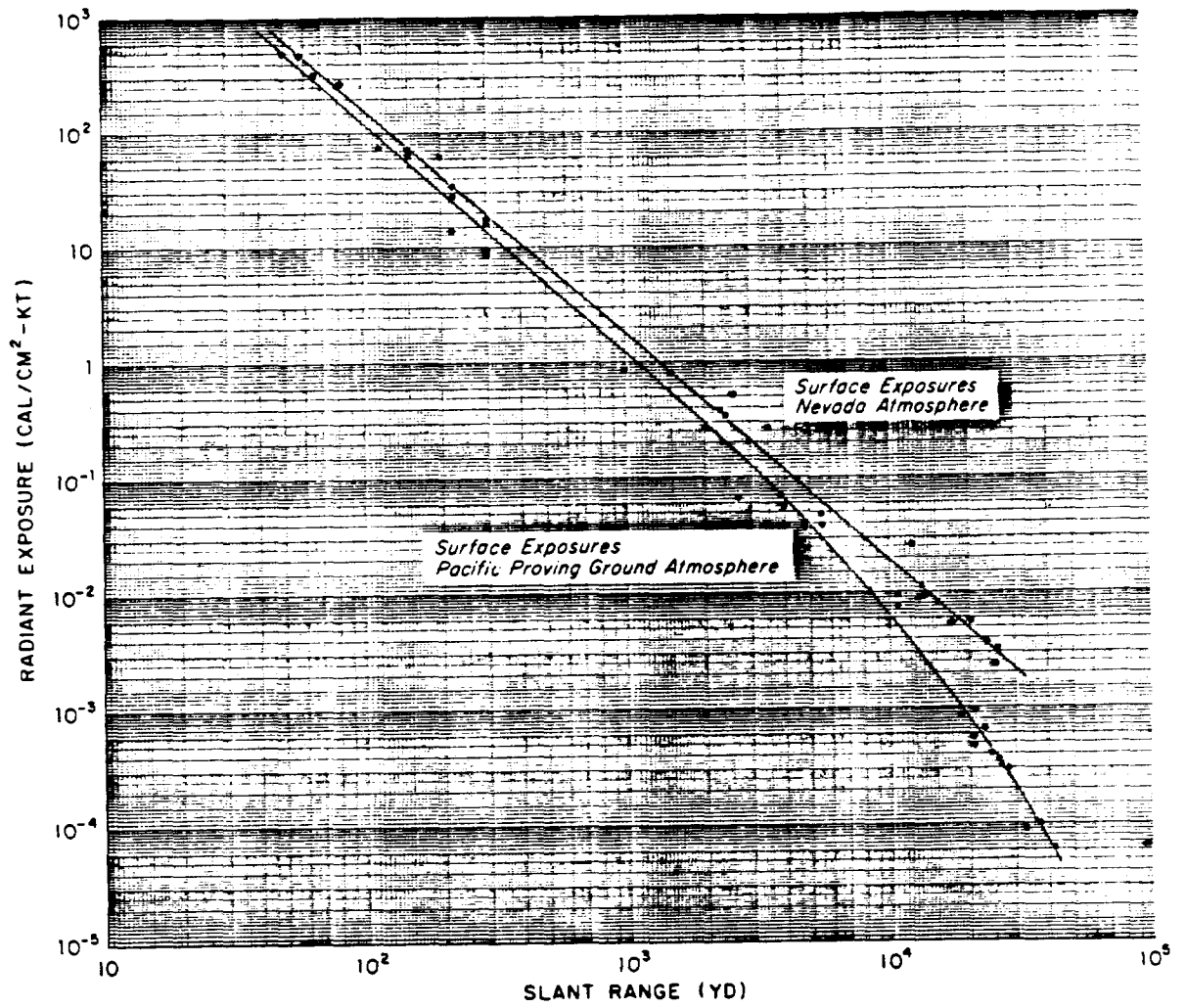


Figure 17-2. Surface burst radiant exposures normalized to 1 KT versus range.

Theoretically, radiant exposures at a distance from water-surface bursts (considered as point sources) would be calculated by use of the expression

$$Q = \frac{kY \times 10^{12} \times \bar{T}}{4\pi D^2} \text{ cal/cm}^2 \quad (17-1)$$

Where

Y is the weapon yield in kilotons.

k, a fraction modifying Y, is a function of (1) the fraction of the total energy appearing as thermal radiation (2) the angle of elevation of the receiver, (3) the shape of the fireball.

$\bar{T}$  is the atmospheric transmissivity (the ratio of the energy incident per unit area on a target in a real atmosphere to that which would be incident on the target in a vacuum).

D is the distance from surface zero to the target (in cm).

However, there are so many unknown factors in Eq. 17-1 that calculated results are unreliable. The value of k may lie between 1/7 and 1/3. Furthermore, there is little reliable verification of the graphical values of  $\bar{T}$  given in Ref. 2. Atmospheric transmissivity is a complex function of several unpredictable variables, such as water-vapor and carbon-dioxide absorption of infra-red radiation, and multiple scattering of all radiation. Furthermore, reflection from partial or total cloud cover, a factor unaccounted for in theoretical calculations, can increase the effective exposure by a factor of as much as 2. Finally, values of Q calculated with the values of k and  $\bar{T}$  given in Ref. 2, are not in agreement with available field-test data (some values differ by as much as a factor of 3). Since theoretically calculated radiant exposures do not agree with empirical data, the curves of Fig. 17-2, which are in good agreement (within  $\pm 25\%$ ) with data, are considered the most reliable current method for estimating radiant exposures.

#### Rate of Energy Delivery

Analysis of thermal data from weapons tests has resulted in establishment of a relationship between weapon yield and the time required for emission of the thermal energy that is effective in burning. A reevaluation<sup>3</sup> of the data for the time to final maximum ( $t_m$ ) as a function of weapon yield has provided an expression that is in excellent agreement with field-test data. Water-surface-burst data indicate a cutoff of radiant exposures after  $10 t_m$ . This cutoff is apparently caused by the formation of a Wilson Cloud (which, however, may not form under atmospheric conditions different from those at the Pacific Proving Grounds where all the tests were held). Furthermore,

data<sup>3,4</sup> indicate that only about 80% of the total energy which is delivered by  $10 t_m$ , is effective in burning. Thus, the effective thermal-energy delivery time is taken as  $10 t_m$  and a plot showing the relationship between  $10 t_m$  expressed in seconds, and yield is given by Figure 17-3.

Thermal-radiation data from shallow underwater bursts are nonexistent; thus, it is impossible to predict with any reliability the thermal radiation effects from such bursts. The only evidence available is the following quotation from Ref. 5 describing the Bikini Baker (Operation Crossroads) shot. . . "The thermal radiation was extremely intense during the first small fraction of a second; . . . the practical effect of the thermal radiation was, of course, almost nil." At Operation Hardtack, no thermal effects were observed from shot Umbrella, which was slightly less than one-third the yield of shot Baker and was detonated at  $5/3$  the depth. Since no other data for shallow underwater bursts are available, it can only be estimated that thermal effects decrease, perhaps linearly, with depth of burst from the effects of surface bursts to noneffectiveness at burst depths scaled to that of Bikini Baker.

### 17.2.3 Criteria for Assessing Thermal Effects on Materials

Criteria for assessing thermal damage are usually expressed in terms of the various radiant exposures and yields that produce the same degree of damage. These criteria have been determined from field-test and laboratory data. At field tests, damage was determined from targets located at known distances from surface zeros of known-yield detonations. References 6 to 15 are some of the American and British reports of both field tests and laboratory experiments to determine material-burn criteria.

The most recent estimates of criteria for destruction of some of the combustibles that may be found topside on a surface ship are given in Table 17-1. The tabulated values of  $\text{cal}/\text{cm}^2$  were determined by measuring the thickness of the specified materials, and using nomographs<sup>16</sup> that correlate material, color, and weight, with the thermal-damage criteria. These estimated values, based on extrapolation from experiments with cellulose products and correlated with field-test and laboratory data, are criteria for the specified untreated materials at a relative humidity of 0%. For a relative humidity of 50%, values should be multiplied by a correction factor of 1.2; for a relative humidity of 70%, by a correction factor of 1.27. While flameproofing helps prevent the spread of fire, recent experiments\*\* indicate that it reduces the ignition point of some materials, so that they will smolder, char, and be destroyed without flaming. The effect of flameproofing on

\*For yields and depths of burst see Table 17-2.

\*\*Personal communication from Stanley B. Martin, USNRDL.

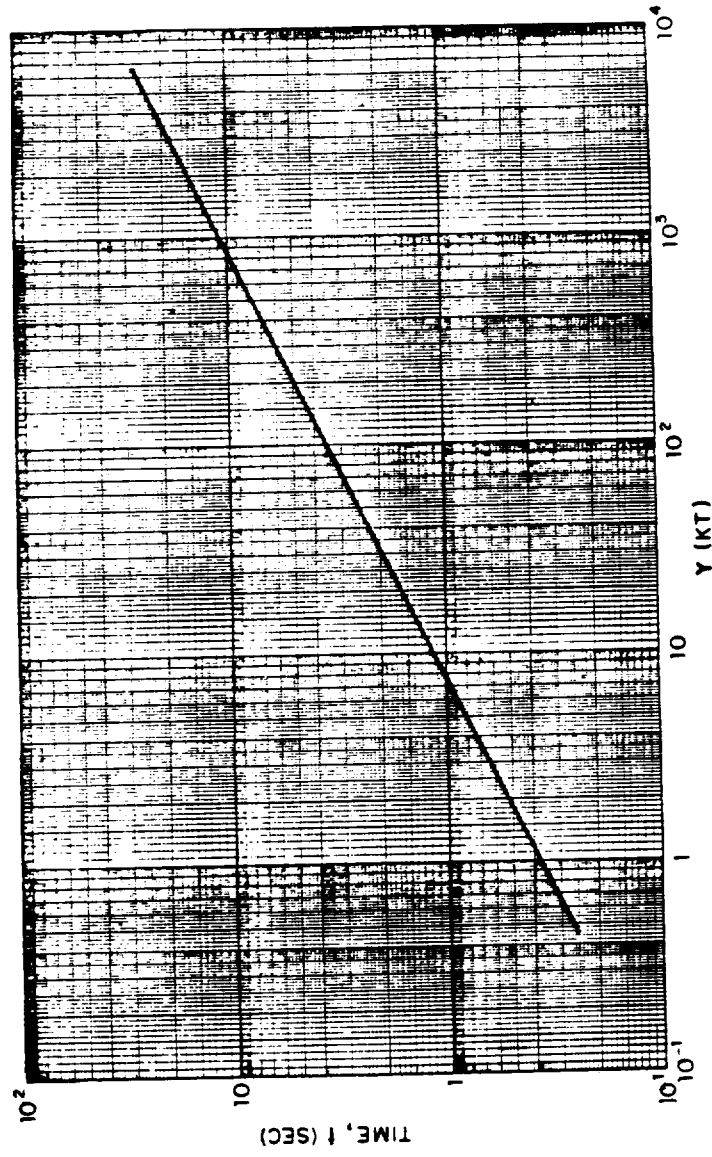


Figure 17-3. Delivery time of effective thermal energy versus yield, water surface bursts.

the materials listed in Table 17-1 has not been tested for the charring effect, although Ref. 14 concluded from tests made with several cotton and woolen fabrics that resistance to destruction was increased by flame-retardant treatment only for the woolen fabrics. Some criteria are based on Ref. 13.

To estimate the effect of thermal radiation on wooden ship decks, use is made of data given in Ref. 2 for charring of white pine, with and without a protective coating. Although ship decks are of a hard wood, and white pine is a soft wood, it is estimated that the effects on coated pine, which will char to a depth of 1 mm with exposure of 40 cal/cm<sup>2</sup> from a 1-KT weapon and 71 cal/cm<sup>2</sup> from a 100-KT weapon, are probably representative for charring of ships' decks.

Table 17-1. Approximate thermal criteria for destruction of some topside combustibles.

Material	Color	Weight	1 KT	10 KT	100 KT	1 MT
		(oz/yd <sup>2</sup> )	(cal/cm <sup>2</sup> )			
Canvas Tarpaulin	Olive Drab	12	12	10	15	23
Kraft Board, W6C (corrugated)	Tan	4.75	4.5	6	10	13
Kraft Board, V3C (corrugated)	Tan	13	11-13	12-13	11-13	17-20
Fibreboard, V3S	--	49	--	--	--	35
Wool Serge	Navy Blue	16	17	17	17	25
Melton (Wool)	Navy Blue	16	13	13	13	20
Wash Cotton Trousers	Khaki	8	15	12	20	30
Wash Cotton Shirt	Khaki	3	5	8.5	12.5	15
Denim Trousers	Blue	9	9	8.5	9	16
Chambray Shirt	Blue	3-5	5-10	6-8	10-12	13-18

17.2.4 Summary

To summarize, no thermal radiation effects are likely aboard surface ships from underwater bursts occurring deeper than at depths scaled to that of Crossroads Baker.\* It is estimated that thermal radiation effects of underwater bursts will increase as burst depth decreases, up to the effects of surface bursts, which are illustrated by the radiant exposures plotted in Fig. 17-2. Below-decks locations will be completely protected from thermal radiation by the shielding afforded by the ships' structures; topside gear or any opaque object in the fireball-to-target line of sight will shield the location in its shadow. Radiant exposures required for destruction of combustibles that may be found on the weather deck are listed in Table 17-1. Criteria for personnel burns, as well as reduction of personnel exposure by shielding and evasive action, are discussed in Chapter 18.

\*See Table 17-2 for shot yields and depths of burst.



### 17.3 FREE-FIELD DATA NECESSARY FOR ASSESSMENT OF NUCLEAR RADIATION EFFECTS

#### 17.3.1 General Introduction

An assessment of nuclear-radiation effects on personnel (presented in Chapter 18) requires a knowledge of the total nuclear-radiation exposure, measured by the nuclear-radiation exposure dose or a time integration of the dose rate received at the point of exposure. The total radiation exposure from a water-surface or underwater nuclear detonation may include contributions from some or all of the following: neutrons, gamma-rays, and beta particles. These different radiations emanate at various times from the fireball or from radioactive materials that result from the detonation. While directional and energy characteristics of the radiations should be understood to permit accurate estimation of the total exposure, it is frequently possible to estimate nuclear-radiation exposures by scaling field-test dose-rate or dose data. However, in some cases exposures must be calculated with theoretical techniques, primarily in situations where the exposures are reduced by shielding materials (as when below-decks spaces are shielded by a ship's structure).

Theoretical calculation of such nuclear-radiation exposures requires knowledge of the nuclear radiation characteristics, such as source strengths, energy spectra, and energy degradations that occur between the source and exposure point as well as of the radiation source and ship geometries. Each component of the total radiation exposure has, in general, a broad energy spectrum that changes with time as the radioactivity decays. Moreover, the decay rate itself differs slightly for different situations, depending on fractionation of the radioactive debris.

#### 17.3.2 Measurement of Nuclear Radiation

The ionization produced during the passage of nuclear radiations through any medium is used both for detection and measurement of the radiation. The amount of ionization produced can be measured, and, depending on the kind of radiation involved, can be expressed in either of two units.

Gamma radiation measured in units of roentgens is termed an exposure dose, which measures the quantity of gamma radiation in terms of the ionization produced in air. One roentgen of gamma radiation produces 1 esu per cc of air, which is equivalent to the release of about 88 ergs of energy per gram of dry air. Instruments have been developed that measure gamma dose rate (the number of roentgens delivered per unit time) and gamma dose (a time-integration of the dose rate during the exposure period). Exposure-dose gamma measurements provide free-field measurements of gamma radiation.

A measurement of the absorption of a quantity of any kind of nuclear radiation in any material is termed the absorbed dose. The rad is the unit used to represent the absorption of 100 ergs of ionizing radiation per gram of the absorbing material or tissue. Thus, dose to personnel is expressed in terms of rads. One roentgen of gamma radiation results in an absorbed dose of about 0.88 ergs per gram of tissue; hence, for gamma radiation, the roentgen and rad are almost equivalent.

### **BEST AVAILABLE COPY**

Neutrons do not produce ionization (the process used to measure radiation) directly in their passage through matter. However, they cause it to occur indirectly by their interaction with certain nuclei, and the number, velocity, and energy of the neutrons involved determines the amount of indirect ionization produced. The effects of neutron radiation, measured in terms of either neutron flux (density) or time integrated neutron flux, (now called fluence) are expressed in terms of rads based on calculations relating fluence to absorbed dose.

Neutron flux, the product of the neutron density and the neutron velocity, is numerically equal to the total number of neutrons passing in all directions through a sphere of one square cm cross-sectional area, per second. Instruments measure neutron flux over limited energy bands and correlate the ionization produced indirectly by the neutrons with the amount of energy that would be absorbed in tissue per unit time. Integrated neutron flux or fluence, the product of neutron flux and time, expresses the total number of incident neutrons per sq cm of detector. Measurements of this type have been made for several energy groups, but particularly for high-energy neutrons, for which the standard detector is common sulfur, because it has been determined that the absorbed dose due to neutrons closely follows sulfur neutron fluence. Empirically determined conversion factors are then used to express the sulfur neutron fluence in terms of absorbed dose. No measurements are available of neutron fluence over the entire energy spectrum. Interpolation and extrapolation have been used to calculate total neutron radiation effects, in terms of rads.

#### 17.3.3 Contributions to Nuclear-Radiation Exposure

Determination of nuclear radiation effects has been facilitated by dividing the radiations into two main categories: (1) fireball-plume-cloud radiations and (2) residual radiations. Fireball-plume-cloud radiations include all those emitted by the fireball and above-surface formations except the base surge, and occur at early times (within or in less than the first minute). Residual radiations include all those emitted by fission products and other bomb residues in the base surge and fallout, as well as by elements in earth, water, or

other materials in which radioactivity has been induced by neutron capture. In the literature, early radiation has been called "initial," and has been rather arbitrarily defined as all radiation emitted within the first minute. Such a definition may be true for water-surface bursts, but cannot hold for underwater bursts and conform with the above definition of residual radiation, since the base surge may be clearly distinguishable and the fission products in the surge may be emitting radiations by 30 sec after burst. Therefore, this report defines "fireball-plume-cloud radiation" as above, with no fixed time limit. For brevity, the initials, F.P.C. radiation, will be used in following discussions.

F.P.C. radiations of significance to the total nuclear-radiation exposure dose for surface or very shallow underwater bursts include (1) prompt gamma rays and prompt neutrons emitted at the time of fission or fusion; (2) gamma rays resulting from inelastic scattering of neutrons; (3) nitrogen-capture gamma rays; (4) early time fission-product gamma rays. The prompt gammas and neutrons are liberated in the process of fission or fusion in a time of less than a microsecond, and are thus emitted at a time when the bomb is still almost completely compacted. Most of the prompt gamma rays are absorbed by the bomb materials and casing and thus do not contribute significantly to the total F.P.C. radiation. Although many of the prompt neutrons are slowed down and captured by the bomb residues, a significant number of neutrons escape to the atmosphere.

As these neutrons traverse the atmosphere, they may undergo either capture or scatter reactions with atomic nuclei along their paths. If neutron capture occurs, the energy of the captured neutron raises that of the capturing nucleus, and the excess energy of the nucleus may be emitted as gamma radiation. In the two types of scattering collisions, the incident neutron loses part of its energy to the struck nucleus, and a neutron degraded in energy results from the reaction. Inelastic scattering occurs when part of the kinetic energy of the incident neutron is converted into excitation energy of the struck nucleus. This energy is then emitted as gamma radiation. Elastic scattering occurs when a portion of the neutron kinetic energy is transferred to the struck nucleus. In this case the total kinetic energy of both particles after collision is the same as before, although the energy distribution may be different.

The gamma rays resulting from inelastic scattering of those neutrons that escape to the atmosphere can contribute significantly to F.P.C. radiation, particularly for bursts of fusion weapons, where large numbers of high-energy neutrons are emitted. The high-energy nitrogen-capture gammas result from the nuclear capture reactions between atmospheric nitrogen and prompt neutrons at or near thermal energies. The early-time fission-product gammas are emitted by

fission products in the fireball, the plumes or column, and the cloud. For underwater bursts, only the early-time fission-product gamma rays are of significance, since prompt neutrons are completely absorbed by a relatively thin layer of water. F.P.C. radiation will be discussed more completely in Section 17.4.

Residual radiation has been subdivided into (a) transit radiation, and (b) deposit radiation. Transit radiation is the radiation from airborne radioactive particles suspended in the base surge and mushroom cloud resulting from water detonations. These radioactive aerosols may pass over or envelop a ship, or enter a ship via any break in the weather envelope. Deposit radiation is the radiation due to radioactive materials, particularly radioactive fallout particles, that may deposit on any of a ship's exterior (or some interior) surfaces. Residual radiation includes (1) gamma rays emitted by fission products in the aerosols or in deposited activity, (2) beta particles emitted from the decaying fission products in the aerosols or deposited activity, and (3) gamma rays emitted from neutron-induced activities.

Residual radiation will probably cause the major portion of all shipboard radiation exposures for all underwater and most surface bursts, especially if the ship is downwind at ranges that are greater than those at which airblast causes loss of the ship. Although exposures to transit radiation are generally of short duration, extremely high dose rates (up to several hundred thousand r/hr) could be received at exposed topside locations of a ship enveloped by a base surge. Section 17.5, Transit Radiation, includes a discussion of the attenuating effect of the ship's structure on dose rates and doses due to the base surge. If a ship's weather envelope were penetrated by any of the contaminated aerosol, ventilation and combustion air could become a minor radiation source within the ship. In addition, the problem of deposit radiation could be somewhat increased if particles carried by the aerosol were deposited in ducts or spaces within the ship. If a ship were caught in fallout or base surge, certain portions of the ship could become dangerous sources of deposit radiation unless countermeasures were employed to remove deposited particles. The extent to which dose rates from radioactive particles deposited topside would be attenuated at below-decks locations will be discussed in Section 17.6, Deposit Radiation. The extent to which the water surrounding a ship may be a source of nuclear radiation from radioactive particles suspended in the water is considered in Section 17.7.

#### 17.3.4 Sources of Weapons-Test Data

Weapons-test nuclear-radiation data from underwater and water-surface bursts have been obtained at the 4 underwater test shots\*

\*Data from the more recent Sword Fish Shot were not available as this report was prepared.

that have been held, and at only 8 of the "water surface" (barge) shots, although 35 barge test shots have been detonated.

Table 17-2. Water shots for which nuclear-radiation data are available.

United States

Water- Surface Bursts					
Operation	Shot	Date	Yield (MT)	Water Depth (Ft)	
Castle	2 (Romeo)	3/1954	11	240	
	4 (Union)	4/1954	7	160	
	5 (Yankee)	5/1954	13.5	250	
	6 (Nectar)	5/1954	1.7	120 (in Ivy-Mike crater)	
Redwing	Flathead	6/1956	[REDACTED]	115	
	Dakota	6/1956		115*	
	NavaJo	7/1956		215	
	Tewa	7/1956		25	
*Shot Dakota occurred later at the same location as Shot Flathead, but no depth measurements were made after Shot Flathead.					
Underwater Bursts					
Operation	Shot	Date	Yield (KT)	Burst Depth (Ft)	Water Depth (Ft)
Crossroads	Baker	7/1946	23.5	90	180
Hardtack	Umbrella	6/1958	[REDACTED]	150	150
	Wahoo	4/1958		500	3000
Wigwam		5/1955	32	2000	15000

Great Britain

Operation	Shot	Date	Yield (KT)	Location
[REDACTED]				

Table 17-2 lists the shots from which data are available, their dates of detonation, yields, and burst conditions, and also lists three British shots from which some data are available.

For each U. S. operation, several ships were instrumented to measure shipboard nuclear radiation. At Operation Crossroads, a whole array of decommissioned ships instrumented with film badges and a few gamma time-intensity recorders were moored at various locations about surface zero. At Operation Castle, two Liberty ships, the YAG's 39 and 40, were modified to have parts of each ship simulate portions of Navy combatant ships. Both ships were equipped for remote-control operation, and traversed the fallout areas of the several shots while numerous instruments aboard recorded the gamma radiation. One ship was equipped with washdown (a system that largely prevents accumulation of deposited activity on the ship's weather surfaces). The two YAG's were used similarly at Operations Redwing and Wigwag, when both were equipped with washdown systems.

At Operation Hardtack, the three destroyers used as target ships were moored at different distances downwind of surface zero of each of the underwater shots, and were extensively instrumented to measure gamma radiation. A fourth ship, the SS MICHAEL MORAN (EC-2), a World War II Liberty ship selected from the reserve fleet for use as a target ship, was instrumented to measure gamma radiation on the weather deck, and was moored upwind of surface zero for Shot Wahoo and crosswind for Shot Umbrella. All four ships were equipped with wash-down systems. In addition, floating coracles designed for the operation were moored at many locations, and were instrumented to yield gamma-radiation histories representative of dose rates at un-shielded weather-deck locations. Floating film packs were also used to measure total exposures.

Some weapon-effects data are available from three British shots. At Operation Hurricane, fallout data are available from island stations located near surface zero. At Operation Mosaic, although the weapons were detonated on towers, it is estimated that the fireball of shot G2 may have touched the sea. Aboard the HMS DIANA, which was positioned more than 50 miles downwind where no health hazard was anticipated, measurements were made of fallout and the ingress of activity through combustion and ventilation air.

### 17.3.5 Summary

## **BEST AVAILABLE COPY**

Available water-shot weapons-test dose and dose-rate data obtained for all the significant components of radiation at various locations (both shielded and unshielded) and at various distances from surface zero indicate that radiation intensities vary with burst depth,

as well as with yield, time, and distance. Some of the data have been scaled to permit estimates of exposures at unshielded locations. However, theoretical calculations of exposures are required in cases where the radiation energies are degraded by passage through materials such as the ship's structure. Scaling and calculational techniques, and their reliability, are discussed in the remaining sections that deal with the individual nuclear radiation classes. Effects of exposures on equipment will also be discussed in these sections. The effects of exposures on personnel are considered in Chapter 18.

## 17.4 FIREBALL-PLUME-CLOUD RADIATION

### 17.4.1 Introduction

As noted in 17.3.3, for surface or very shallow underwater bursts, four components contribute significantly to the total F.P.C. radiation\* incident on a target. The relative contribution of each component depends primarily on the weapon type.<sup>17</sup> (The prompt, or fission-process, gamma rays are emitted within a fraction of a second after burst, and are ignored in this discussion since they are almost completely absorbed by the bomb materials.<sup>17</sup>) A brief review of the 4 components follows. Many of the prompt neutrons emitted in the fission or fusion process are slowed down and captured by the bomb materials. However, a sufficient number escape so that the resulting prompt neutron flux forms a significant direct contribution to F.P.C. radiation. In addition, gamma rays, resulting from inelastic scattering of neutrons and nitrogen-capture gamma rays also contribute significantly. These three components of F.P.C. radiation are all due to neutrons, and will result only from surface or very shallow underwater bursts, since the prompt neutrons are completely absorbed by a thin (about 3 ft) layer of water. The early-time fission-product gamma rays emitted during the first minute after detonation (once the bomb materials have vaporized) by the rapidly decaying radioactive fission fragments are the fourth significant component of F.P.C. radiation. As noted in 17.1.2, the fission products will be carried into the air and mixed with the water thrown up by a water-surface or underwater burst. Thus, F.P.C. radiation is also emitted by the fission products carried in the column, plumes, and cloud.

Those characteristics of the above four F.P.C. radiations that affect their interaction with ships are discussed in this section, along with shipboard shielding against F.P.C. radiation and available field-test dose and dose-rate data. Curves that may be used to estimate F.P.C. neutron dose vs distance are presented, as well as curves for free-field F.P.C. gamma dose. When both doses are expressed in rads they are additive. In the discussion of the interaction of the target ship with F.P.C. radiation, the effects of neutrons and gamma rays are considered separately, since the two kinds of radiation differ in many respects. No method of calculating F.P.C. dose at shielded locations is presented, since no such method exists explicitly in current literature. Current information as to the effects of F.P.C. radiation on shipboard equipment will also be summarized.

\*Fireball-plume-cloud radiation is defined in 17.3.3.

**BEST AVAILABLE COPY**



17.4.2 Factors Affecting the Interaction of F.P.C.  
Radiation With a Target Ship

(1) Factors Affecting Neutron Radiation. The amount of neutron radiation received at a target some distance from a nuclear detonation is dependent on several factors: the characteristics of the nuclear device; the distance of the target from the detonation (the neutron source); and the shielding around the target point.

The device characteristics markedly affect both the number of neutrons emitted and the energy spectrum at the source.<sup>17</sup> The bomb materials, particularly the hydrogenous high explosives used, capture neutrons efficiently and hence affect the number and energy of the prompt neutrons that escape into the air. Furthermore, several times as many neutrons are released per kiloton of fusion yield as per kiloton of fission yield.<sup>18</sup> The neutron-energy spectrum at the source affects the distribution of energies (the spectrum) at the target, and the neutron energy spectrum at the target, in turn, affects the neutron radiation dose at the target. Prompt neutrons released by the detonation of a fission weapon have a continuous energy spectrum that peaks at about 1 Mev at the source, while almost all the neutrons resulting from detonation of a fusion device are 14 Mev at the source.<sup>18</sup> According to Ref. 19, field-test data indicate that the slow neutrons with energies of less than about 1 ev contribute no more than 2% of the total neutron dose received at distances of biological interest, whereas the faster neutrons with energies greater than 0.75 Mev contribute about 75% of the dose.

The distance from the detonation to the target affects both the number of neutrons reaching the target and the energy spectrum at the target. As the prompt neutrons leave the environment of the bomb they undergo collisions with nuclei of elements present in the atmosphere and either are captured or scattered (lose energy) with each collision. The mean free path between the collisions is dependent on neutron energy, and can vary from about 100 meters (thermal neutrons) to greater than 300 meters (14 Mev neutrons). Each collision will result in either a decrease in neutron energy or in neutron capture and hence removal. The longer the path to the target, the more collisions are possible; therefore fewer neutrons will reach more distant targets since more capture reactions are possible. The neutron energy spectral characteristics at the target depend on the relative importance of the scatter and capture processes during these collisions. Capture is usually much more probable for very low energy neutrons. Hence, after neutrons traverse a few mean free paths in air, just as many low-energy neutrons are lost by capture as are produced when higher energy neutrons lose energy through the scattering process. The result is an equilibrium neutron energy spectrum after the radiation has traversed a few hundred meters of air or a few centimeters of iron or other solid material.

[REDACTED]

Shielding around the target point attenuates neutrons at a higher rate than does air, and thus reduces the neutron dose. The most effective neutron shielding involves a combination of scatter and capture materials. Some elements (such as barium or iron) are effective in slowing down fast neutrons ( $\geq 3$  Mev) through inelastic scattering. Hydrogenous materials, such as water or paraffin, are very effective in slowing down fission neutrons (most of which have energies of less than 3 Mev) to thermal energies, and boron is effective in capturing thermal neutrons.

(2) Factors Affecting Gamma Radiation. Gamma radiations that contribute a significant portion of the total F.P.C.-radiation dose are (a) the gamma rays (of about 4 Mev average energy) produced when the neutrons of greater than 4-Mev energy undergo inelastic scattering, (b) the high-energy (up to about 11 Mev) gamma rays emitted when slow neutrons undergo radiative capture by atmospheric nitrogen nuclei, and (c) the early-time fission-product gamma rays that have an energy spectrum of about 3 Mev average energy, with energies up to 7 - 8 Mev. The amount of this F.P.C. gamma radiation that interacts with a target is dependent on several factors: the weapon type, the distance of the target from the source, the air density, the angle of incidence of the radiation, and the shielding around the target point. All these factors affect the gamma energy distribution at the target. The effects of these factors are briefly discussed in the following paragraphs.

The weapon type (fission or fission-fusion) determines the number and energy of the prompt neutrons emitted, and thus controls whether the gamma radiations resulting from inelastic scattering of neutrons and those from nitrogen capture of neutrons contribute significantly to the total F.P.C. gamma radiation. Furthermore, the weapon type and yield also affect the significance of the fission-product gamma radiation.<sup>17</sup> A few gamma-ray spectral measurements have been recorded at targets during weapon tests, but more detailed measurements have been made in laboratories.<sup>20,21</sup>

The dose rate of the F.P.C. gamma radiation at a target decreases rapidly with distance from the source due to both the inverse-square effect\* and air attenuation. The gamma rays are both scattered and absorbed, to some extent, by passage through any material. Scattering through the

---

\*This inverse-square relationship is valid only for a point source of radiation, but may be used to approximate the amount of direct radiation incident on a target at a distance equal to at least several times the diameter of a source of finite size.

**BEST AVAILABLE COPY**

[REDACTED]

interaction of the gamma rays with particles in any medium (including air) results in diversion of the radiation from its initial path and in loss of energy (Compton effect). The amount of attenuation is dependent on both the energy of the incident rays and the density of the material traversed. The higher the gamma-ray energy, the less the attenuation for a given density; conversely, the higher the density of the medium, the greater is the attenuation for a given gamma-ray energy, particularly for the energies of F.P.C. gamma rays and ship materials. The effect of decreasing the density of material (where the material is air) between the source and target is illustrated in the enhancement of fission-product gamma radiation noted for megaton-yield bursts. F.P.C. gamma radiation at a particular distance scales linearly with yield for land surface bursts up to about 100 KT; however, progressively greater-than-linear scaling with increasing yield is noted for megaton-yield bursts. This enhancement is partially due to the greater amount of gamma radiation resulting from inelastic scattering and nitrogen capture of the neutrons produced in a fusion detonation, and partially to the "hydrodynamic effect," in which the shock wave produces rarefaction of the atmosphere, eliminating much of the air attenuation for the fission product gamma rays. The velocity of the shock front for high-yield bursts is sufficiently higher than that for low-kiloton-yield bursts to produce a significant enhancement of the F.P.C. fission-product gamma radiation.<sup>22</sup> The source-to-target distance, the angle of incidence of the radiation, and to an extent the ship orientation to the burst are of significance in calculations where source-shield geometries must be considered, such as for locations within a ship where the hull and decks act as attenuating shields for the radiation. The greater the source-to-target distance, the more the radiation will be scattered. Scattered radiation is more greatly attenuated by a shield than is direct radiation, because its energy has been reduced by scattering. The angle of incidence of the radiation is significant because radiation incident on the "shield" at more oblique angles traverses greater thicknesses, hence is more attenuated than radiation following the shortest path. In addition, the radiation will have to traverse greater thicknesses of the ship's structure to reach interior locations if the ship is bow-on or stern-on to the burst than if it is beam-on.

#### 17.4.3 Field-Test Fireball-Plume-Cloud Radiation Data and Estimates of Free-Field Fireball-Plume-Cloud Radiation Dose

(1) F.P.C. Neutron Radiation. Little neutron radiation data from water-surface bursts is available, and most of the estimates have been based on data from land-surface, tower, and air bursts. At Operation Hardtack, neutron flux measurements were made at two of the barge shots.<sup>23</sup> Examination of the neutron flux curves of the various detectors (various energy ranges) for shots Yellowwood [REDACTED] and Walnut [REDACTED] reveals that the slopes of the flux-vs-distance curves are not all the same. However, the differences may have been due to the positioning of the

**BEST AVAILABLE COPY**

[REDACTED]

detectors(not on a radial line) and the device characteristics (shielding inherent in the weapon configurations). A plot of neutron dose versus distance, calculated from the flux data, showed agreement within a factor of 2 to 2.5 with values predicted according to Reference 2.

Estimates of total neutron dose vs distance from burst are derived from two sources, The Nuclear Radiation Handbook<sup>24</sup> and A Study of the Sulfur Neutrons From Fission Weapons.<sup>25</sup> Doses at given ranges from unboosted fission weapons, calculated according to Ref. 25, are higher by a factor of 1.5 to 2 than those calculated according to Reference 24. Since the conclusions of Ref. 25 are based on more extensive data than were available when Ref.24 was prepared, the results of Ref. 25 are recommended for use.

The main conclusions of the Ref. 25 analysis are as follows:

(1) The neutron dose closely follows the sulfur neutron fluence (nvt) for both boosted and unboosted fission weapons. The ratio of the sulfur neutron fluence intercept to the biological dose intercept is about a factor of 2 higher for boosted than unboosted weapons. However, boosting also increases the sulfur neutron fluence by about the same factor. Since these factors are compensating, there is no net effect on dose.

(2) The sulfur neutron intercept fluence per kiloton is an inverse function of the thickness of the weapon's high explosive component for thickness greater than about 10 cm, but appears relatively insensitive to changes in HE thickness below this value.

Plots of neutron dose vs distance for the probable range of atmospheric density are given in Fig. 17-4. One pair of curves gives values for a "typical fission weapon," the other pair for a fusion weapon. The "average value" of intercept fluence per KT [REDACTED] given in Ref.25 was used to calculate the values of the fission curve. Furthermore, the correlation of sulfur neutron flux with biological dose given was adjusted to provide results in terms of rads (absorbed dose). The values for the fusion curves are calculated from Ref. 24, since no more recent methods are available. It must be noted that because of variations in, and paucity of, data, dose estimates at best should be considered reliable only to + 200%.

It has been found that neutron radiation for yields under 1 MT can increase the total F.P.C. radiation dose by as much as a factor of 2, at close-in ranges. For yields of over 1 MT at ranges where measurements have been possible, the neutron dose is relatively insignificant compared to the gamma dose.

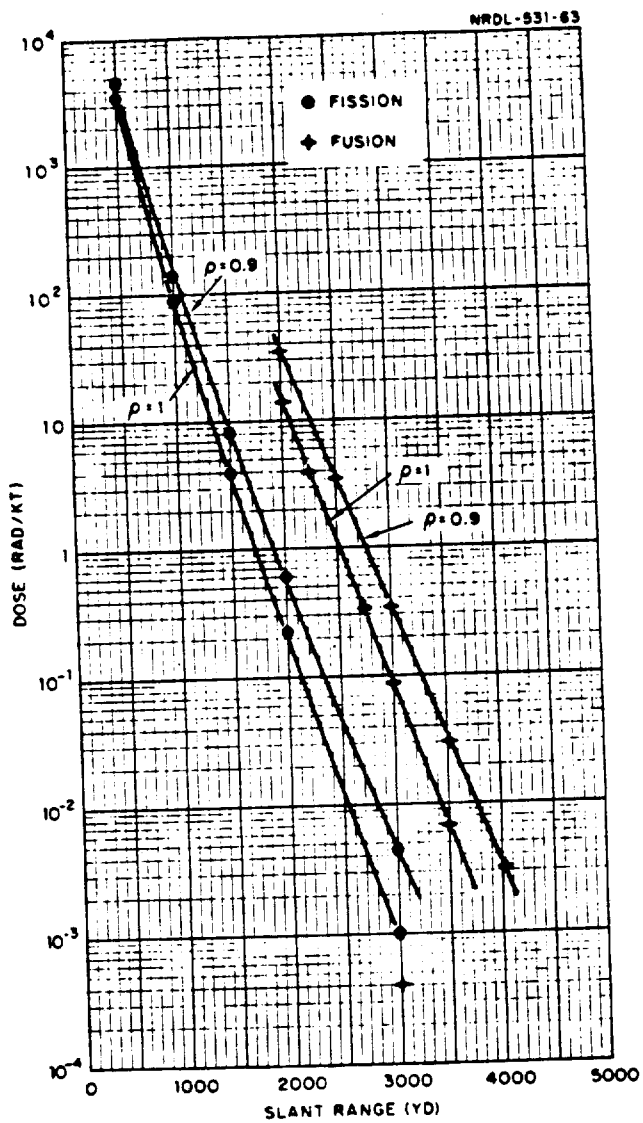


Figure 17-4. Neutron dose normalized to 1 KT versus distance.

(2) Gamma Radiation. Measurements of F.P.C. gamma radiation from water-surface bursts were made at Operations Castle<sup>26</sup> and Redwing<sup>27</sup> for devices ranging in yield/ [REDACTED]

[REDACTED] Analysis of available data from shots Flathead, Dakota, Teva, and Navajo permitted construction of the curves of Fig. 17-5 (F.P.C. Gamma Dose vs Range for 1 MT) and the Dose Multiplying Factor, Fig. 17-6. Both Figs. are redrawn from Ref. 28. Use of these two figures permits prediction of free-field F.P.C.-gamma-radiation doses from water-surface bursts of yields from 100 KT to 10 MT. Additional data are needed, however, particularly to verify the values of the dose curves at ranges greater than 12,000 ft and of the dose-multiplying-factor for yields [REDACTED]

[REDACTED]

For underwater bursts, fragmentary measurements of F.P.C. gamma radiation were made at Operations Crossroads (Baker)<sup>29, 30</sup> and Wigvam<sup>31</sup>. However, those measurements are not sufficiently detailed to permit reliable predictions of gamma dose rate or gamma dose as a function of time and distance. Somewhat better measurements of F.P.C. gamma radiation were obtained at Operation Hardtack, Shots Umbrella and Wahoo<sup>23, 32, 33</sup>. The GTR data obtained<sup>32</sup> indicate that the stem of the water plume produced an early (less than 15-sec) significant peak gamma dose rate that fell off rapidly with distance. Data from Refs. 32 and 33 are plotted on Fig. 17-7. Several GTR's were used and the standard-GTR measurements are estimated<sup>32</sup> to be more reliable than those of the ASEL-GTR; however all available data are plotted. It should be noted that within the first minute, significant gamma doses were measured, but the major portions of those doses were due to transit radiation (discussed in 17.5). The F.P.C. gamma dose, estimated<sup>32, 33</sup> to have been insignificant, is plotted in Fig. 17-8. The values shown in the figures are, in general, independent of direction from burst, but because of the paucity of data, are considered reliable only within a factor of ten, and apply only to the particular test conditions.

#### 17.4.4 Effect of Geometry on the Interaction of F.P.C. Gamma Radiation with a Target Ship

No shipboard measurements have been made of F.P.C. gamma radiation from water-surface bursts. At Operation Hardtack, efforts were made to measure this radiation from underwater bursts at both exposed and shielded locations aboard target destroyers. However, no doses were recorded at the shielded locations within the first minute. The ships

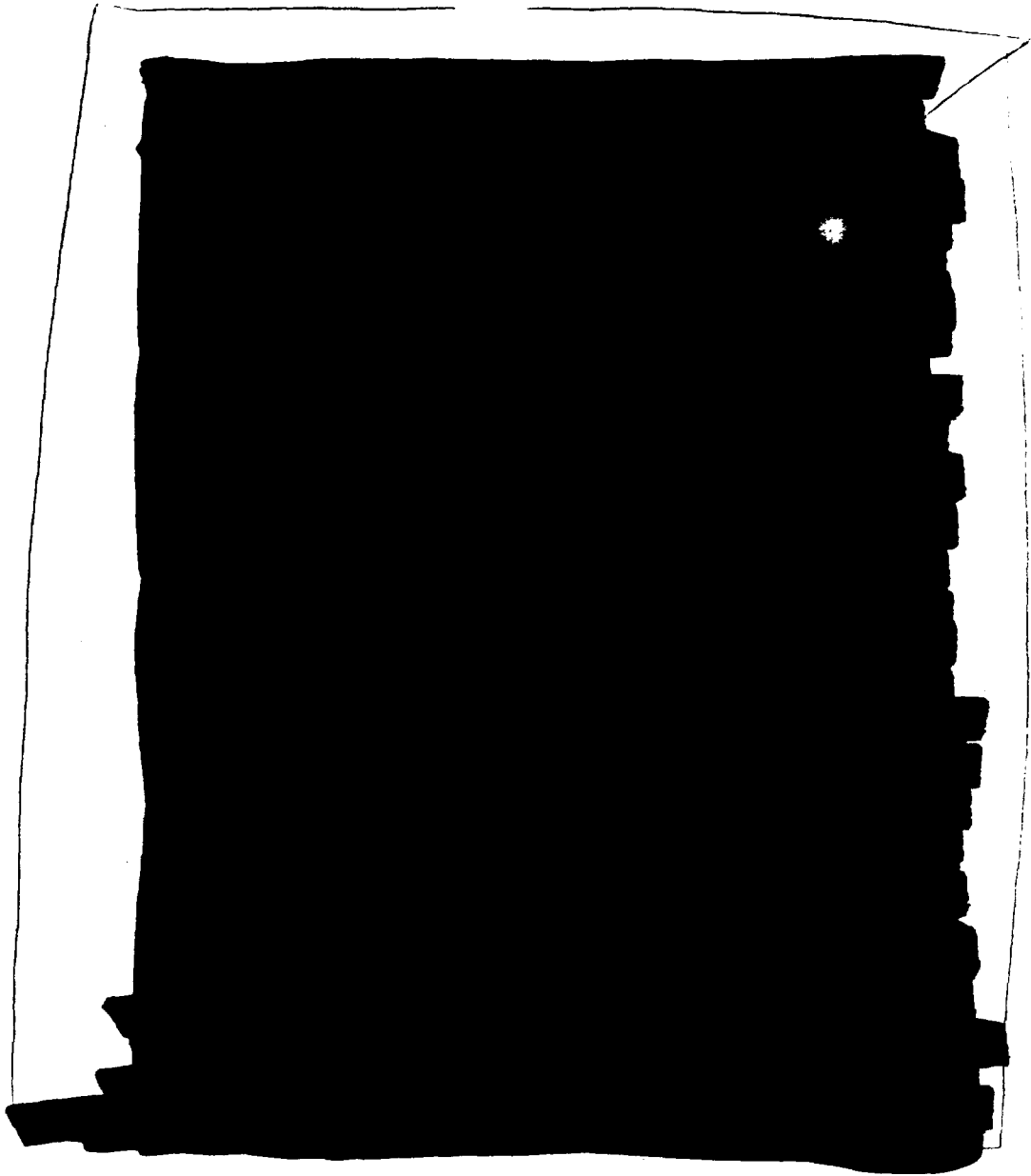


Figure 17-5. F.P.C. gamma dose versus range for 1-MT surface bursts.

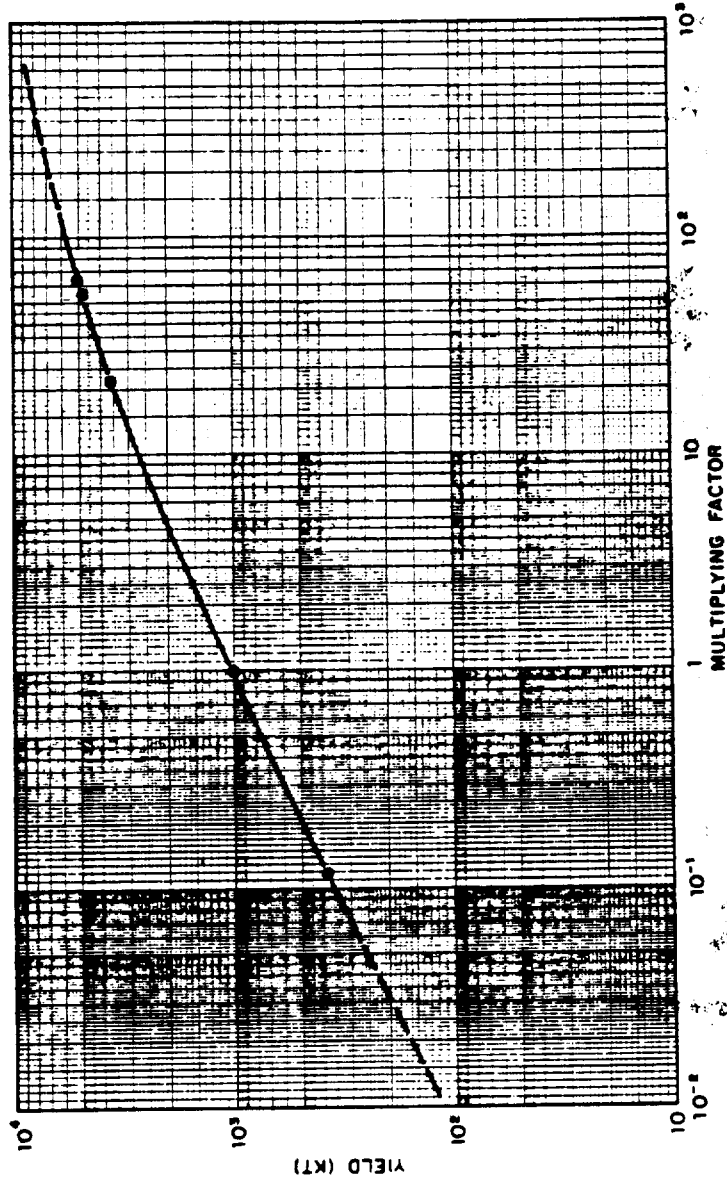


Figure 17-6. Yield versus multiplying factor for F.P.C. gamma dose, surface bursts.



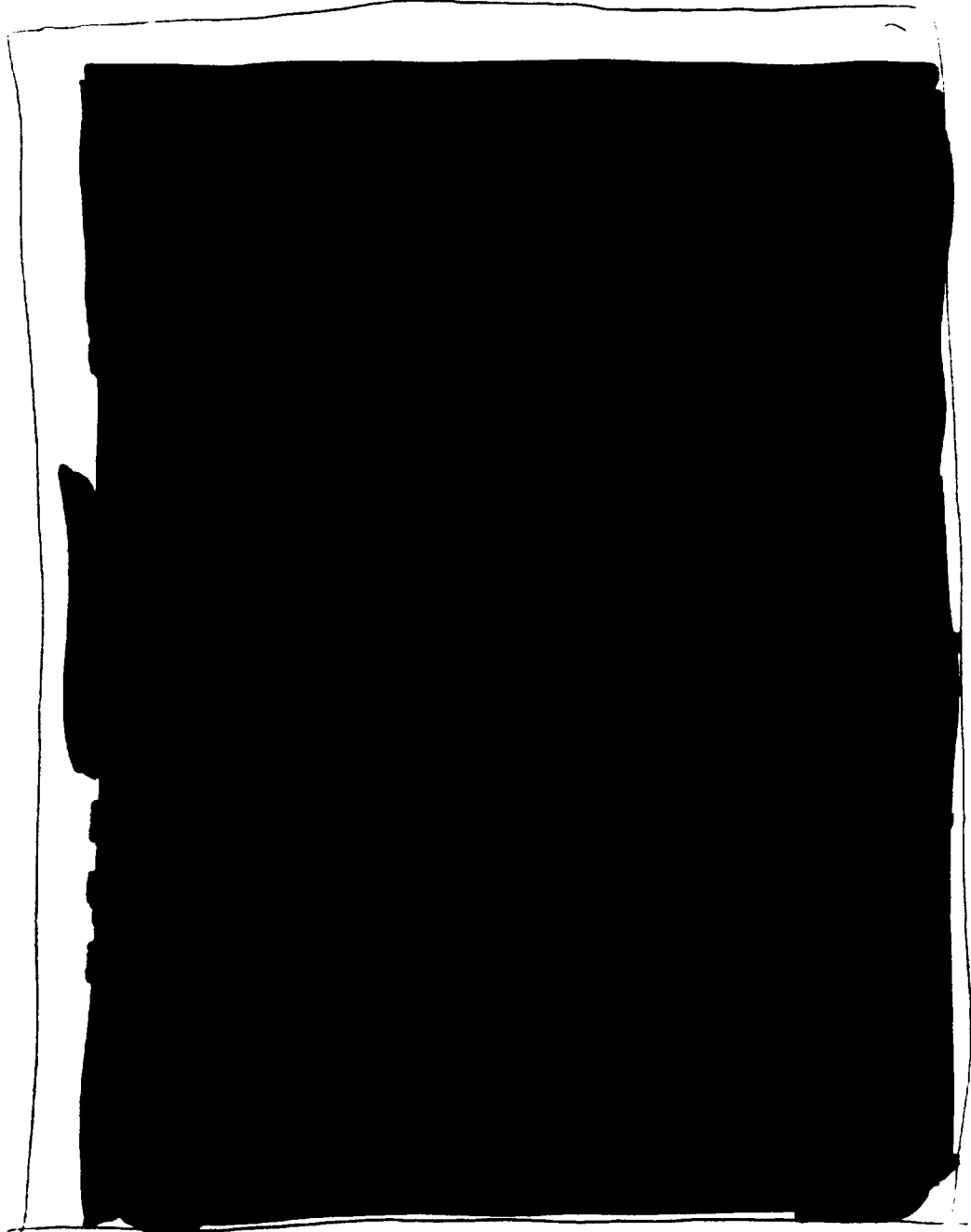


Figure 17-7. Peak F.P.C. gamma dose rate versus distance, Shots Wahoo and Umbrella.

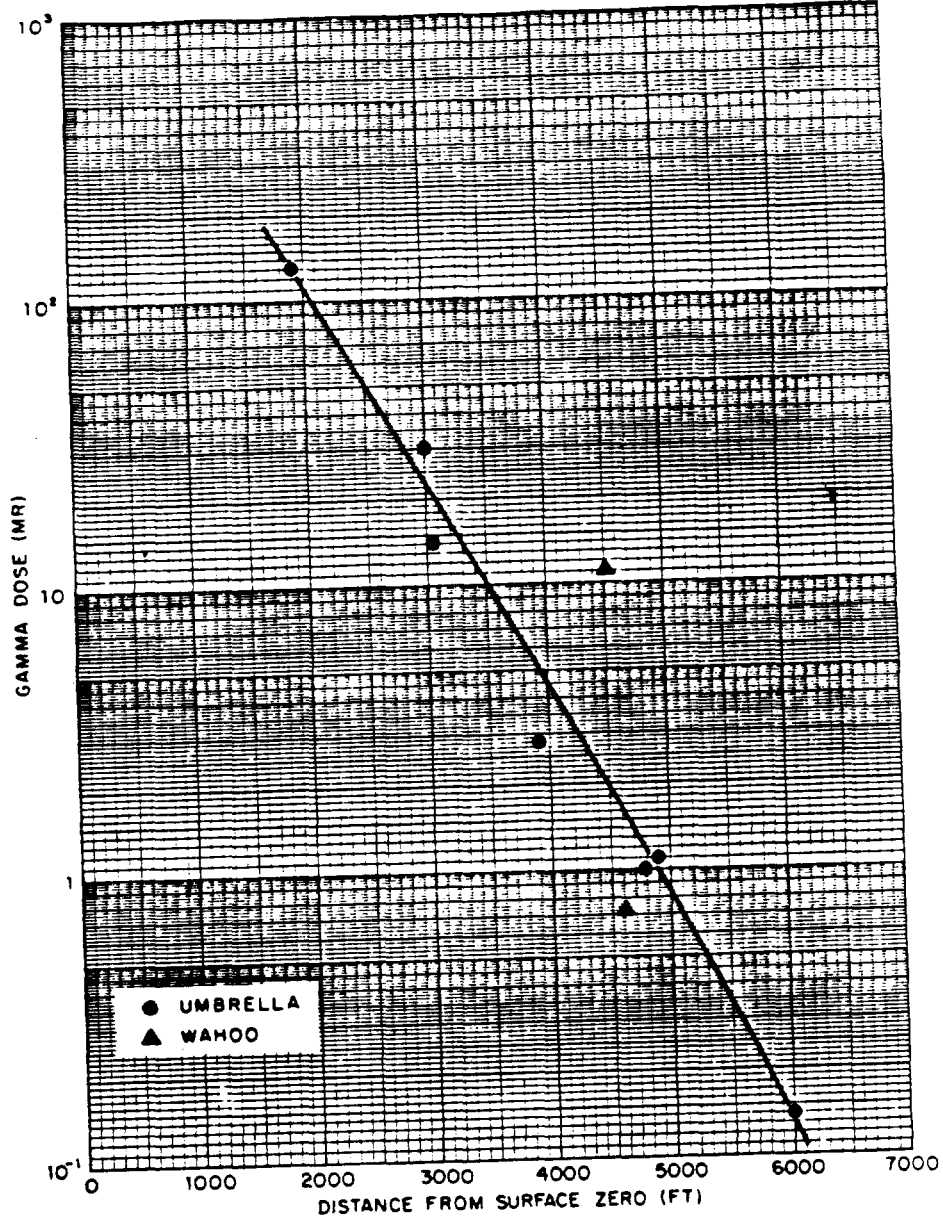


Figure 17-8. F.P.C. gamma dose versus distance, Shots Wahoo and Umbrella.

were positioned at various distances from surface zero, from 2900 to 8900 ft for shot Wahoo and from 1900 to 7900 ft for shot Umbrella.<sup>23, 32, 33</sup>

Reference 34 summarizes experiments the British conducted in 1949 aboard a cruiser, the Arethusa, to determine the shielding afforded by the ship's structures against the F.P.C. gamma radiation resulting from a nuclear airburst. Gamma radiation emitted by cobalt-60 and sodium-24 sources was used to simulate the F.P.C. gamma radiation aboard a ship located beyond the range of complete destruction from an air burst. However, since the angle of elevation of the source from the water line was only  $10^\circ$ , it is estimated that the results may also be used to indicate levels of F.P.C. gamma radiation for water-surface bursts, although the isotope gamma energies were only about  $1/6$  (Co-60) to  $1/3$  (Na-24) of the F.P.C.-gamma-radiation energies for a nuclear burst. Radiation levels were measured in three groups of compartments, that were in vertical alignment and in some compartments that extended across the width of the ship, such as the mess decks and the 4th-deck engine and boiler rooms. Several significant conclusions were reached as a result of these experiments, relating geometry and ship orientation to F.P.C. gamma dose. It was found that, in general, the protection afforded by the ship was greatest (by as much as a factor of 30) for bow exposures, and least for exposures on the beam. This effect was particularly noticeable in compartments situated below the upper deck, and was due, presumably, to the added protection afforded by bulkheads near the bow of the ship. As would be expected, the ship orientation did not affect to so great an extent the exposures at locations in compartments within the bridge structure. It was also found that for compartments that extended across the full width of the ship, there was a considerable variation (by as much as a factor of 11) between the dose received at the near-incident and near-exit sides of a compartment relative to the source of radiation.

#### 17.4.5 Effects of F.P.C. Radiation on Shipboard Electronic Equipment

The possibility that shipboard electronic equipment might malfunction as a result of exposure to the high rapidly delivered radiation exposures emanating from a nuclear detonation was indicated by laboratory tests carried out in 1956.<sup>35</sup> These preliminary high-intensity short-duration neutron-irradiation tests, in which the Los Alamos Scientific Laboratory's Godiva pulse reactor was the neutron source, indicated the sensitivity of semiconductors to neutron irradiation.

At Operation Plumbbob, in Nevada, numerous components used in electronic circuits were exposed to F.P.C. radiation from airburst Shots Hood and Priscilla.<sup>36</sup> It was concluded that, of components normally used in electronic circuits, semiconductor devices are the most susceptible to damage by nuclear radiation, and in locations where physical survival of equipment is possible, fast-neutron bombardment alone could be responsible for permanent damage to semiconductor devices. Data indicated

that, during a nuclear detonation, exposure to  $10^9$  nvt (neutrons/cm<sup>2</sup>), with negligible gamma radiation, can cause malfunction of semiconductor devices, and audio units were severely damaged by exposure to  $1.1 \times 10^{14}$  nvt.

[REDACTED]

Many industrial firms have been investigating the effects of pulsed nuclear radiation on electronic equipment (as indicated in Ref. 39), particularly the temporary disablement of avionics controls in a weapon system, an effect that would jeopardize the success of the weapons' mission.

#### 17.4.6 Summary

The F.P.C. radiation incident on a target within the first minute following a water-surface or shallow underwater burst includes neutron radiation, gamma radiation due to inelastic scattering and nitrogen capture of the prompt neutrons, and fission-product gamma radiation.

For surface bursts, the free-field F.P.C. neutron and gamma doses vs distance from surface zero for weapons of various fusion-to fission ratios can be estimated from Figs. 17-4, 17-5 and 17-6. For weapons of 1 MT or less, the gamma dose is negligible at distances of about 3,700 yards (11,000 ft) or more.

For underwater bursts, the neutron dose may be disregarded. The only available gamma data, from Shots Umbrella and Wahoo at Operation Hardtack, indicate that for underwater bursts of about 10 KT the gamma

**BEST AVAILABLE COPY**

dose is negligible. However, the data do not permit scaling or extrapolation to other yields and burst conditions.

No explicit method is given in current literature for calculating F.P.C. radiation doses at shielded locations aboard ship (although it would be possible to adapt the method of calculating transit radiation dose), and no field-test data exist to indicate the radiation doses that might be expected at such shielded locations. Results of tests made with radioactive isotopes to simulate the source of F.P.C. gamma radiation indicate that, at some locations, the protection afforded by a ship the size of a cruiser can reduce the free-field exposures by as much as a factor of 30. However, since the energy of F.P.C. gamma radiation is high, protection afforded by smaller ships (which are more lightly constructed), such as destroyers, would be less than that indicated by the test results.

Exposures of electronic equipment to F.P.C. radiation at field tests and to laboratory-simulated F.P.C. radiation indicate the sensitivity of such equipment to high-intensity short-duration pulses of such radiation. It was found that electronic equipment such as semiconductors and electronic fuze components are particularly vulnerable. In some cases, permanent damage occurred; in other cases, transient disturbances occurred that could cause malfunction of equipment in a tactical situation.

## 17.5 TRANSIT RADIATION

### 17.5.1 Introduction

Transit radiation has been defined (Section 17.3) as the gamma radiation\* from airborne particles suspended in the cloud and base surge formed by water bursts. Assessment of effects of such radiation is based on the dose or the time-integrated dose rate received at the exposure point. Thus, all available weapons-test dose and dose-rate data are of value in devising scaling techniques that would permit estimation either of dose or of dose-rate histories due to transit radiation at various ranges from surface zero for detonations of any yield. Transit-radiation data measured at weapons tests at unshielded (topside) shipboard locations are discussed in 17.5.2, and similar data obtained at below-decks locations are discussed in 17.5.3. In some cases, specific measurements of transit radiation were made; in other cases, where only one total-dose or dose-rate history was recorded, attempts were made to separate the transit from the deposit radiation. When the washdown system was in operation, deposit radiation was reduced; thus, the relative contribution of transit radiation to the total exposure was greater on a washed ship than on an unprotected ship, although the absolute amount of transit radiation did not change.

Weapons-test data available from the few water shots at which measurements have been made are insufficient to permit reliable extrapolations or scaling techniques. Therefore, attempts have been made to develop semi-theoretical models for predicting transit-radiation doses, employing available data to correct and verify the models. Two such models for predicting transit radiation at unshielded locations aboard ship are discussed in 17.5.4.

Transit dose rates and doses at interior locations in a ship will always be less than those recorded at the same time on the ship's weather deck, because of the attenuation afforded by the intervening structure. Such attenuation is generally expressed in terms of shielding factors, where the shielding factor for a given location is usually defined as the ratio of the dose rate at the given location to the dose rate at 3 ft above the weather deck. As noted in Ref. 41, the shielding factors depend not only on the arrangement and thickness of ship structure and materials, but also on the distribution of radioactive particles in space as well as on the radiation energy spectrum. The spectrum varies slightly with bomb type, but may vary considerably through fractionation of the different isotopes involved. It also varies with time after burst. A theoretical method for calculating ship-shielding factors and thus dose rates at interior shipboard locations is presented in 17.5.4. The effect

---

\*Beta radiation from transit sources contributes only a negligible amount to the total dose received at unshielded locations, and none at all at shielded locations.

of the geometry of the ship on transit radiation doses at unshielded locations is discussed in 17.5.6, and the effects of transit radiation on electronic equipment are indicated in 17.5.7.

#### 17.5.2 Weapons-Test Data for Unshielded Shipboard Locations

##### 1. Water-Surface Bursts

All the test shots classified as surface bursts (Table 17-2) were over relatively shallow water, considering the high yields involved, and the proximity of the sea bottom and the motion of bottom material probably influenced the subsequent radiation effects. Thus, these shots probably did not produce the same effects that would have occurred had they been water-surface bursts at sea (over deep water). However, radiological data from these tests can be useful in estimating radiation effects from water-surface bursts at sea.

Operation Castle: According to Ref. 40, no separate measurements of transit radiation were recorded for either Shot 4 (Union) or Shot 5 (Yankee). However, crude estimates indicated that on the YAG 39 target ship with the washdown system operating, doses at least greater than 0.8 r accumulated between 1 and 3 hr after Shot Union, and doses greater than 23 r accumulated between 1 and 12 hr after Shot Yankee. In neither case was the target ship directly downwind in the path of fallout. Taking estimated differences in geometry into account, these figures led to an estimate that, at the end of fallout, as much as half the dose accumulated on the weather decks of a washdown-protected ship was due to transit radiation. On a ship not protected by washdown the transit dose was estimated to be of minor significance relative to the deposit dose.

Operation Redwing: For the two water-surface bursts and one shot partly on land and partly over water (Shot Tewa), various records of dose rate and dose with and without washdown are available.<sup>41, 42</sup> Reference 41 concluded that "the air contributions to the gamma-radiation fields aboard ship were highly significant during the period of fallout." The only separate transit-radiation records for Shot Tewa are "estimated" (i.e., adjusted for instrumentation) 2 $\pi$  free-field dose rates and doses. The highest such readings were a dose rate of 3.5 r/hr at 4 hr after burst and a total dose of 9 r accumulated by 25 hr after burst, after the YAG-39 had completed maneuvers in an area north of surface zero while the wind direction was at 105°. For Shots Navajo and Flathead, gamma radiation was recorded in washed and unwashed weather-deck areas aboard the YAG's starting at several hours after burst, but no estimates of transit radiation alone are available. Incremental-collector and GTR (gamma intensity time recorder) records<sup>42</sup> are available, and transit radiation doses and dose rates have been calculated<sup>43</sup> from the records by estimating fallout arrival times and,

after making appropriate corrections, subtracting the deposit dose (dose accumulated after fallout started) from the GTR records. However, such results must be considered speculative.

2. Underwater Bursts

**BEST AVAILABLE COPY**

Transit radiation data available for underwater bursts are from the four low-kiloton shots listed in Table 17-2. The magnitudes of the measured transit doses were significant in all four cases. Furthermore, the data indicate that the significance of transit radiation as a contaminating mechanism may be associated with the phase of the bubble when it breaks through the surface. At Operation Crossroads, Shot Baker, the shallow burst that produced a broad column and mushroom cloud, the deposited activity from the rainout or fallout, rather than transit radiation, was the major source of contamination. However, there was practically no fallout from any of the other three deeper bursts, and in each of those three tests the transit radiation was the source of the gamma doses measured on the target ships. Available data are summarized in the following paragraphs.

Operation Crossroads, Shot Baker: A few dose-rate histories were recorded at Shot Baker,<sup>44,45,46</sup> and are estimated to be partly due to transit radiation. References 44 and 45 reproduce time-dose-rate records from four of the target ships. Examination of those records indicates that significant gamma doses were delivered during the times the ships were enveloped by the base surge. For instance, during envelopment by the base surge, peak dose rates of about 3500 r/hr, 180 r/hr, and 150 r/hr were recorded on LCT 874 (2420 yd from surface zero and slightly downwind), on APA 77 (USS CRITTENDEN, 1500 yd from surface zero and slightly downwind), and on LCI 332 (1890 yd from surface zero and slightly upwind), respectively. However, the departure of the surge caused no noticeable decrease in the dose-rate curves. Furthermore, on LCI 332 although the dose rate increased from about 50 r/hr to about 150 r/hr during envelopment by the base surge between 2 and 5.6 min, the dose rate suddenly increased to about 870 r/hr at 7 min when the surge was about 300 yd downwind from the ship. According to Ref. 29, at weather deck locations, it was "estimated that 50 percent of the total dose was radiated from the mist during the time in which the vessels were engulfed by the mist," and the same study gives a contour map of transit-radiation doses, obtained by subtracting deposit doses (computed by means of fallout collections) from total doses (measured by film badges).

Operation Hardtack: The two underwater bursts of this operation (Shots Umbrella and Wahoo) provide the best transit-radiation records of any weapons test, and results indicate that exposure to the base surge of a shallow or moderately-deep underwater burst can result in high doses within the first 15 to 30 min. Dose-rate histories were recorded<sup>33</sup> aboard the three DD's and the EC-2 at shots Umbrella and



Wahoo, and many total doses were registered on film packs. Also, many of the base-surge dose-rate records were measured by GTR's located on coracles that were floating in the water.<sup>32</sup> These coracle records best describe free-field dose rates, where the free field is defined as the gamma field near the water surface, unmodified by any projections above that surface. Since the GTR's were only a few feet above the water surface, it is estimated that some of them were washed by the water and some of the records include radiation from contaminated water. However, the dose contribution from the water is separable from the total dose because some of the coracles were also equipped with underwater GTR's; thus the above- and below-surface GTR records could often be compared with each other and with available shipboard records. Inspection revealed that most of the coracle records can be considered equivalent to readings at unshielded locations on a ship's deck. Analysis of the records led to the conclusion given in Ref. 33, which deals specifically with shipboard radiation, that "at least 95 percent and 98 percent for Shots Umbrella and Wahoo, respectively, of the total doses observed on the unwashed decks were due to remote-source (i.e., transit) radiation."

Base-surge dose rates were recorded at times ranging from less than 30 sec to more than 20 min after burst.<sup>32, 33</sup> Peak dose rates as high as 100,000 r/hr and total transit doses as high as 1000 r were recorded.

At Shot Umbrella, on the EC-2 at 1650 ft crosswind, a dose of over 1000 r was recorded, with a peak dose rate of more than 100,000 r/hr at less than 1 min after burst. Aboard the DD-592 at 3000 ft downwind, a dose of over 500 r was recorded, with a similarly high peak rate of about 100,000 r/hr at 30 sec. On the DD-593 at 7900 ft downwind, a dose of only 65 r was recorded with a peak rate of about 5500 r/hr at 100 sec.

At Shot Wahoo, aboard the EC-2 located 2300 ft upwind from surface zero, a peak dose rate of 17,500 r/hr was recorded at 0.75 min after burst, and a transit dose of about 300 r was accumulated within 30 min. Aboard the DD-593 at 8900 ft downwind, a peak dose rate of about 9000 r/hr was recorded at about 5 min after burst, and the transit dose was 300 r.

Dose rates were recorded aboard ship until 6 hr after burst. After passage of the base surge, rates were quite low, characteristically being less than 1 r/hr at times later than 1 hr after burst (all ships used washdown).

Operation Wigwam: One dose-rate history recorded aboard the YAG-39 at 13 to 20 min after burst<sup>31</sup> must have been due to transit radiation alone, since no deposit material was collected in that time interval. The peak recorded dose rate was approximately 600 r/hr, when the ship was about 28,000 ft from surface zero. Some transit radiation was recorded the following day at extremely low levels.

**BEST AVAILABLE COPY**

## 17.5.3 Weapons-Test Data for Shielded Locations

1. Water Surface Bursts

Operation Castle: Interior-location dose rates were not recorded<sup>40</sup> for shot 4. At shot 5 (Yankee), some transit radiation was received but not separately recorded<sup>40</sup> at unshielded locations on the YAG-39. Since washdown was operating, some (but not all) of the deposit radioactivity was washed off the ship, and thus the dose rates and doses recorded<sup>40</sup> at various interior locations on the ship were considered partly (but not entirely) due to transit radiation. Peak dose rates, which occurred at about H + 5 hr, were about 1 r/hr in the interior of the superstructure, 0.4 r/hr in the bottom of No. 2 Hold, and 0.02 r/hr in the starboard boiler. The respective total doses to 12 hr were about 7.5, 3, and 0.15 r.

Operation Redwing: As stated in 17.5.2, the only unshielded transit-radiation data at this operation are those for Shot Tewa; thus Tewa is the only shot for which a comparison of shielded and unshielded transit radiation would be possible. Although the dose rates at various interior locations were recorded, the transit and deposit contributions were not separated, nor are records for interior locations explicitly presented. Reference 41 gives ratios of interior dose rates and doses to total dose rates and doses recorded at the same times on the weather decks of the target ships. Such ratios are, in general, less than 0.5.

2. Underwater Bursts

Operation Crossroads, Shot Baker: Although film badges recorded total gamma exposure doses in many shielded locations, the transit component of these doses is not known. Reference 29 estimated that on the weather deck, the transit component was about 50%, but at interior locations, the same reference states that details of badge placement varied, resulting "in wide variation of doses received by badges subjected to approximately the same radiation." Also, according to this report, conversion of film density to radiation dose "may be in error by as much as a factor of two," and the "influence of shielding on the badge readings is apparently many times the shielding effect which might be expected from consideration of the plating thickness interposed between the badge and the exterior of the vessel." Thus, it is impossible to reliably estimate the transit component of the radiation records at interior locations at Shot Crossroads Baker.

Operation Hardtack: Radiation histories were obtained on one ship at Shot Wahoo and on all three ships at Shot Umbrella. Film-pack doses were also recorded. It is estimated that transit radiation was responsible for 95% and 98% of the total doses recorded in shielded

**BEST AVAILABLE COPY**

locations at Shots Umbrella and Wahoo, respectively. The preceding statement is based on the estimate<sup>33</sup> that at least 95% and 98% of the total dose on the washed decks of the destroyers was due to transit radiation from Shots Umbrella and Wahoo, respectively, and the contribution of all other radiation to the total dose at below-decks locations was of little significance. At Shot Umbrella, doses of more than 200 r were recorded in many compartments of the two closest ships (at 1900 and 3000 ft from surface zero). The ratios of doses in compartments to those on washed weather decks ranged from 0.1 to 0.7 for non-machinery spaces and from 0.02 to 0.2 for machinery spaces.<sup>33</sup> The ratios of peak dose rates showed similar variation. At Shot Wahoo, doses of more than 500 r were recorded in most compartments aboard the closest ship (at 2900 ft) and doses of more than 200 r were recorded aboard the next closest ship (at 4900 ft).

Existing data indicate that, at least under certain conditions, the transit radiation may contribute the major portion of the nuclear radiation aboard ship. These conditions occur when (1) yields, water depths, and burst depths are such that a contaminated base surge forms; and (2) when the radioactive particulate material formed is of such a nature that the washdown system is highly effective in preventing shipboard contamination. Since available data are insufficient for reliable scaling and extrapolating transit-radiation effects for any yield or burst condition (depth of burst and depth of water) it is obvious that methods for theoretical calculations of such exposures are required.

Operation Wigwam: During the period when transit radiation was being recorded on the deck of the YAG-39, from 13 to 20 min after burst, there was no record of deposit dose. The peak dose rates of 300, 150, and 18 r/hr recorded<sup>31</sup> during this interval at the wheelhouse, internal, and deep-hold stations, respectively, therefore may be assumed to have been due to transit radiation. These interior peak dose rates thus were found to be 50%, 25% and 3% respectively, of the recorded exterior peak dose rate of 600 r/hr.

#### 17.5.4 Theoretical Calculations of Transit Radiation for Unshielded Locations

##### GENERAL

No theoretical models for estimating transit radiation from water-surface bursts have been developed, but two models are available for subsurface bursts. Order-of-magnitude estimates for surface bursts are given in Ref. 47, which states "the fireball formed by a surface shot will vaporize water below it; this water, the explosion products, and entrained air will form a radioactive mushroom cloud. Below the cloud a tenuous stem or column of water will be raised and the column collapse will probably create a relatively minor base surge .....

Certain analyses indicate that the transit dose should be about 10-30 percent of the deposit dose during the period of deposition, the percentage increasing with increasing distance from surface zero."

An idealized theoretical model for predicting peak dose rates and doses for underwater bursts is presented in Chapter 7 of Reference 47, whereas a more generalized model for calculating such histories is given in Reference 48. The model of Ref. 47 is briefly described, followed by a summary of the model presented in Reference 48.

THE MODEL OF REFERENCE 47

In this model, let

$t_1$  = time in hours of initial arrival of activity (leading edge of base surge)

$t_f$  = time in hours of final arrival (trailing edge)

$d$  = dose rate from airborne activity at any time  $t$  after burst

$d_0$  = dose rate corrected for decay to reference time of 1 hr

$d = d_0 t^{-1.2}$ , assumed radioactive decay

$d_0 = 0$  for  $t < t_1$  and for  $t > t_f$

$d_0 = d_0(R, \theta)$  for  $t_1 \leq t \leq t_f$ , where  $R$  and  $\theta$  are polar coordinates of the point with reference to surface zero.

In Ref. 47, for the specific shots under discussion, estimates of  $d_0$ ,  $t_1$  and  $t_f$  are plotted as functions of distance  $R$ . Then the total transit dose,  $D$ , may be expressed by

$$D = \int_{t_1}^{t_f} d \, dt = \int_{t_1}^{t_f} d_0 t^{-1.2} \, dt$$

and evaluated by

$$D = \frac{5d_0}{t_1^{0.2}} \left[ 1 - \left( \frac{t_1}{t_f} \right)^{0.2} \right] \quad (17-2)$$

For convenience in calculating, the quantity in brackets is also plotted in Ref. 47.

In this simple model,  $d_0$  may be thought of as resulting from an average amount of active material distributed through that portion of

**BEST AVAILABLE COPY**

the base surge passing any point, in the sense that multiplying  $d_0$  by the assumed decay rate,  $t^{-1.2}$ , and then integrating from  $t_1$  to  $t_f$  gives the correct value of the total transit dose at the point. When integrated from  $t_1$  to  $t_f$ , the expression gives an idealized estimate of the dose-time history that smoothes out the effects of nonuniformity in the actual values of  $d_0$ . Comparison of some results from Shot Wahoo with calculated values of  $d_1$ , the maximum dose rate to be expected from airborne activity (the value of  $d$  at time  $t_1$ ) indicates that the calculated value of  $d_1$  gives a close estimate of the maximum observed dose rate. Note that in this model, the maximum dose rate occurs at  $t_1$ ; in the real case, the maximum dose rate occurs somewhat later.

#### THE MODEL OF REFERENCE 48

A geometrical model of the base surge is used as the source of radiation for the theoretical method of calculating transit radiation developed in Ref. 48. The geometrical and radiological parameters of the right circular truncated cone used as the model depend on yield and burst depth, and the model is designed to be applicable to weapon yields from 1 KT to 100 KT. Surface and near-surface bursts are not covered. The geometries used are suggested by photographic records of weapon tests and by theoretical scaling relationships,<sup>49</sup> but are adjusted to agree with radiological test data. Similarly, the radiological properties of the model, although guided by simplifying assumptions, are adjusted after comparison with weapon-test data.

It is noted that this model takes into account only burst depth; water depth is not considered, although the development of Ref. 49 tacitly assumes shallow bursts are bottom bursts. It has been suggested that the base-surge radii calculated for shallow bottom bursts are approximately valid for all shallow bursts, but recent data (from Operation Hydra II) indicate that such an assumption is questionable. Numerical calculations required for prediction of dose rates and doses have been programmed for machine (IBM-704) computation at NRDL.

#### A. Simplifying Assumptions

The following simplifying assumptions were used in developing the model:

1. Air attenuation of radiation occurs but there is no attenuation by the water droplets that form the base surge.
2. Gamma-spectrum and buildup-factor calculations are replaced by use of an effective attenuation factor,<sup>50</sup> a substitution that takes into account absorption and scattering of gamma rays over the entire radiation spectrum. (Note that the effective attenuation factor is different from an "average" or "effective" energy.)

3. Activity is homogeneously distributed in the base surge.
4. There is no fractionation of fission products; therefore, gamma decay rates used are those for the gross fission-product mixture.<sup>51</sup>
5. Possible deformation of surge by wind is neglected so that the surge has circular symmetry. Beginning at 15 seconds after burst, the surge moves downwind as a unit at the specified surface windspeed,  $u$  (ft/sec), and at  $t$  sec after burst, the center of the source is located at a distance  $u(t - 15)$  ft downwind from surface zero.
6. Total activity due to the burst is multiplied by a number  $\phi$ ,  $0 < \phi < 1$ , that depends on scaled depth but does not vary with time. This assumption is equivalent to assuming that a fraction  $\phi$  of the total activity is the base surge (given conditions 2 to 5) and that there is no loss of activity by rainout, evaporation, etc.

**B. Classification of Underwater Burst Depths**

A given underwater burst of yield  $Y$  (KT) at a depth of  $d$  ft is classified as follows:<sup>49</sup>

- Very Shallow:  $21 Y^{1/3} < d < 75 Y^{1/3}$
- Shallow:  $75 Y^{1/3} < d < 240 Y^{1/4}$
- Deep:  $240 Y^{1/4} < d < 600 Y^{1/4}$
- Very Deep:  $600 Y^{1/4} < d$

Near-Surface shots,  $0 < d < 21 Y^{1/3}$ , are not covered by the model of Ref. 48. Figure 17-9 (from Ref. 49) shows the categories for 1 to 100 KT. Weapon tests falling in the four categories used are:

- Very Shallow: Crossroads Baker
- Shallow: Hardtack Umbrella
- Deep: Hardtack Wahoo
- Very Deep: Wigwam

Table 17-2 gives the yields and depths of these shots.

The physical interpretation of the classification, from Ref. 49, is as follows:

Near-Surface bursts are those that are so shallow that the layer of water above them is vaporized by the explosion. The phenomena of this type of burst and the associated hazards are unknown. The radiological

**BEST AVAILABLE COPY**

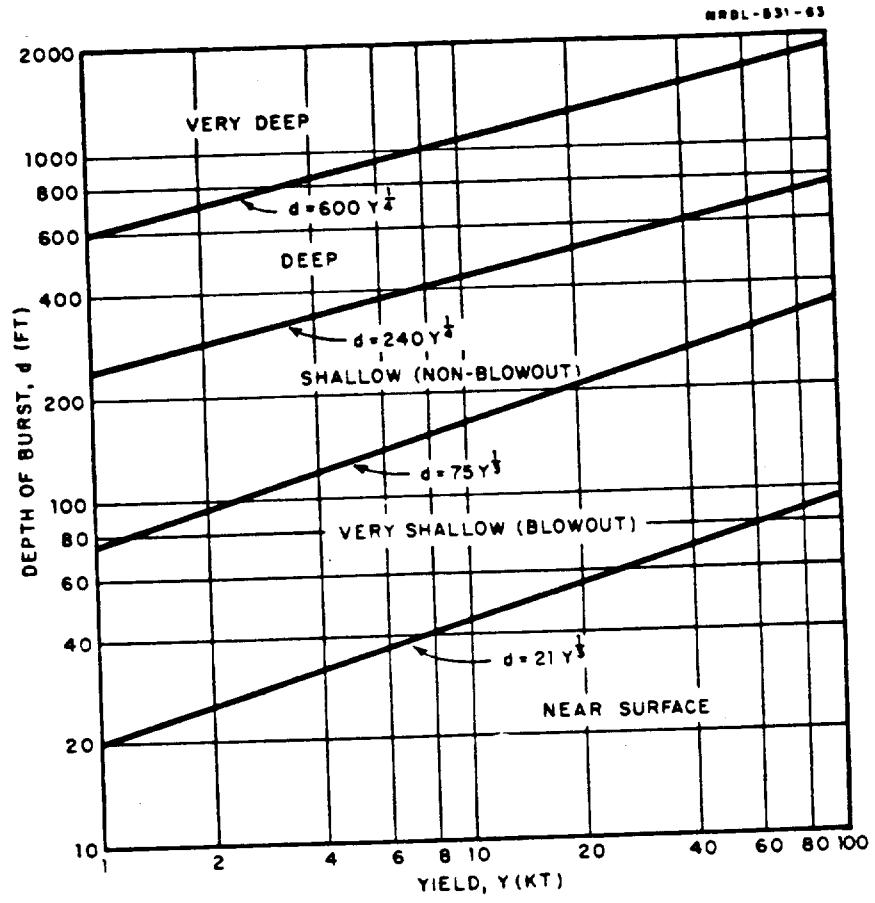


Figure 17-9. Classification of underwater burst depths.

hazard of the base surge is considered unimportant compared with air-blast and fallout hazards from bursts in this category.

Very-Shallow bursts are those for which the bubble breaks the surface during the first cycle while bubble pressure is greater than atmospheric pressure, causing blowout of fission products.

Shallow bursts are those for which the bubble vents during the first cycle, but at a time when bubble pressure has dropped to atmospheric pressure or less.

Deep bursts are those for which the bubble completes at least one oscillation (expansion and contraction) before breaking through the surface.

Very Deep bursts are so deep that the bubble breaks up before reaching the surface. The minimum burst depth for this category is taken as that at which the bubble completes three expansion-contraction cycles before breaking through the surface.

Although the physical category into which a burst falls may be influenced by bottom depth as well as burst depth, the influence of the bottom is not considered in this model. For bursts close to the dividing line between two categories, it is suggested<sup>48</sup> that an appropriately weighted average of the results for these categories be used.

### C. Base Surge Forms

The two geometrical forms of the base surge used in the model were suggested by photographic and radiological data, and are shown in Fig. 17-10. It is emphasized that the geometrical forms used for computation purposes, which yield transit-dose-rate and dose values in agreement with test data, are not necessarily the actual visible shape of the surge.

Very Shallow and Shallow. The form is a right-circular hollow truncated cone, with the lower interior angles of both inner and outer faces equal to  $70^\circ$ . The inner radius is taken as  $2/3$  of the outer radius.

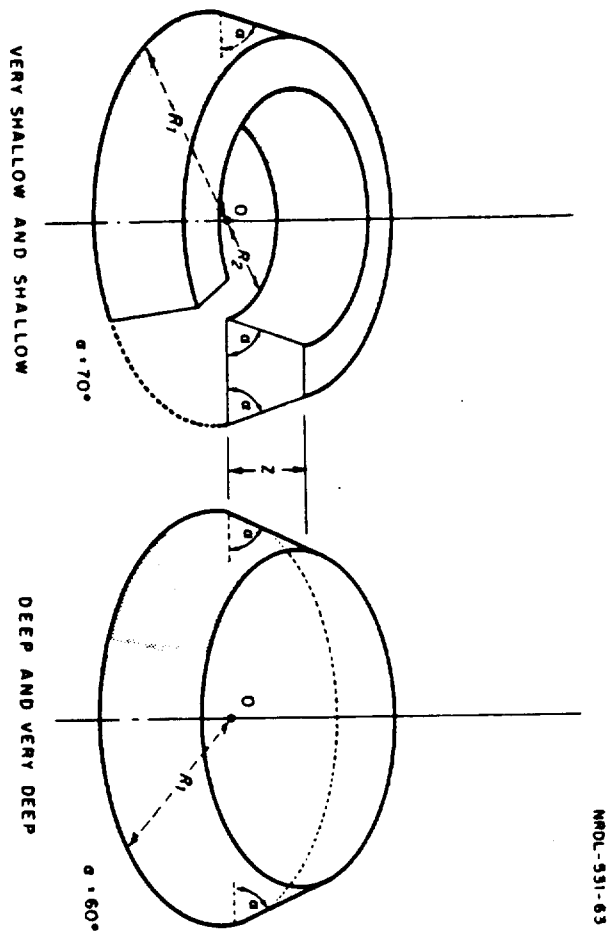
Deep and Very Deep. The form is a solid right circular truncated cone with the lower interior angle of the face equal to  $60^\circ$ .

In both forms, the height of the base surge,  $Z$ , as a function of time  $t$  (sec) is the same:



[REDACTED]

17-45



NRDL-531-63

Figure 17-10. Base surge geometry.

[REDACTED]

$$Z = 1000 \left( \frac{Y}{10} \right)^{1/6}, t \leq 60$$

$$Z = \left[ 1000 + \frac{t - 60}{180} \times 1000 \right] \left( \frac{Y}{10} \right)^{1/6} = \frac{50}{9} \left[ t + 120 \right] \left( \frac{Y}{10} \right)^{1/6}, 60 < t < 240$$

$$Z = 2000 \left( \frac{Y}{10} \right)^{1/6}, t > 240$$

(17-3)

The expressions for Z were suggested by inspection of data from Operations Wigwam and Hardtack. They are used here for all depths of burst in the ranges under consideration. Actually, of the two Hardtack shots considered, the shallow one (Umbrella) produced a somewhat higher base surge. One would expect that decreased burst depth for a given yield generally would result in increased surge height, as long as the shot remained below the Near-Surface category. However, the scatter of height observations at each of the Hardtack shots is so great that no attempt has been made to scale height with yield or depth.

D. Scaling of Base Surge Size

Several dimensionless expressions are used in Ref. 49 for scaling the base-surge radius R, (ft) at time t (sec).

For Very Shallow and Shallow bursts:

$$R_{sc} = \frac{R_1}{D_{max}}; t_{sc} = \frac{t}{\left[ \frac{D_{max}}{d_{sc}} \right]^{1/2}}$$

where  $R_{sc}$  (dimensionless) is the scaled (or reduced) radius,  $D_{max}$  (ft) is the maximum diameter of the column of water produced on the surface, and  $t_{sc}$  is scaled time in terms of  $(\text{sec}/\text{ft}^{1/2})$ . The maximum diameter of the water column,  $D_{max}$ , can be expressed in terms of yield Y (KT) and/or scaled burst depth  $d_{sc}$ .

For Very Shallow bursts:  $D_{max} = 710 Y^{1/3}$

For Shallow Bursts:  $D_{max} = 377 Y^{1/3} d_{sc}^{1/6}$

where  $d_{sc} = \frac{d}{Y^{1/3}}$ .

For Deep and Very Deep bursts:  $R_{sc} = \frac{R_1}{A_{max}}; t_{sc} = \frac{t}{A_{max}^{1/2}}$

where  $A_{max}$  (ft), the maximum radius of the bubble produced by the burst,

can be expressed in terms of yield and burst depth:

$$A_{\max} = \frac{1500 Y^{1/3}}{(d + 33)^{1/3}}$$

(The number 33 represents atmospheric pressure at the surface in ft of water; thus,  $d + 33$  represents hydrostatic pressure.)

Values of scaled base-surge radius and scaled time for the four underwater test shots, based on visual extent of the surge, are given in Table 17-3, reproduced from Ref. 49, which contains a discussion of the principles of scaling used. The following expressions for scaled radius were developed by graphical methods of fitting to the values of Table 17-3, and the application of correction factors to bring calculated dose rates into agreement with observed ones.

$$\left. \begin{aligned} \text{Very Shallow and Shallow: } R_{sc} &= \left[ 5.85 \log_{10} (t_{sc} + 0.73) + 0.802 \right] C \\ \text{Deep: } R_{sc} &= \left[ 16.7 \log_{10} t_{sc} + 4.54 \right] C_D \\ \text{Very Deep: } R_{sc} &= \left[ 7.32 \log_{10} (t_{sc} - 1) + 7.83 \right] C \end{aligned} \right\} (17-4)$$

The term  $C$ , which has the value 0.8 is the correction factor applied to bring calculated dose rates into agreement with observed ones. The value indicates that the "radiological" radius of the surge is less than the visual photographic radius.

#### E. Radiological Aspects of the Model

##### 1. General Characteristics

The radiological characteristics specified for the model include source strength, activity distribution, and air-attenuation behavior. In the model, the source is homogeneous. Source strength is proportional to yield,  $Y$ . Energy emission rate is that of unfractionated fission products. An "effective attenuation factor"<sup>50</sup>  $\bar{\mu}$ , for air attenuation is used in dose-rate computation. Dose-rate computations for a given point are made at 15-sec intervals, starting at 30 sec after burst. Dose is computed from these dose rates in 15-sec increments. The model predicts excessively high dose rates at times earlier than 30 sec because only air attenuation is considered. At these early times, attenuation by water thrown up by the explosion, or inhomogeneities in the distribution of radioactivity, which have been ignored, probably accounts for much of the difference. These early dose rates probably make a significant contribution to the total dose only in the region near surface zero where other weapon effects, especially underwater shock, are of dominating importance.

**BEST AVAILABLE COPY**

Table 17-3. Scaled base surge data.<sup>49</sup>

Baker and Umbrella		Wahoo		Wigvam	
$t/(D_{max})^{1/2}$	$R/D_{max}$	$t/(A_{max})^{1/2}$	$R/A_{max}$	$t/(A_{max})^{1/2}$	$R/A_{max}$
[REDACTED]	[REDACTED]	[REDACTED]	[REDACTED]	[REDACTED]	[REDACTED]

2. Calculation of Dose Rates

The dose rate,  $d$ , due to transit radiation, is calculated by means of the expression,

$$d = k I \text{ r/hr} \tag{17-5}$$

where  $k = 1.703 \times 10^{-6}$  r/hr per Mev/cm<sup>2</sup>-sec, a constant that includes the energy-absorption coefficient,  $\mu_A$  (assumed to be  $3.35 \times 10^{-5}$  cm<sup>-1</sup> average for radiation of energy from 100 Kev to 2 Mev), and constants for converting Mev/cm<sup>2</sup> sec to r/hr

BEST AVAILABLE COPY

and

$$I = \frac{1}{\mu} N J_0 \text{ Mev/cm}^2 \text{ -sec} \quad (17-6)$$

= the gamma intensity per unit area (energy flux density) at the point of measurement, P

where  $\frac{1}{\mu}$  = the effective free mean path, plotted on Fig. 17-11 reproduced from Ref. 50. (The effective mean free path is an empirical figure that takes into account buildup factor.)\*

$$N = \frac{1}{4\pi} \int \frac{e^{-X}}{X^2} dV, \text{ and represents the ratio of (1) the dose rate at P}$$

due to the given source, to (2) the dose rate that would be measured at a point within an infinite volume with the same source density. (In the expression for N, all distances are expressed in units of effective mean free path.) For points on the water surface,  $0 \leq N \leq 0.5$ . (The 0.5 value corresponds to a base surge with a semi-infinite volume.)

---

\*Three types of buildup factor, corresponding to the three types of spectra (photons, energy flux, or dose rate) may be defined by the equation expressing the ratio of total (scattered and unscattered) to unscattered numbers of photons, energy flux, or dose rate. The dose rate (or dose) buildup factor is:

$$B_1 = \frac{d_{1u} + d_{1s}}{d_{1u}}$$

where  $d_{1u}$  represents the dose (rate) from unscattered radiation and  $d_{1s}$  represents the dose (rate) from scattered radiation.

V = volume of the base surge that corresponds to the burst conditions considered (expressed in effective-mean-free-path units).

X = distance from P to element dV of the source of radiation, measured in effective-mean-free-path units.

$J_0$  = volume source density in Mev/cm<sup>3</sup> -sec.

Values for  $J_0$  are calculated by evaluating the expression

$$J_0 = \phi \frac{Y(1.5 \times 10^{23})E(t)}{V} \text{ Mev/cm}^3 \text{ -sec} \quad (17-7)$$

where

$\phi$  = the fraction of the total fission-product activity that is in the base surge. It has been assigned the values shown in Table 17-4 for optimum agreement with test data.

Y = weapon yield, in KT

V = base-surge volume in cm<sup>3</sup>

$1.5 \times 10^{23}$  = the number of fissions per kiloton of weapon yield

E(t) = the energy emission rate of the fission products<sup>51</sup>

$$= 2.78 t^{-1.23} - 2.41 t^{-1.45} \text{ Mev/sec-fission} \quad (17-8)$$

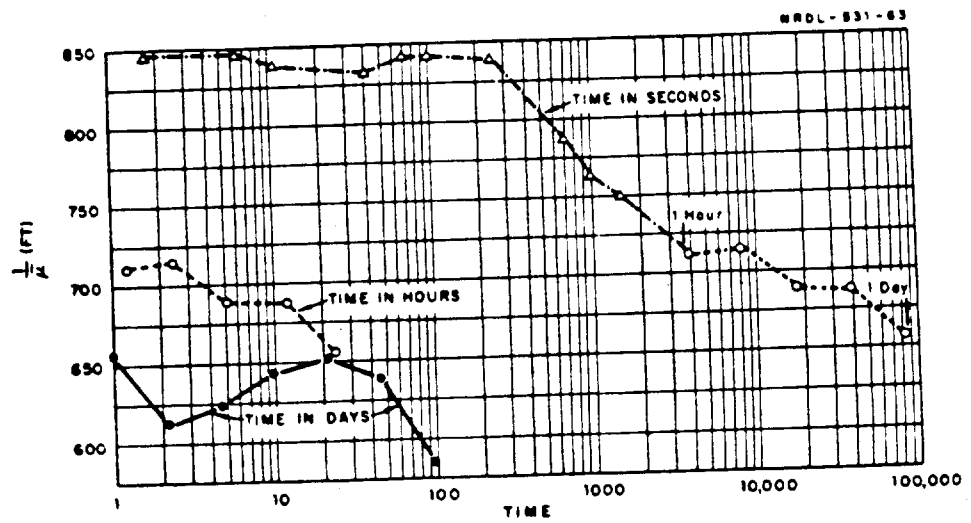


Figure 17-11. Effective mean free path as a function of time after fission.

Table 17-4. Fraction of fission products,  $\phi$ , assigned to base surge.<sup>48</sup>

Class of Burst	$\phi$
Very Shallow	$\frac{1}{10}$
Shallow	$\frac{1}{10}$
Deep	$\frac{1}{3}$
Very Deep	$\frac{1}{10}$

For Very-Shallow and Shallow bursts, the volume for the "hollow" base-surge geometry can be expressed

$$V_s = \pi Z \left[ (R_1 - R_2) - Z \cot \alpha \right] (R_1 + R_2) \quad (17-9a)$$

For Deep and Very-Deep bursts, the volume for the "solid" base surge geometry can be expressed

$$V_d = \frac{\pi Z}{3} \left[ 3R_1^2 - 3R_1 Z \cot \alpha + Z^2 \cot^2 \alpha \right] \quad (17-9b)$$

where (see Figure 17-10)

$Z$  = height of base surge

$R_1$  = outer radius of base surge

$R_2$  = inner radius of base surge

$\alpha$  = interior angle between each face of the surge and the base, or water surface.



For Deep bursts at increasing scaled depths approaching the Very Deep category, the transition between the two corresponding values of  $\phi$  will have to be determined by additional theoretical or experimental work.

Complete derivations of the mathematical forms of N for both deep and shallow bursts are presented in Reference 48. Summaries of the derivations are presented in the following paragraphs, along with Equations 17-10 to 17-12, which are explicit expressions for N. The dose rate, d, due to transit radiation from underwater bursts, can then be calculated by the substitution into Equation 17-5 of Equations 17-6 to 17-8, the appropriate form of Equation 17-9, and the suitable value of N as expressed by Equations 17-10, 17-11 or 17-12. Such calculations have been machine programmed at USNRDL.

(1) "Deep" Geometry

Consider a solid truncated cone, (Fig.17-10) of radius  $R_1$ , height Z, interior angle  $\alpha$  between face and base, with the base centered at O; and a receiver at point P in the plane of the base at a distance S from the axis of the cone. Then,

$$N = 1/4\pi \iiint \frac{e^{-\sqrt{r^2 + z^2}}}{r^2 + z^2} r dr d\alpha dz$$

where cylindrical coordinates are used with center at P, z-axis parallel to axis of cone and polar axis PO, and the integration is over the volume of the truncated cone. (All distances are expressed in mean-free-path units.)

To facilitate computation, the z-integration is replaced by a finite summation over n increments  $\Delta z$  where  $n \Delta z = Z$ . Let  $z_1$  be the midpoint of the  $i^{th}$  increment:  $z_1 = \frac{(2i + 1) Z}{2n}$ . In effect, the

truncated cone is replaced by a set of n circular disks of thickness  $Z/n$  and of radius  $R_1 - z_1 \cot \alpha$ ,  $i = 1, 2, \dots, n$ . Then,

$$N = 1/4\pi \sum_{i=1}^n \frac{Z/n}{r} \iint \frac{e^{-\sqrt{r^2 + z_1^2}}}{r^2 + z_1^2} r d\alpha dr.$$

The value  $n = 10$  was used in computing base surge dose rates. There are 2 forms for the integral depending whether  $S \leq R_1 - z_1 \cot \alpha$ , or  $S \geq R_1 - z_1 \cot \alpha$ . There are thus 3 cases for the summation over the entire volume:

**BEST AVAILABLE COPY**

1.  $S < R_1 - Z \cot \alpha$ .

$$N = \frac{Z}{2\pi n} \sum_{i=1}^n \left[ \pi \left\{ E_1(z_1) - E_1 \left[ \sqrt{(R_1 - z_1 \cot \alpha - S)^2 + z_1^2} \right] \right\} + \int_{R_1 - z_1 \cot \alpha - S}^{R_1 - z_1 \cot \alpha + S} \frac{e^{-\sqrt{r^2 + z_1^2}}}{r^2 + z_1^2} r \arccos \frac{r^2 + S^2 - (R_1 - z_1 \cot \alpha)^2}{2rS} dr \right] \quad (17-10)$$

2.  $S > R_1$ . Using similar procedures,

$$N = \frac{Z}{2\pi n} \sum_{i=1}^n \left[ \int_{S - (R_1 - z_1 \cot \alpha)}^{S + (R_1 - z_1 \cot \alpha)} \frac{e^{-\sqrt{r^2 + z_1^2}}}{r^2 + z_1^2} \arccos \frac{r^2 + S^2 - (R_1 - z_1 \cot \alpha)^2}{2rS} dr \right] \quad (17-11)$$

3.  $R_1 - Z \cot \alpha \leq S < R$ . Equation 17-9 applies to all terms in the summation from  $i = 1$  to the largest  $i$  such that  $S < R_1 - z_i \cot \alpha$ . Equation 17-10 applies to all terms in the summation from the smallest  $i$  such that  $S > R_1 - z_i \cot \alpha$  to  $i = n$ .

(2) "Shallow" Geometry

Consider a hollowed-out truncated cone (Fig. 17-10) with outer and inner radii  $R_1$  and  $R_2$ , height  $Z$ , interior angle  $\alpha$  between each face and base, and a receiver in the plane of the base at a distance  $S$  from the axis of the cone. Let the coordinate system be the same as in the deep case. Then, if the dose-rate ratio  $N$  for the solid truncated cone of the deep case is  $N(R_1, Z, \alpha, S)$ ,

$$N = N(R_1, Z, \alpha, S) - N(R_2, Z, \pi - \alpha, S) \quad (17-12)$$

for the hollow truncated cone.

BEST AVAILABLE COPY

### 17.5.5 Theoretical Calculations for Shielded Locations

It is desirable to know the interaction of a ship's structure with transit radiation in order to determine to what extent a ship will shield personnel from such radiation. Comparison of topside and below-decks weapons-test transit-radiation data which have been obtained simultaneously could provide such information. However, test data on below-decks transit-radiation exposures are insufficient to permit extrapolation to exposures from bursts of any yield and for any burst condition. Therefore theoretical methods of estimating such exposures or of calculating ship-shielding effects are necessary.

A below-decks transit-radiation exposure is due to the transmission through the ship's structure of gamma rays emanating from the airborne radiation sources surrounding the ship. To predict such exposures, it is necessary to know the source characteristics and the shielding effectiveness of the structural components of the ship. This effectiveness is a function of the amount and type of material between the point of interest and the external radiation source, the source-shield-receiver geometry, and the energy spectrum of the gamma radiation that composes the radiation field. Effectiveness, defined in terms of the shielding factor, is a dimensionless ratio of the gamma dose rate at the point of interest to that at a point of measurement in the external radiation field above the point of interest. A method has been developed for calculating the shielding factor without knowledge of the actual below-decks dose rate. Thus, it is possible to estimate the radiation attenuation at any below-decks location, or to calculate the dose rate at that location as the product of the shielding factor for the location and the topside transit-radiation dose rate, if the latter dose rate is known.

Present information is such that neither topside transit-radiation dose rates nor base-surge characteristics expected from water-surface bursts can be specified, since they have never been observed, as was noted in Section 17.5.2. Therefore, it is not feasible to calculate theoretically below-decks exposures due to such bursts. However, transit-radiation exposures from three underwater bursts have been measured, (Section 17.5.2) and the base-surge radioactive-source characteristics (the primary source of transit radiation) have been defined, with limitations, for underwater bursts, in general. In addition, a base-surge model exists (Section 17.5.4) that, for practical purposes, predicts topside exposures that agree with available data from underwater bursts. Therefore, it has been possible to develop theoretical methods for calculating below-decks transit radiation exposures for such bursts.

The general problem of computing ship-shielding factors involves:

- (1) specification of the geometric configuration and the radiation

**BEST AVAILABLE COPY**

energy spectrum of the radioactive sources; (2) specification of the major ship characteristics, particularly the shielding configuration for the point considered and the nature of the shielding materials; (3) development of methods for computing the interaction of the radiations with the ship.

Basically, the method presented of calculating ship-shielding factors for the transit dose (from a volume radioactive source surrounding the ship) is a point-by-point calculation. The radioactive source region is considered to be made up of an aggregate of point isotropic sources. The dose rate from each source is calculated at a given location by computing the radiation attenuation along the entire path length, and the total dose rate is found by summing over all sources. All the energies in each source spectrum as well as all the sources must be summed. In practice, the summation process is replaced, to whatever extent possible, by integration.

The theoretical development of ship-shielding calculations is based on an idealized concept of the interaction of radiations with a ship. The expression of the shielding factor for the transit dose was developed from the expression of dose rate due to a point source. For a point isotropic source emitting 1 photon/second of energy  $E_1$  (Mev/photon), the exposure dose rate  $d_1$  (r/hr) at a distance  $x$  (cm) from that source in a homogeneous medium can be expressed by:

$$d_1 = \frac{k \mu_{A1} E_1 B_1 e^{-\mu_1 x}}{4\pi x^2} \text{ r/hr} \quad (17-13)$$

where  $k$  = a factor to convert Mev absorbed in a  $\text{cm}^3$  or gm of the medium per second to r/hr.

If  $\mu_A$  is in units of  $\text{cm}^{-1}$ ,  $k = 5.086 \times 10^{-2}$  r/hr per Mev/ $\text{cm}^3$ -sec

If  $\mu_A$  is in units of  $\text{cm}^2/\text{gm}$ ,  $k = 6.6 \times 10^{-5}$  r/hr per Mev/gm-sec

$\mu_{A1}$  = the energy-absorption coefficient for air corresponding to the quantum energy  $E_1$

$B_1$  = the infinite-medium dose buildup factor\*

$\mu_1$  = the linear total absorption coefficient for the medium.

Then the exposure dose rate  $d$  (r/hr) at the same distance  $x$  (cm) from a point isotropic source emitting  $n_1$  (photons/sec) quanta of energy  $E_1$  (Mev/photon) in a homogeneous medium can be expressed as the sum of the exposure dose rates due to all the emitted energies:

\*This buildup factor is defined as the ratio of the dose from both unscattered and scattered radiation to the dose from unscattered radiations only.

$$d = k \sum_1 \frac{\mu_{A1} n_1 E_1 B_1 e^{-\mu_1 x}}{4\pi x^2} \quad r/hr$$

We can define

$$d_0 = k \sum_1 \mu_{A1} n_1 E_1 = \sum_1 (d_0)_1 \quad r\text{-cm}^2/hr \quad (17-14)$$

and

$$(d_0)_1 = f_1 (d_0) \quad (17-15)$$

where  $d_0$  = a symbolic dose-rate measure of source strength.

$f_1$  = the fraction of  $d_0$  due to the source energy  $E_1$ .

Goldstein and Wilkins<sup>52</sup> present a method of calculating the deep penetration of photons in infinite homogeneous media for point-isotropic or infinite uniform-plane mono-directional sources. This "Moments" method employs a different dose buildup factor for each energy and medium. Because of their complexity, the calculations were performed on a computer and the results are presented in both tabular and graphical form in Ref. 52. Differential energy spectra for point-isotropic and plane monodirectional sources for various energies from 0.5 to 10 Mev and for penetrations up to 20 mean free paths in several media, as well as buildup factors, are included.

To determine the exposure-dose rate and the shielding effectiveness of a ship at a below-decks location when the ship is enveloped by a base surge, the unshielded dose rate due to a monoenergetic point source (Eq. 17-13) must be extended to represent the corresponding dose rate due to a volume source, and then must be modified by a factor that accounts for the attenuation of the dose rate by the shielding afforded by the ship's structure. Finally, it must be summed over all emitted energies. The theoretical method that has been developed at NRDL for this purpose is based on an idealized concept that considers the exposure point shielded by a slab from a semi-infinite volume of uniformly-distributed radioactive point sources. The basic slab geometry considered in the mathematical derivation is that of a circular truncated cone, and numerical techniques are used to convert results for circular slabs of radius R to rectangular slabs that give the same dose-rate reduction. The conversion technique is explained in Ref. 53.

The basic dose-rate equation for the monoenergetic point source can be extended to express the volume-source case; that is, to express the exposure-dose rate at a perpendicular distance h below a slab of finite thickness and infinite extent, while an infinite radioactive volume source above the slab is emitting n (photons/cm<sup>3</sup>-sec) quanta of energy

$E_0$  (Mev/photon). The procedure is as follows:

$$d_{h\infty} = k\mu_{A_0} nE_0 \int_0^{\infty} \frac{Be^{-(\mu x)'}}{4\pi x^2} dv \quad r/hr \quad (17-16)$$

where  $nE_0$  = the source strength in units of Mev/cm<sup>3</sup>-sec

and  $x$  = distance (cm) from the exposure point to the incremental element of volume,  $dv$

$(\mu x)'$  =  $\mu_1 x_1 + \mu_2 x_2$  where  $x_1$  is the path length in air,  $x_2$  is the path length in the slab, and each  $\mu_j$  is the total linear absorption coefficient for the corresponding medium.

$B = B [E_0, (\mu x)']$  is the dose build up factor, as defined for Equation 17-13.

Further,  $d_0$ , a symbolic dose-rate measure of source strength may be written:

$$d_0 = k\mu_A nE_0 \quad r/hr\text{-cm} \quad (17-17)$$

Note the difference in units for  $d_0$  from a volume source (Eq. 17-17), and from a point source (Eq. 17-14). When the concept is used for a plane source in 17.6.5,  $d_0$  will have the units r/hr. This results from a difference in the significance of  $n$ , which has the units  $\frac{\text{photons}}{\text{sec}}$ ,  $\frac{\text{photons}}{\text{cm}^3\text{-sec}}$  and  $\frac{\text{photons}}{\text{cm}^2\text{-sec}}$  respectively. (See also footnote after Equation 17-27, Section 17.6.4.)

Then the exposure dose rate at the exposure point shielded by a slab of infinite radius is defined by:

$$d_{h\infty} = d_0 \int_V \frac{Be^{-(\mu x)'}}{4\pi x^2} dv \quad r/hr \quad (17-18)$$

However, ships are not infinite in extent. The slab of shielding represents a ship's structure above the exposure point, and, in general, is composed of a number of slabs of different sizes and thicknesses (corresponding to a ship's decks and plating and determined by the location of the exposure point). Therefore, the slab must be bounded, and for the idealized conditions of the problem, the individual slabs are considered contiguous and are treated as a single whose total thickness equals the sum of the thicknesses of the individual slabs. Although the shielding slabs are rectangular, it was found more feasible to calculate the shielding effectiveness in terms of circular slabs that

**BEST AVAILABLE COPY**

provide the same shielding. Factors for converting circular slabs to equivalent rectangular slabs are presented graphically in Ref. 19. Further, it is necessary to integrate over the source region to find the exposure dose rate for any constant thickness of absorber.

It was found possible<sup>53,55</sup> to express the results of Goldstein and Wilkins for the dose buildup factor, B, of Eq.17-13, for any given medium and quantum energy, by an expression of the form.

$$B = \left[ 1 + a(\mu x) + b(\mu x)^2 \right] e^{c(\mu x)} \quad (17-19)$$

The constants, a, b, and c may be related to the quantum energy E, and evaluated for various media. Values of the constants for buildup in iron and air or water are given in Ref. 55, Table 2. An expression of the form of Eq.17-19 makes it possible to integrate over a source region, since the buildup factor has analytic form and the resulting expression is integrable. The integrated expression for exposure dose rate due to sources distributed in a volume of air or water beyond the surface of a circular slab is given in Ref. 54. For simplicity of notation, the integral forms will be used in the remainder of this discussion.

Then the dose rate at an exposure point shielded from the volume source by a finite circular slab of radius R may be expressed:

$$d_{hR} = d_0 \int_0^R \frac{B e^{-(\mu x)^c}}{4\pi x^2} dv \quad (r/hr) \quad (17-20)$$

Explicit calculation of the dose rate at a shielded location in every case involves knowledge of the source strength,  $d_0$ , a quantity that may not be known. However, the shielding effectiveness of the location is expressed in terms of an attenuation factor, or shielding factor, representing the ratio of dose rate at a shielded location to that at an unshielded location (approximately over the exposure point and usually considered to be 3 ft above the slab (deck)). In such ratios, the source strength,  $d_0$ , cancels. Although shielding factors do not provide actual dose or dose-rate values for below-decks locations, it is frequently desirable to evaluate the shielding factor for a given location to determine the degree to which the ship's structure would attenuate transit radiation. The following ratios are used in practice to evaluate the shielding factor:

**BEST AVAILABLE COPY**

$$SF = \frac{d_{hR}}{d_{3R}} = \left[ \frac{d_{h\infty}}{d_0} \times \frac{d_{hR}}{d_{h\infty}} \right] \div \frac{d_{3R}}{d_0} \quad (17-21)$$

where  $d_{h\infty}$ ,  $d_0$ , and  $d_{hR}$  are defined in Eqs. 17-16, 17-18, & 17-21, and  $d_{3R}$ , the dose rate at a point 3 ft above the finite slab, may be expressed:

$$d_{3R} = d_0 \left[ \int_0^R \frac{Be^{-(\mu x)'} }{4\pi x^2} dV \right]_{h=-3} \quad (r/hr) \quad (17-22)$$

It is apparent that, when Eqs. 17-16 to 17-19, 17-21 and 17-22 are used, the dose-rate ratios have the following equivalences:

$$\left. \begin{aligned} \frac{d_{h\infty}}{d_0} &= \int_0^{\infty} \frac{Be^{-(\mu x)'} }{4\pi x^2} dV \quad (cm) \\ \frac{d_{hR}}{d_{h\infty}} &= \frac{\int_0^R \frac{Be^{-(\mu x)'} }{4\pi x^2} dV}{\int_0^{\infty} \frac{Be^{-(\mu x)'} }{4\pi x^2} dV} \\ \frac{d_{3R}}{d_0} &= \left[ \int_0^R \frac{Be^{-(\mu x)'} }{4\pi x^2} dV \right]_{h=-3} \quad (cm) \end{aligned} \right\} \quad (17-23)$$

Reference 54 presents curves of the quantities needed to find the shielding factors for various  $h$  and  $R$  values. Note that Reference 54 uses the following symbols:

**BEST AVAILABLE COPY**



$I_{\infty}$  instead of  $d_{h\infty}$

$I$  instead of  $d_{hR}$

$I_0$  instead of  $d_0$

The computation of  $d_{hR}$  in general involves three steps: (1) the calculation for radiation received from above (through the decks); (2) and (3) the radiation coming through the sides of the ship. In the present method, actual deck and bulkhead thicknesses measured from ship's plans are multiplied by an empirical factor of 2 to take into account machinery and piping.

The evaluation of the integrals of Eq. 17-23 for all the energies in the source spectra would be an exceedingly lengthy task, even when machine-computed. It has been found practicable to minimize computations by replacing the large number of energies (as many as 171)<sup>56</sup> actually present with "pseudospectra" derived from the fission-product spectra.<sup>57</sup> The pseudospectra for given times after fission and a given radiation-source configuration consist of only 5 energies: 0.25, 0.40, 0.75, 1.25, and 2.75 Mev. Each of these energies is weighted in such a way for each time, as to give virtually the same attenuation (absorption and scattering) as the more complex actual spectrum would give. The weighting fractions for the five (5) energies and for three (3) times after fission (70 sec., 1.12 hr, 23.8 hr) and for iron and air or water are given in Ref. 57. The details of the theory and method of evaluating the integrals are presented in Ref. 53, along with the limitations of the results of the calculations. It is pointed out in Ref. 53 that the major limitations arise from the use of a buildup factor to account for the dose-rate contribution of photons scattered one or more times in the attenuating media before reaching their receiver. The calculations of unscattered flux are exact, but the calculations of scattered flux rely on the infinite-medium buildup factors of Goldstein and Wilkins.<sup>52</sup> These buildup factors are stated by the authors to be accurate, probably within  $\pm 10\%$ . However, in this method of calculating ship-shielding factors, they are applied to finite media, and it is assumed that slabs that are actually separated (as ship decks) behave in the same way, with respect to attenuating scattered radiations, as a single slab having the same total thickness. It is estimated that the errors in the slab calculations will be small compared to the uncertainties and errors introduced in attempting to idealize the ship structure, the geometry, and the characteristics of the radiation sources.

**BEST AVAILABLE COPY**

Results of machine computations have been plotted graphically to permit evaluation of the ratios of Eq. 17-23 for a range of slab thicknesses and exposure point locations. These graphs are given in Ref. 54 for the five (5) pseudospectrum energies, along with the ratios that permit conversion of circular to equivalent rectangular slabs.

To illustrate the results of shielding calculations from airborne activity, Figs. 17-12 to 17-15 (reproductions of Figs. 7 to 10 of Ref. 55) are included. The shielding factor is plotted vs total decking thickness for a number of locations within USS RANGER (CVA-61). The monoenergetic calculations have been weighted in accordance with the pseudospectra for unfractionated U-235 fission products at 70 sec and 1.12 hr after fission. Two sets of calculations were made for each time, one set using only the nominal plating thicknesses ( $t$ ) to give a minimal estimate of the shielding, and the other set using twice the plating thicknesses ( $2t$ ) to give expected shielding factor values. As indicated in Ref. 55, for airborne activity a considerable portion of the incident radiation penetrates through the side of the ship rather than through the weather deck. Therefore, the correlation of shielding factor with total plating thickness overhead is not an accurate measure of the radiation attenuation. However, it represents the best yardstick currently available.

#### 17.5.6 Effect of Geometry at Unshielded Locations

No data are available either from water-surface bursts or the earlier underwater bursts to establish experimentally the effect of the geometry of the ship or of the aerosol on transit-radiation levels at unshielded locations. However, analysis<sup>32</sup> of shipboard data from the Hardtack shots "indicates that the ship's superstructure has a detectable influence on the total gamma dose.... Because of the paucity of GTR data, the analysis was based on doses registered on film packs" (fixed at various locations in the ship). Furthermore, "the gamma records resulting from the passage of airborne radioactive material are sufficiently characteristic that records from shots Wahoo and Umbrella can usually be distinguished by inspection, particularly at downwind location." The differences in the records are due to differences in the geometries of the base surges resulting from the two shots.

Film packs were located at various frame numbers, on both sides of the ships (toward and away from surface zero). According to Ref. 32, plots of film-pack doses vs frame number, for both shots, show a fairly consistent difference between film pack doses on the opposite sides of the closer ships, a difference consistent with the attitude of the ship. In general, film packs on the side of the ship toward surface zero registered significantly higher doses than those on the side away from surface zero. In addition, the same plots give a characteristic curve shape for each ship, regardless of the ship's attitude

**BEST AVAILABLE COPY**

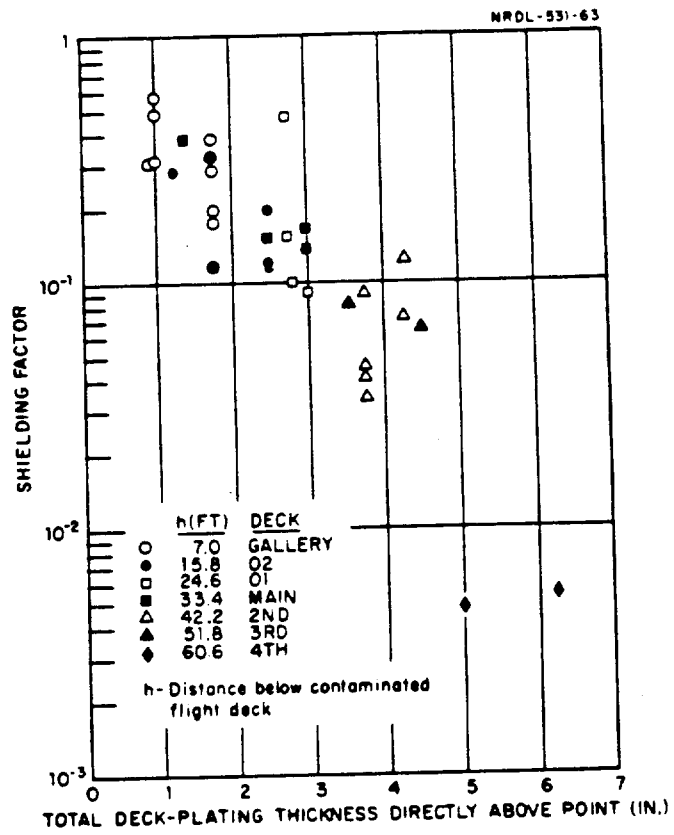


Figure 17-12. Minimal shielding (1t) calculations, USS RANGER, airborne activity 70 seconds after fission.

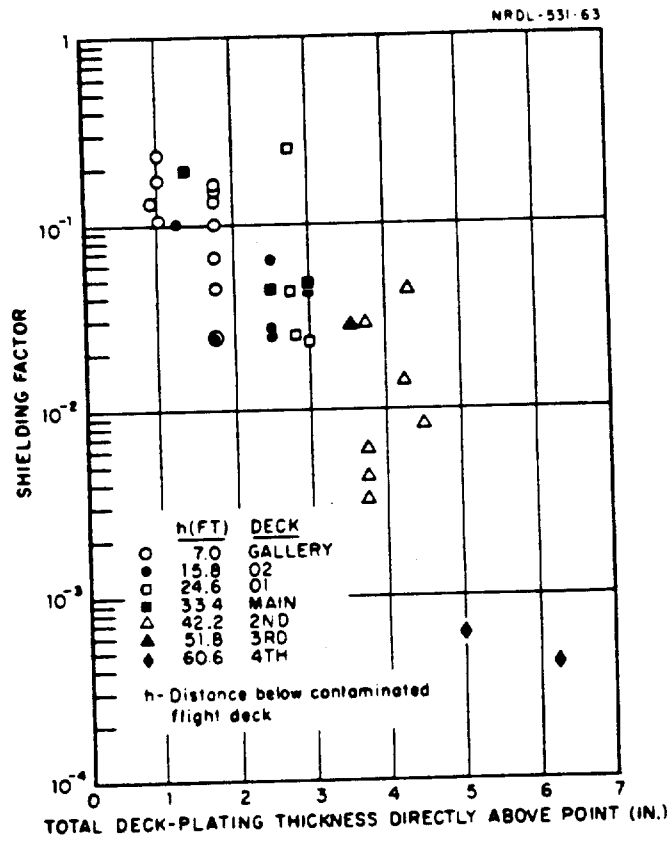


Figure 17-13. Expected shielding (2t) calculations, USS RANGER, airborne activity 70 seconds after fission.

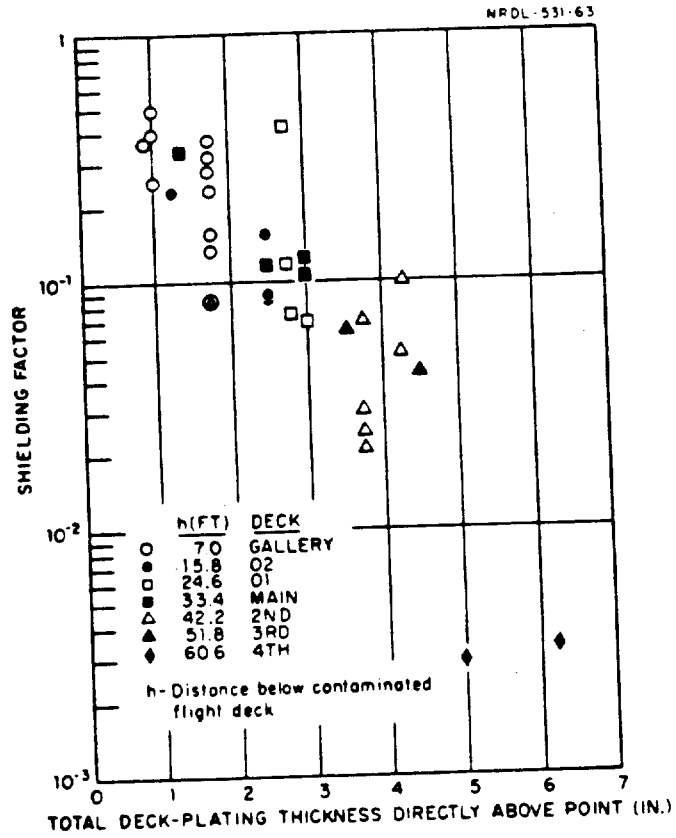


Figure 17-14. Minimal shielding (1 t) calculations, USS RANGER, airborne activity 1.12 hours after fission.

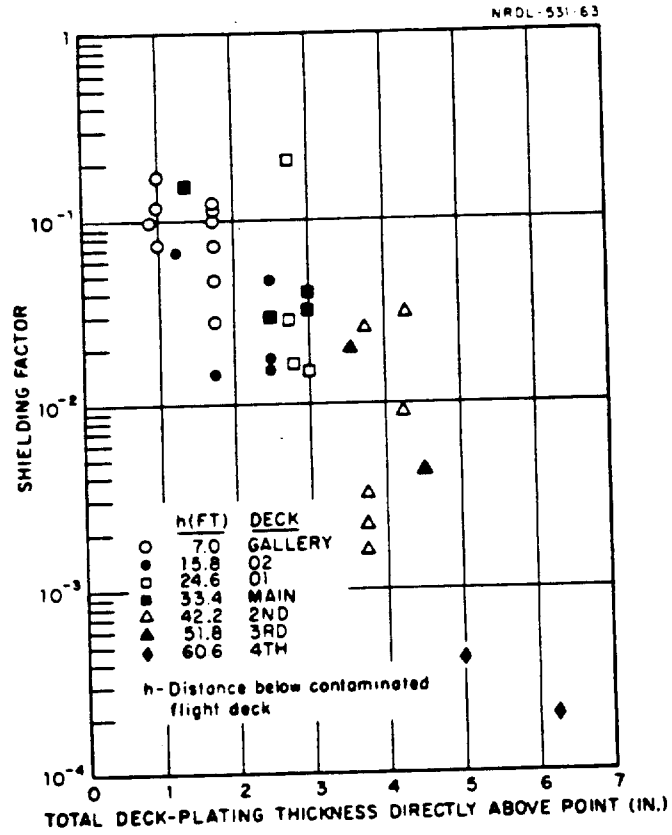


Figure 17-15. Expected shielding ( $2t$ ) calculations, USS RANGER, airborne activity 1.12 hours after fission.

or distance from surface zero. The regularity of the curve shapes is definite evidence of superstructure effect. It was found that "the total solid angle of unshielded base surge subtended by an absorbing volume bears a direct relationship to the total dose received." The average of film-pack doses for the platform film packs, and even for completely unshielded positions on the superstructure decks is high, because of the large solid angle subtended at the films due to their elevated positions. Where even a relatively thin section of the superstructure subtended more than 10% of the total solid angle (at the film), an approximate shielding factor was estimated, using the ship's plans and a gamma energy of 1 Mev. The calculation of shipboard doses from free field isodose contours requires the use of "conversion factors" that compensate for superstructure shielding. Such factors were calculated from film pack and GTR data for exposures aboard the target ships at Shots Wahoo and Umbrella, and are given in Table 3.33 of Ref. 32. The individual factors vary from a low of about 0.15 (for an exposure dose at frame 100 along the centerline of the superstructure deck of the DD474 for Shot Wahoo) to a high of 1 for an exposure dose between frames 120 and 130 on the superstructure deck of the DD592 at Shot Umbrella. The average variation of the factors (on the same ships) from the mean for both shots lies between 4% and 14%. It is suggested in Ref. 32 that use of the conversion factors may be extended to inner compartments, but that it is impossible to estimate the true accuracy of the procedure; therefore, the conversion factors should be used with caution, particularly in the case of moving ships. Conclusions<sup>32</sup> state that a reduction equal to a factor of 2 or greater in weatherdeck dose, due to superstructure shielding, was observed at certain locations.

The different geometries of the base-surge radiation fields for the two shots were responsible for the differences in gamma dose-rate records. Interpretation of the photographic data<sup>49</sup> indicates that at Shot Wahoo, there were probably both a primary and a secondary base surge. The passage of the two surges caused numerous significant peaks in the downwind dose-rate histories.<sup>32</sup> The Shot Umbrella base surge appears to have formed a single ring relatively clear of airborne radiation material at its center,<sup>49</sup> and in most cases the Shot Umbrella records contain a single high peak in dose rate followed at a later time by a prolonged and relatively low increase in dose rate.<sup>32</sup> The differences between the Wahoo and Umbrella records indicate that depth of burst has a pronounced influence on the radiation fields produced, but it is impossible at this time to extrapolate from these two documented cases to predictions of effects of bursts at other depths, particularly since more pronounced differences probably occur as the depth of burst approaches zero. However, this effect has been taken into account in an approximate way in the base-surge model discussed in Section 17.5.4, The Model of Reference 48.

### 17.5.7 Effects of Transit Radiation on Electronic Equipment

It was decided to investigate the effects of transit radiation on electronic equipment because weapon-test data indicated that initial radiation might affect such equipment. Experiments carried out at USNRDL<sup>58</sup> indicate that malfunction of certain electronic equipment is probable and failure of the equipment is possible, as a result of exposure to high-level transit gamma-radiation. Components, such as photomultiplier tubes and semiconductors, were irradiated with laboratory-produced gamma rays having simulated intensity-time characteristics of the base surge of Shot Wahoo. It was determined that, in particular, semiconductors of the germanium type were significantly affected by doses of about 2000 r delivered under such conditions. It was concluded from the laboratory experiments that, for equipment currently in use (designed 4-5 years ago when transistors were used conservatively), complete failure is not likely; however, reliability and accuracy may be reduced as a result of such gamma irradiation. No quantitative assessment of the extent of the reduction is available at this time. It has been further estimated that, in some cases, the more completely transistorized equipment manufactured currently may fail completely. Examples where such dangers occur are in those circuits where exact frequency control is essential, where diode-controlled reference voltages must be maintained accurately, and where high-impedance circuitry is used.

### 17.5.8 Summary

No weapons-test data exist upon which to base conclusions regarding the gamma dose rates due to transit radiation at early times after water-surface bursts. The target ships that were sent into the fallout areas at the surface-burst tests did not contact any contaminant earlier than an hour after detonation, by which time any base surge (if it existed), the major source of transit radiation, would have completely dissipated. During fallout, at an hour or more after detonation, the transit-radiation contribution to the total recorded weather-deck dose was estimated to be of minor significance, particularly in comparison with the deposit dose on a ship not protected by washdown.

Data from Shots Wahoo and Umbrella indicate that on ships with the wash-down system in operation, for underwater bursts that break through the surface with no more than one bubble expansion, radiation doses were due primarily (between 95 and 98%) to transit radiation. Doses from 300 to 1000 r may be expected within the first 15 min after burst at completely unshielded locations on the weather decks of ships that are stationary from about 2000 ft upwind to about 9000 ft downwind of surface zero. At some weather-deck locations, the superstructure affords sufficient shielding from base-surge radiation to reduce the free-field dose by a factor of 2 or more. Data also indicate that the transit-radiation doses at below-decks locations in destroyers may vary from about 2% of the weather-deck

**BEST AVAILABLE COPY**



dose to as high as 70% of the weather-deck dose for a well-shielded location, and for a lightly shielded location, respectively.

No theoretical models have been developed for estimating transit radiation from water-surface bursts, primarily because the early phenomenology of such bursts (that is, the magnitude and distribution of activity in the base surge) has never been reliably defined. Several theoretical models have been developed for estimating transit-radiation dose rates and doses from underwater bursts. The "radiological model" presented in Section 17.5.4 does not define the actual physical shape of the base surge, but use of the model does permit approximate calculation of transit-radiation doses at any specified surface location, for underwater bursts of 1-to 100-KT yields. Calculated results are in good agreement with measurements taken at Shots Wahoo and Umbrella. Several methods of calculating gamma doses at shielded locations have been developed, and the method referenced in Section 17.5.5 is one of the most recent. Certain features of several earlier systems are incorporated, along with the latest theoretical efforts to account for the spectral distribution of the various energies at the exposure point and for the scattering characteristics of the various energies involved and the media penetrated.

Experiments have been carried out recently at USNRDL, to investigate the penetration of an aircraft carrier by a distant gamma-ray source.<sup>59</sup> Doses were measured in many below-decks spaces of a light aircraft carrier, using a  $\text{Co}^{60}$  source with various angles of incidence at distances of 80 to 100 ft, to simulate the radiation from a base surge. Such experiments permitted measurements of the attenuation of the gamma radiation, by ship shielding. No comparisons have yet been made between these experimental results and theoretically calculated results.

**BEST AVAILABLE COPY**

## 17.6 DEPOSIT RADIATION

### 17.6.1 Introduction

"Deposit radiation" was defined (Sec. 17.3.2) as "the radiation due to radioactive materials, particularly radioactive fallout particles that may deposit on a ship's exterior (or some interior) surfaces." Deposit radiations include both gamma rays and beta particles emitted by the radioactive deposited material, and may also include gamma rays emitted from neutron-induced activities. Assessment of the effects of the gamma radiation is based on the dose or time-integrated dose rate received at the exposure point. Thus, all available weapons-test data on residual gamma-dose and dose-rate can be of value either (1) in devising scaling techniques or (2) as guidance for calculational techniques that would permit estimation of either gamma dose or dose-rate histories due to deposit radiation at various ranges from surface zero for detonations of any yield. Beta particles have only a limited range in air (up to about 10 ft), and the range decreases so rapidly with increasing density of medium traversed that the average distance a beta particle of given energy can travel in water, wood, or body tissue is roughly 1/1000 of that in air. Thus, there will be no transmission through the steel of a ship (of still greater density than water or wood) of the beta particles emitted by the deposit radiation. However, beta radiation can affect personnel if beta activity is deposited on the skin or ingested. Those effects of beta radiation will be considered in Chapter 18, where radiation effects on personnel are discussed.

Deposit gamma-radiation dose and dose rate are functions of the photon energy emitted by deposited radioactivity. This emitted energy will depend on the time after burst and on the composition of the deposited material, which may differ not only with weapon composition, but also with the location of the detonation point with respect to the water surface. Furthermore, the amount of deposited activity remaining on board a ship will depend on whether shipboard countermeasures, such as washdown, are used, and on the effectiveness of the countermeasures for the particular deposited material.

It is expected that the deposited radioactivity from a true surface burst (at the surface of deep water and with no ship involvement) would result from (1) "slurry" fallout droplets composed of water, sea-salt, and weapon materials, and perhaps (2) some contaminated droplets from the base surge. Evaporation of such fallout probably would leave a residue invisible to the unaided eye.

All available data on fallout from water-surface bursts are for barge shots over comparatively shallow water, which are not true water-surface bursts. Droplets of slurry fallout from all the barge shots have been analyzed,<sup>60</sup> and as a result of the analysis have been defined

as "drops of saturated solution of sodium chloride in water, containing in suspension crystals of sodium chloride and small radioactive spheres ...ranging in size from about 50 to 250 microns in diameter."<sup>60</sup> The analysis has also indicated traces of sea-bottom material and iron and coral ballast from the shot barge.<sup>60</sup> However, these insoluble materials appeared in sufficiently minute quantities that the fallout could still be characterized as slurry (expected from water-surface bursts) and not as solid-particulate contaminant (characteristic of land-surface bursts), which leaves a visible residue.

The deposited material from underwater bursts in deep water is expected to be very similar to that from water-surface bursts. If the burst involves a ship, the fallout particles would probably include vaporized ship materials, while if the burst were in shallow water, ocean-bottom materials would be included in the fallout particles, which might leave a visible residue. Tests have indicated<sup>61</sup> that wash-down removes the "wet mist" type of fallout more effectively than the particulate type.

#### 17.6.2 Weapons-Test Data for Unshielded Locations

##### 1. Water-Surface Bursts

Operation Castle: Efforts were made to document the characteristics of the radioactive fallout resulting from three of the lagoon barge shots of Operation Castle. Gamma dose rates at 1 hr at the islands close to surface zero were estimated<sup>62</sup> to be as high as 4700 r/hr for Shot 2, 440 r/hr for Shot 4, and over 1000 r/hr for Shot 6. Insufficient fallout material from Shots 4 and 6 was gathered in the close-in incremental fallout collectors for a meaningful particle analysis; however, considerable activity was exhibited by the liquid samples gathered in the 30-min collectors at Shot 4.<sup>62</sup> At Shot 2, millipore filters exposed topside on the YAG 39 test ship were intensely radioactive and indicate that the activity probably arrived in the form of liquid droplets.<sup>63</sup> It was estimated that the fallout from Shot 2 arrived as a fine mist at the stations 50 nautical miles downwind, since the identification flags on the free-floating sea stations were more highly radioactive than the total fallout collections at the same stations. A moist fallout would be absorbed by flapping flags more easily than a dry particulate.<sup>64</sup>

Except for patches of chalky substance (of high intensity) on the windward surfaces of aircraft on the YAG 40 test ship, following Shot 2, no visible deposited material was found on the test ships. However, fallout was collected on special filters and on a film by electrostatic precipitation. Studies of the filters and film and their autoradiographs showed that the fallout consisted of microscopic solid crystals and small droplets. Small particles less than 10 microns in diameter appear to have arrived at the earth's surface in the solid or semiliquid state; in

**BEST AVAILABLE COPY**

[REDACTED]

addition, fallout included liquid drops having a range of size up to several millimeters in diameter. The presence on the filters of many particles invisible under the microscope was indicated by the autoradiographs. It was concluded that the bomb debris mixed to some extent with the large amount of sea water and the relatively small amount of coral that were taken into the fireball.<sup>64</sup> In addition, although no gross fallout was photographed on the YAG 40, small sparsely-spaced particles were photographed intermittently, following Shot 5.<sup>40</sup>

Fallout dose and dose-rate measurements were also made on the two test ships, the YAG 39 (with the washdown operating) and the YAG 40 (unprotected), which were guided (some distance apart) by remote control through the fallout regions of the detonations.<sup>40</sup> Following Shot 4, the maximum average cumulative dose up to 5 hr on the unprotected YAG 40 flight deck was almost 100 r. Less than 10% of that dose was recorded for a similar location on the YAG 39, with washdown in operation. The highest cumulative doses were recorded at 11 hr after Shot 5, when an average dose of almost 500 r was recorded on the YAG 40 main deck forward. Less than 10% of that dose was recorded for a similar location and exposure time on the washed YAG 39. At 2 hr after Shot 4, peak dose rates of 40 - 50 r/hr were recorded on the YAG 40, whereas dose rates on the YAG 39, with washdown in operation, were reduced to less than 10% of those on the unprotected ship. Following Shot 5, dose rate averages on the YAG 40 flight deck peaked at between 80 and 90 r/hr at about 3 hr after shot, while dose rates on the YAG 39 were again less than 10% of those on the YAG 40. The portion of the total dose due to deposited activity or to airborne activity is questionable. Castle data indicated that the transit dose was of minor significance on an unprotected ship, since about 95% of the total dose recorded on the weather deck of the unwashed YAG 40 was estimated to have been due to deposited activity. For bursts of this type, washdown appeared very effective in removing activity deposited on the YAG 39 decks, since only half the total dose accumulated at the end of fallout on the washdown-protected ship was estimated to have been due to the deposit dose.<sup>40</sup>

Operation Redwing: Data are available on fallout from only two of the barge shots, and from Shot Tewa, which was almost a land-surface shot, since it was on a reef where the water was only 25 ft deep. Data are also available from Shot Zuni, an island-surface shot. Characterization<sup>42</sup> of the fallout indicated that all the fallout collected from barge shots Flathead and Navajo consisted of slurry particles, whose inert components were water, sea salts and a small amount of insoluble solids, principally oxides of calcium and iron. The diameters of the spherical slurry droplets at time of arrival ranged from 57 to 121 microns for Flathead, and from 75 to 272 microns for Navajo. Nearly all the active fallout collected from Shot Tewa

**BEST AVAILABLE COPY**

[REDACTED]

consisted of solid particles, with an insignificant number of slurry particles revealed by microscopic examination. The fallout analysis of Ref. 42 was not of close-in fallout, since the samples used were collected on the support ships, which were 20 miles or more from surface zero.

Shipboard fallout measurements were made at Operation Redwing<sup>41, 61</sup> during maneuvers (similar to those at Operation Castle) of the YAGs through the predicted fallout areas. Since the ships were manned, low-activity areas were traversed, and instead of one ship with washdown and one without, each ship was equipped with a partial washdown system. Therefore, more accurate appraisals could be made of washdown effectiveness than was possible at Operation Castle where the two ships were, of necessity, some distance apart and hence experienced somewhat different fallout conditions.

During the Shot Flathead operation,<sup>61</sup> the YAG 40, at 40 miles north of surface zero, intercepted slurry-type fallout at H + 8.2 hr, and remained in fallout until H + 23.7 hr. As the ship maneuvered, a peak value (in time) of the average (over the deck) dose rate of 0.011 r/hr was recorded at H + 17 hours on the washed area of the main deck, while a "peak mean" dose rate of 0.266 r/hr was recorded on the unwashed area of the main deck. A similar washdown effectiveness is demonstrated by the mean total accumulated dose of 0.126 r recorded by 23.7 hours on the washed area, while 3.04 r was recorded in the unwashed area. Thus, results observed at Operation Castle were confirmed, since the average dose and dose rate in the washed area were less than 10% of that in the unwashed area. It should be noted that the average dose in the unwashed area<sup>41</sup> had increased to about 6 r at 48 hr, when the ship returned to base.<sup>41</sup>

During the Shot Navajo operation,<sup>61</sup> the YAG 39, at 22 miles north of surface zero, intercepted fallout of salt-water slurry at H + 2.4 hours, and remained in the fallout area till long after fallout cessation, which occurred at about H + 13.4 hr. A peak mean dose rate of 0.177 r/hr was recorded on the washed area of the main deck at H + 6 hr, a value significantly lower than the unwashed-area peak mean dose rate of 1.4 r/hr. The accumulated mean gamma deck doses recorded at the end of washdown (at 9.4 hr) were 0.721 r and 5.48 r in the washed and unwashed areas, respectively, whereas at the end of fallout (at 13.4 hr), mean total doses of about 1.0 r and 7.5 r were recorded in the washed and unwashed areas respectively. Apparently, washdown was not as effective in removing the fallout from this shot as it was in the other cases, probably because the system was operated intermittently, since it was necessary for personnel to be on deck at several times during the maneuvers. The average dose on the unwashed area increased to about 10 r, recorded by about 43 hr.<sup>41</sup>

BEST AVAILABLE COPY

Notes

DNA 1240H-2

*Compare this to fallout patterns in the area of the YAG 40 to the end of washdwn at H + 15.2 hours was 49.3 r, while in the washed area, a total of 10.3 r was recorded.<sup>42</sup> The recorded dose in the unwashed area increased to 100 r by about 5 1/2 hr, indicating the effect of the deposited activity. Furthermore, it is estimated from the records in Ref. 41, that the deposited activity contributed about 95% of the total radiation dose recorded by 24 hr on the unwashed weather deck, an estimate in agreement with that of Operation Castle.*

## 2. Underwater Bursts

Operation Crossroads, Shot Baker: It was estimated<sup>29</sup> that deposit dose composed about 50% of the total radiation doses registered by film badges at exposed locations on ships at Shot Baker, and the remainder of the dose was attributed to transit radiation from the base surge. It was further estimated<sup>29</sup> that residual activity was deposited on the ships by rainout from the mushroom head of the cloud, in a ring whose radius was slightly less than 1000 yards from surface zero. In the ring, the mean total dose level due to deposited material was 4000 r, of which 3500 r was attributed to fallout from the mushroom cloud. In the center of the ring, deposit doses ranged down to below 1000 r. Table 1 of Enclosure J of Ref. 65 gives calculated estimates of first-hour doses (based on dose-rate readings) from material deposited on target ships. The ships were located at ranges varying from 500 to 2000 yards around surface zero, and first-hour dose estimates varied from 140 r, aboard the LCI-332 at 2000 yards E of surface zero, to 3850 r on the Pensacola at 500 yards SW of surface zero.

Operation Hardtack: Large base surges were generated by Shots Umbrella and Wahoo, but no visible fallout occurred. Weather-deck dose and dose-rate data were obtained principally for Shot Umbrella, due to power failures on two test ships at Shot Wahoo. All the test ships were within 2 to 3 miles of surface zero.<sup>33</sup> Dose and dose-rate data were also obtained from the coracles, most of which were within 2 miles of surface zero, although a few were positioned at more than 4 miles from surface zero. During Shot Wahoo, 11 of the 18 coracles broke moorings. Their positions during the time of principal interest did not change more than 300 ft, although before recovery, several drifted 4 to 12 miles.<sup>32</sup> It was concluded in Ref. 33 that practically no material was deposited aboard the test ships, since the dose rates fell from extremely high to extremely low values with the passage of the base surge, and very little dose was accumulated after the first few minutes. However, of the samples collected in the AFI (air filtration instrument) in 2- and 10-minute intervals,<sup>32</sup> the first samples in both series from Umbrella were heavily loaded with visible residue resembling pulverized coral. There was also evidence that heavy liquid deposition associated with radioactive material occurred during the first few minutes.<sup>32</sup> Air

**BEST AVAILABLE COPY**

samples were also collected in test compartments following Shot Umbrella,<sup>66</sup> and analysis of the samples indicated that 90% to 95% of the activity in the samples was due to particles with radii of less than 1 micron. It was demonstrated at previous tests that washdown is very effective with small particles carried in an invisible mist, and washdown was operating on the test ships at both shots. Thus, it is possible that had washdown not been operating, radioactive material might have been deposited and remained on the weather decks of the test ships. No data were obtained at distances such as 10 to 20 miles from surface zero, to permit "scaled" comparison with data from the barge shots of previous operations.

Operation Wigvam: The YAG-39 encountered an invisible cloud of airborne radioactive material between H + 16 and H + 19 min. Residual contamination was left on the ship, but decay and the washdown system reduced the radiation levels quite rapidly, so that at H + 1 hr, the average gamma dose rate on the weather deck was about 9 mr/hr. The YAG-40 avoided the "cloud," and made numerous traverses of the contaminated area on D and D + 1 days, but encountered no fallout. It was estimated that very little residual activity remained on the hull of the ship.<sup>31</sup>

### 17.6.3 Weapons-Test Data for Shielded Locations

#### 1. Water-Surface Bursts

Operation Castle: A study was undertaken to obtain data on the effectiveness of ships' structures in shielding interior compartments from gamma radiations during and after a contaminating event. Data for this study were obtained from Shots 2, 4, and 5, and the recorded dose and dose-rate values at exterior and interior locations on the test ships are presented graphically in Chapter 2 of Ref. 40. Results of analysis of the data, presented in Chapter 3 of Ref. 40, indicate that the shielding factor (the dimensionless ratio of the dose rate or dose within a compartment to that measured above the weather deck) at locations between the 2nd deck and weather deck were in the range from 0.1 to 0.2 on YAG 40, and from 0.15 to 0.30 on the washdown-protected YAG 39. In superstructure compartments on both ships, the shielding factors generally were in the range from 0.1 to 0.6. It was pointed out that the shielding factor actually represents shielding from all sources of radiation - transit, deposit, and water-borne. However, it was concluded that "shielding factors on the YAG-40 are believed to be a good approximation to the shielding factors for activity deposited on the deck surfaces."

Operation Redwing: Dose and dose-rate values recorded at exterior and interior shipboard locations for the Operation Redwing shots indicate the extent to which the ships' structures attenuated the gamma radiations emitted by radioactive material surrounding and deposited on the ships. The dose to 30 hr in the upper No. 2 hold of the YAG 39 was

**BEST AVAILABLE COPY**

15% of the average unwashed weather-deck dose, for both Shots Flathead and Navajo, and was 15 to 17% of the weather-deck doses recorded at Shots Zuni and Tewa. Zuni was a land-surface shot, and Tewa was detonated on the edge of a reef, involving a little water. The average unwashed-deck dose up to 30 hr on the YAG-39 varied widely in magnitude for the four shots (0.4 r at Zuni, 2 r at Flathead, 9.5 r at Navajo, and 190 r at Tewa). On the YAG-40, where the unwashed-deck doses to 30 hr also varied greatly (65 r at Zuni, 4 r at Flathead, 1.5 r at Navajo and 85 r at Tewa), the doses in the upper No. 2 hold were between 7% and 12% of the unwashed-deck doses.<sup>41</sup>

The shielding factors quoted in the preceding paragraph probably closely approximate ship shielding against activity deposited on the deck surfaces, although they were calculated on the basis of average total deck doses. The basis for the preceding statement is derived from data in Refs. 41 and 61. It is estimated from data obtained for Shot Tewa that about 95% of the average accumulated dose to 30 hr on the unwashed deck of the YAG-39 was due to deposited activity, and about the same proportion held for the YAG-40 deck dose for Shot Zuni. Thus, for those two shots, it is estimated that in the upper No. 2 hold, the ships' structures shielded out about 85% of the radiation from activity deposited on the weather-deck surfaces. Although the airborne-and deposit-radiation proportions of the total deck doses recorded for Flathead and Navajo were not estimated, it seems reasonable to postulate that the ships' structures were as effective in attenuating radiation from activity deposited by barge shots as they were in attenuating radiations from the more nearly solid particulate material deposited by land-surface shots. Since the effect of the ships' structures on the total doses was about the same (for the same locations) for all four shots, it is postulated that in the upper No. 2 hold, the ships' structures shielded out about 85% of the deposited-activity radiations from the barge shots, as well as from the land-surface shots.

## 2. Underwater Bursts

Operation Crossroads, Shot Baker: Below-decks dose records from Shot Baker are of dubious value. The exact placement of film badges within compartments was not specified, and not only was there "wide variation of doses received by badges subjected to approximately the same radiation,"<sup>29</sup> but also "four of the sixteen unshielded badges (on 13 different ships) registered less dosage than some badges located inside the structure on the same vessel."<sup>29</sup> Shielding-factor estimates have been made, based on averaged data. Although no distinction is apparent between shielding factors for amidships and for bow and stern compartments, the values vary with the thickness of steel, and lie between values of about 0.25 and 0.025.<sup>55</sup> However, the proportion of the total below-decks dose due to activity deposited on the decks is a matter of conjecture, since it was estimated that only about 50% of the total deck dose was due to deposited activity.

**BEST AVAILABLE COPY**



Operation Hardtack: There are no data from either Shot Umbrella or Shot Wahoo to indicate the effectiveness of ships' structures in attenuating activity deposited on the weather decks, since practically no material was deposited on the decks of the test ships.<sup>33</sup>

Wigvam: Deck deposit on the YAG-39 was negligibly low, and doses measured at shielded locations are believed to reflect the effect of the ship's structure on transit dose, not on deposit dose. The YAG-40 avoided the "cloud" and all deck deposit.<sup>31</sup>

#### 17.6.4 Theoretical Calculations for Unshielded Locations

Several methods have been developed for predicting deposit dose from both water-surface and underwater bursts, but it is estimated that none of the systems currently available is dependable within a factor of 10. One method used at present to estimate the region of fallout from a water-surface burst (but which does not provide quantitative estimates of dose) employs a computer-programmed calculation of the Dynamic Model or D-Model<sup>67</sup> (developed at USNRDL), that predicts fallout contours from land-surface bursts of specified yields for specified wind conditions. Another method has been used to predict deposit dose from water-surface and underwater bursts,<sup>68</sup> based on the assumption that the deposit dose is caused by radiations from radioactive sources deposited and remaining on flat surfaces in the vicinity of a point. The method assumes that the deposited activity builds up linearly with time during the period of deposition. For underwater bursts, times of initial and final arrival of activity are taken to be times of arrival (at the specified point) of the leading and trailing edges of the base surge. For surface bursts, these times are taken as initial and final times of fallout from the mushroom cloud and are estimated by determining the time required for assumed winds to move a source region of the same lateral dimensions as the initial cloud past the point in question. A brief summary of the D-Model and changes required in it before it can be used to predict deposit doses or dose-rates from water-surface bursts, and a brief summary of the method used in Ref. 68 follow:

1. Water-Surface Bursts. The Dynamic, or D-Model, was designed to predict dose rates and doses resulting from land-surface-burst fallout particles of 50 microns or larger in diameter. The model, programmed for the IBM-704, permits computation of dose-rate contours for bursts of given yields taking place in given wind configurations. The D-Model assumes that the initial radioactive-particle cloud is composed of up to about 100 identical coincident right circular cylinders with axes perpendicular to the land surface. Each cylinder represents a selected particle-size class, and is divided horizontally into identical coaxial discs, each of which represents an equal portion of the selected particle-size class. The number of discs used depends on yield. The particle-size distribution of fallout in time and space is determined by following the trajectory of

**BEST AVAILABLE COPY**

each disc for each particle-size class until the disc hits the ground. The effect of this process is to determine the distribution of fallout by tracking a maximum of 9000 different discs (depending on yield), each representing a given particle-size range originating at a given altitude in the cloud. The fraction of activity associated with each particle-size class must also be known, to permit deposit dose-rate estimates. Dose-rate and dose values calculated from this model are in agreement with measurements made following the surface and underground shots of Operation Jangle.

Use of the D-Model to predict reasonably accurate fallout contours for water-surface bursts will be possible only with several fundamental changes of parameters used in the computer program. Weapons-test data have indicated that slurry-type fallout droplets from water-surface bursts differ from land-surface-burst fallout particles in size range, composition, density, and mass-activity relationships. In addition, the time-history of the formation of slurry droplets and their falling rates are different from those of earth particles. It follows, therefore, that fallout patterns for water-surface bursts would differ from those for land-surface bursts. Furthermore, it must be understood that there is no such thing as a dose-rate contour at sea because fallout mixes fairly rapidly with the water, although on a large ship located at a fixed point, deposit dose could build up as on a land target. Work is in progress at NRDL to determine the required changes in parameter values that would permit application of the D-Model to water-surface-burst fallout prediction. When the appropriate program changes are effected, the output of the D-Model will indicate deposit that would take place on a large, flat, unwashed surface, and must be interpreted, together with ship size and countermeasure system, to provide dose or dose rate information.

Predictions that are given in Ref. 68 for deposit dose from a water-surface shot have been based on a compromise of predictions of effects of a land-surface shot as given in Refs. 2 and 69, and as computed from the land-surface D-Model.<sup>67</sup> It has been impossible to determine the degree of accuracy of the predictions of Ref. 68, since no water-surface shot of this type has been fired. It was assumed that the base surge is a minor mechanism of transport of radioactivity, that fallout from the cloud is the main source of deposited activity, and that the cloud dimensions are comparable to or exceed those of the base surge. It was further assumed that the deposited activity builds up in a linear manner with time during the period of deposition. The times of initial arrival and final arrival of activity were estimated on the basis of fallout from the cloud as determined by the falling rates of particles and by the assumed prevailing winds. Then the deposit dose,  $D$ , accumulated at a point during the time interval from  $t_1$ , time of initial arrival of activity, to any time after burst,  $t$ , may be expressed by:

$$D = \int_{t_1}^t d \, dt \quad (17-24)$$

**BEST AVAILABLE COPY**

where  $d$  = dose rate from deposited activity at time  $t$

=  $d_0 t^{-1.2}$ , where  $t^{-1.2}$  results from the assumed radioactive-decay law.

$d_0$  = dose rate\* corrected for decay to reference time of 1 hr

= 0 for  $t < t_1$

=  $d_0^{(\max)}$  for  $t > t_f$

=  $d_0^{(\max)} \left[ \frac{t - t_1}{t_f - t_1} \right]$  for  $t_1 \leq t \leq t_f$

$d_0^{(\max)}$  is the experimentally determined or calculated maximum dose rate (corrected to 1 hr). Usually it will be equal to

$$d_0^{(\max)} = d(t_f) t_f^{1.2}$$

and is a function of position in the fallout field. When calculated by the D-Model it is the summation of dose rates contributed by each disc landing at a given point, each corrected back to 1 hr from its actual time of arrival.

$t_f$  = time of final arrival of activity.

Then,

$$D = \frac{1.25 d_0^{(\max)}}{t_1^{0.2} \left( \frac{t_f}{t_1} - 1 \right)} \left[ \left( \frac{t_1}{t} \right)^{0.2} \right] \left[ \left( \frac{t}{t_1} \right) - 5 \left( \frac{t}{t_1} \right)^{0.2} + 4 \right] \text{ for } t_1 \leq t \leq t_f \quad (17-25)$$

$$\text{and } D = \frac{5 d_0^{(\max)}}{t_f^{0.2}} \left[ 1 - \left( \frac{t_f}{t} \right)^{0.2} \right] \text{ for } t > t_f \quad (17-26)$$

The estimated maximum dose rate  $d^{(\max)}$  at a given time  $t$  is fairly sensitive to the shape of the curve describing the buildup of  $d_0$  with

\*The symbol  $d_0$  used in this section has no relationship whatever to the  $d_0$  used in Secs. 17.5.5 and 17.6.5. It is unfortunate that the references cited use the same symbols for different concepts, but in the present work it has been decided not to add to the possibility of confusion by increasing the total number of symbols.

BEST AVAILABLE COPY

time. However, in any case, its possible range is less than:

$$d_o^{(max)} t_f^{-1.2} < d^{(max)} < d_o^{(max)} t_1^{-1.2}$$

The lower limit would result if all the activity were suddenly deposited at  $t_f$ ; the upper limit would result if essentially all the activity were suddenly deposited at  $t_1$ . (These two situations are of course not real; they are introduced only to show the bounds of possible values of  $d^{(max)}$ ).

For the linear buildup assumed differentiation shows that  $d^{(max)}$  always occurs at  $t = 6t_1$ , since

$$d = d_o^{(max)} \left( \frac{t-t_1}{t_f-t_1} \right)^{t-1.2} \quad (t_1 \leq t \leq t_f), \quad (17-27)$$

Thus if  $t_f \leq 6t_1$ , as is generally the case then

$$d^{(max)} = d_o^{(max)} t_f^{-1.2} \quad (17-28)$$

and if  $t_f \geq 6t_1$

$$d^{(max)} = \frac{5 d_o^{(max)} (6t_1)^{-1.2}}{\left( \frac{t_f}{t_1} - 1 \right)} \quad (17-29)$$

Values of  $t_1$  and  $t_f$  may be estimated from Ref. 2, or may be obtained from a fallout model.

The calculated results of the above equations represent doses caused by radiations from sources deposited and remaining on an infinitely large flat retentive surface, where no drainage or runoff of the active material occurs. The calculations could apply to the dose on the deck of an aircraft carrier with no operating washdown system. If washdown were operating, the dose would be reduced to 0.1 or perhaps 0.05 of the calculated value. The dose is substantially less, also, for ships with weather decks of smaller size. Figures 20 and 21 of Ref. 67 graphically present factors that may be used to calculate the reduction of the infinite-plane dose or dose rate which results when the deposited activity lies on a finite area.

**BEST AVAILABLE COPY**

2. Underwater Bursts. The Ref. 68 method of predicting the deposit dose resulting from underwater bursts employs the same basic theory as that for predicting deposit dose from surface bursts, but defines the parameters differently. Times  $t_1$  and  $t_f$  are estimated from the base-surge dimensions and rate of motion. Such values must be obtained from a base-surge model (see Vol. 1 of the Handbook). Further test data are required to determine whether deposit dose is significant for an underwater burst.

#### 17.6.5 Theoretical Calculations for Shielded Locations

A computational method has been developed at NRDL<sup>70</sup> to calculate the effectiveness of a ship's structure in attenuating the gamma radiation from activity deposited on the weather deck. Results of the calculations, in terms of the shielding factor, can be obtained for any specific location within the ship. The method, essentially a means of calculating the value of the ratio of the dose rate at a given location within the ship to the dose rate at a given exterior location, is independent of the quantitative value of either dose rate.

The NRDL computational method employs an idealized concept of the interactions of radiations with a ship's structure, and is based on several simplifying assumptions: (1) deck-deposited activity is a uniform distribution of isotropically emitting point sources on horizontal surfaces only; (2) buildup factors\* computed for infinite media are applicable for the finite shielding layers of a ship; (3) material in separate layers, like decks of a ship, has the same scattering characteristics as a single slab of the total thickness; (4) a deck-plating-thickness multiplying factor of 2 accounts for shielding material other than deck plating (bulkheads, beams, machinery, etc.); (5) pseudospectra, consisting of five energies, can be used in calculations to replace actual fission-product spectra for given times after fission, and can be weighted for each time to give virtually the same attenuation as the more complex actual spectrum would give. A brief discussion of the method follows; details of the method are given in Refs. 53 and 70.

The theory was developed from the basic expression (Eq. 17-13 in 17.5.5) for the exposure dose rate  $d_1$  (r/hr) at a distance  $x$  (cm) from a point isotropic source emitting 1 photon/sec,  $n_1$ , of energy  $E_1$  in a homogeneous medium:

$$d_1 = \frac{k\mu A_1 n_1 E_1 B_1 e^{-\mu_1 x}}{4\pi x^2} \quad \text{r/hr} \quad (17-13)$$

The exposure dose rate due to a polyenergetic point source is found by summing the above equation over all the emitted energies.

\*The buildup factor, as defined in Section 17.5.5, is the ratio of the dose from (1) both scattered and unscattered radiations to (2) the dose from unscattered radiations only.

**BEST AVAILABLE COPY**

In the theoretical method developed at NRD, it was found possible to express the results of Goldstein and Wilkins<sup>22</sup> for the dose buildup factor, B, of Equation 17-13 for any given medium and quantum energy, by an expression of the form given in Equation 17-19 of 17.5.5:

$$B = \left[ 1 + a(\mu x) + b(\mu x)^2 \right] e^{c(\mu x)} \quad (17-19)$$

The constants a, b, and c can be related to quantum energy E and evaluated for various media. Further, since the expression for the buildup factor is analytic, it is possible to integrate Eq. 17-13 over a source region. The integrated expression for dose rate due to sources distributed over the top of a circular slab of radius R<sub>0</sub> is given in Ref. 55. For simplicity and abbreviation of notation, the integral form will be employed in this discussion.

The ship-shielding factor for deposit radiation is evaluated by using three dose-rate ratios similar to those used to calculate the shielding factor for transit radiation:

$$SF = \frac{d_{hR}}{d_{3R}} = \left[ \frac{d_{h\infty}}{d_0} \times \frac{d_{hR}}{d_{h\infty}} \right] \div \frac{d_{3R}}{d_0} \quad (17-30)$$

where  $d_{hR}$  = exposure dose rate (at a given below-decks location) due to activity deposited on the weather-deck of the ship.

$d_{3R}$  = exposure dose rate at 3 ft above the weather-deck, over the below-decks location.

$d_{h\infty}$  = exposure dose rate at a location considered to be a given distance below an infinite slab of shielding, with radioactive sources distributed uniformly over the top surface of the slab.

$d_0$  = a symbolic dose-rate measure of source strength.

For the plane source case,  $d_0$  has the units r/hr. It is a quantity equivalent to that given by Eq. 17-14 or Eq. 17-17 of Section 17.5.5, but with an n whose units are photons/cm<sup>2</sup> - sec. See Note after Eq. 17-17, and footnote after Equation 17-24 of Section 17.6.4.

Since the individual dose rates on the right hand side of Eq. 17-30 are initially unknown, it was found possible to obtain the desired shielding factor by substituting equivalent ratios into the calculations.

**BEST AVAILABLE COPY**

A brief summary of the theory follows:

When the point-source case (Eq.17-13) is extended to express the exposure dose rate at a distance  $h$  below a slab of infinite extent, with radioactive monoenergetic sources distributed uniformly over the top surface, the dose rate  $d_{h\infty}$  due to the plane source emitting  $n$  (photons/cm<sup>2</sup>-sec) quanta of energy  $E_1$  (Mev/photon) can be expressed as the integral:

$$d_{h\infty} = k\mu_{A1} n E_1 \int_0^{\infty} \frac{Be^{-(\mu x)'} }{4\pi x^2} dA \quad (r/hr) \quad (17-31)$$

The source strength per unit area, may be expressed by  $nE_1$  Mev/cm<sup>2</sup>-sec and  $x$  = distance (cm) from the exposure point to an incremental element of area,  $dA$

$(\mu x)' = \mu_1 x_1 + \mu_2 x_2$ , where  $x_1$  is the path length in air and  $x_2$  is the path length in the slab, and each  $\mu_j$  is the total linear absorption coefficient for the corresponding medium.

The symbolic dose-rate measure of source strength,  $d_0$ , may be expressed:

$$d_0 = k\mu_{A1} n E_1 \quad (r/hr) \quad (17-32)$$

However, since a ship is not infinite in extent, it is necessary to determine the effectiveness of a finite slab in shielding the exposure point from the radioactive material. Furthermore, for the idealized concept of the problem, it is assumed that the shielding layers (corresponding to the plating of the ship's decks) are contiguous. It was found more feasible to calculate the shielding provided by the rectangular slabs of ship structure by considering the shielding provided by circular slabs that give the same dose-rate reductions. Graphs that equate circular shields to rectangular shields in terms of radius  $R$  and semi-length and semi-width  $a$  and  $b$  are given in Reference 71.

Then, the dose rate at an exposure point shielded by a finite slab of radius  $R$  from the plane distributed source may be expressed by:

$$d_{hR} = d_0 \int_0^{\pi R^2} \frac{Be^{-(\mu x)'} }{4\pi x^2} dA \quad (r/hr) \quad (17-33)$$

**BEST AVAILABLE COPY**

The dose rate at 3 ft above the slab over the exposure point may be expressed by:

$$d_{3R} = d_0 \left[ \int_0^{\pi R^2} \frac{Be^{-(\mu x)'} dA}{4\pi x^2} \right]_{h = -3} \quad (r/hr) \quad (17-34)$$

From inspection of Eqs. 17-32, 17-33, and 17-34 it is apparent that dose rate ratios required in Eq. 17-30 to evaluate the shielding factor have the following equivalences:

$$\left. \begin{aligned} \frac{d_{h\infty}}{d_0} &= \int_0^{\infty} \frac{Be^{-(\mu x)'} dA}{4\pi x^2} \\ \frac{d_{hR}}{d_{h\infty}} &= \frac{\left[ \int_0^{\pi R^2} \frac{Be^{-(\mu x)'} dA}{4\pi x^2} \right]}{\left[ \int_0^{\infty} \frac{Be^{-(\mu x)'} dA}{4\pi x^2} \right]} \\ \frac{d_{3R}}{d_0} &= \left[ \int_0^{\pi R^2} \frac{Be^{-(\mu x)'} dA}{4\pi x^2} \right]_{h = -3} \end{aligned} \right\} \quad (17-35)$$

The evaluation of the integrals of Eq. 17-35 for all the energies in the source spectra would be an extremely lengthy task, even when machine-computed. Therefore, the actual spectra have been replaced with pseudospectra, as described in 17.5.5. Evaluation of the ratios of Eq. 17-35 has been carried out for the five gamma-ray energies of the pseudospectra, for various distances below the slab, and for slab thicknesses of 0 to 10 inches. Results are presented graphically in Ref. 71. Note that Ref. 71 uses the following symbols:

- $I_{\infty}$  instead of  $d_{h\infty}$
- $I_0$  instead of  $d_0$
- $I$  instead of  $d_{hR}$

**BEST AVAILABLE COPY**



## 17.6.6 Simulant Experiments

An experiment was conducted on a Naval ship to evaluate shielding effectiveness of the ship's structure against gamma radiation from an external source. Results are reported in Refs. 71, 72, 73, 74 and 75. In the experiment, to approximate a condition of uniform contamination, a 145-curie  $\text{Co}^{60}$  source (1.25 Mev gamma energy) was pumped through plastic tubing laid out on the flight deck of the COWPENS (AVT 1), a light aircraft carrier. Two dosimeters were placed at each of various locations on the flight deck and in below-decks spaces. Numerous dosimeter readings were averaged and then divided by exposure time to provide dose rate as a function of time from the centerline of the ship. The measured flight-deck dose rates were corrected for the size of the "contaminated" area, since experimental data and computations indicated that the observed dose rate on deck would be increased by 4.5% if the entire deck were contaminated. Adjusted readings were used to determine the shielding factors. Two portions of the ship, designated A and B, were investigated. The A section had more and smaller compartments than the B section.

Figure 17-16 illustrates schematic cross-sections of the COWPENS at the frames where the measurements were obtained. Measurements on the Gallery Deck, the Forecastle, and the Main Deck were made about frame 35 (the A Section), while measurements on the Hangar Deck and the 2nd and 3rd Decks were made about frame 85 (the B section). Dosimeter arrays at each location were supported 3.5 ft above the various decks. The shielding factors obtained experimentally are listed in Table 17-5. Also listed in the Table, for the same locations and source energy, are shielding factors calculated by the theoretical method described in 17.6.5, using twice the total deck-plating thickness above each location. The factor of 2 was derived from measurements made in the B section.<sup>75</sup>

Experimental results indicated that on large ships, such as aircraft carriers, at locations on the 2nd and 3rd Decks and below, the ship's structure attenuated radiations to less than 1% of the level on the weather deck.

## 17.6.7 Summary

A survey has been made of available information on the interaction of surface ships with deposit radiation resulting from water-surface or underwater bursts. Results of the survey, which included weapons test data, experimental data using simulants, and theoretical calculations, are summarized in the following paragraphs.

**BEST AVAILABLE COPY**

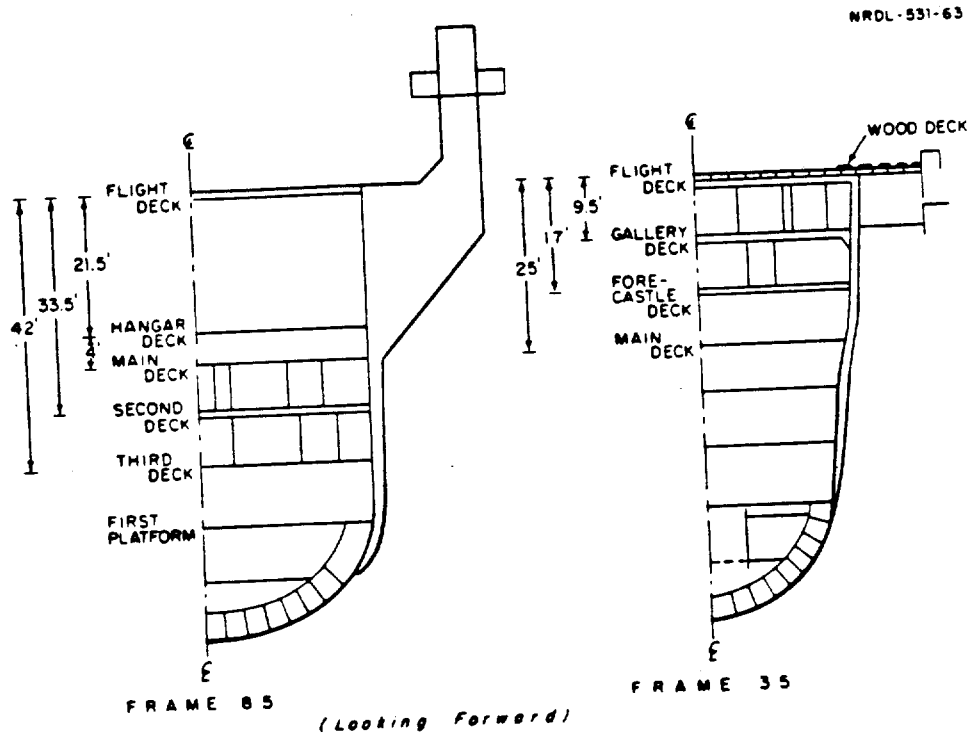


Figure 17-16. Schematic cross-section through COWPENS (AVT) at two frames.

Table 17-5. Experimental and computed shielding factors for COWPENS (AVT 1).\*

Deck	Transverse Distance To Center Line (ft)	Experimental Shielding Factor	Computed Shielding Factor
A Section			
Gallery	2 to Starboard	0.175	0.2396
	14 to Starboard	0.156	0.2350
	22 to Starboard	0.152	0.2099
Forecastle	2 to Starboard	0.0818	0.1315
	14 to Starboard	0.0688	0.1264
	22 to Starboard	0.0539	0.1079
Main	2 to Starboard	0.0376	0.07205
	14 to Starboard	0.0366	0.07033
	22 to Starboard	0.0231	0.06069
B Section			
Hangar	0	0.156	0.1978
	16 to Port	0.143	0.1830
	28 to Port	0.100	0.1453
Second	0	0.0355	0.04519
	17 to Port	0.0214	0.02283
	27 to Port	0.00892	0.008455
Third	0	0.0119	0.01513
	17 to Port	0.0110	0.01195
	29 to Port	0.00428	0.004313

\*Data from Reference 74.

Water-Surface Bursts. Data indicate that slurry-type radioactive particles will deposit on weather decks of ships caught in the fallout resulting from water-surface shots, and the deposited particles generally are not visible. On the unwashed areas of test ships, a dose increase of 40% to 50% was recorded during the 24-hr period following cessation of fallout from 2 test shots. The increase indicated that although it was invisible, deposited activity was present. The wash-down countermeasure has been effective in removing slurry deposit, and has reduced doses on washed weather decks to about 10% of the unwashed deck doses.

The interaction of a ship's structure with radiations from the deposited material serves to attenuate the gamma rays, the amount of attenuation being dependent on the thickness and density of the structural shielding. The effectiveness of the shielding is indicated in terms of the shielding factor, which is the dimensionless ratio of the below-decks dose or dose-rate to that at 3 ft above the weather deck. At below-decks locations where deck plating served as part of the shield, test data from target ships indicated that doses were 10% to 20% of weather deck values. Test data showed that the aluminum superstructure also to some extent attenuated the gamma radiations from deck-deposited activity; depending on the location of the exposure point, doses were reduced to 10% to 60% of weather deck doses.

Underwater Bursts. A burst at mid-depth in comparatively shallow water, such as Shot Baker, Operation Crossroads, may be expected to produce a large base surge, as well as fallout. Records are not available to indicate whether the deposited activity from Shot Baker was visible; but it is expected that for a burst of this type, some bottom material (which would be visible) would be included in the fallout. It was estimated that first-hour doses ranging from 3800 r to 140 r resulted on the weather decks of ships from 500 yd to 2000 yd from surface zero, respectively. Below-decks dose records, of dubious reliability, indicate shielding factors from 0.25 to 0.025 for various locations.

Deeper underwater test shots produced base surges; however, no visible fallout occurred, and data indicated negligible deposited activity on the target ships. However, very small (less than 1 micron) radioactive particles were found in some of the activity samplers at Operation Hardtack. Particles, such as those in the samplers, may have been deposited on the weather decks and rapidly removed by the washdown systems operating on the target ships, since very little dose was accumulated on the weather decks after the passage of the base surge (in the first few minutes).

Shielding Factors. One theoretical method described for calculating shielding factors is rather cumbersome and has not been proven entirely

reliable. Experiments were carried out using a distributed  $\text{Co}^{60}$  source on the flight deck of the COWPENS to simulate deck-deposited activity, and shielding factors at below-decks locations were measured. Results indicated that the ship's structure attenuated radiations to less than 1% of the level on the weather deck. Shielding factors for the same energy and the same locations were computed, using twice the deck-plating thickness above each location. A correlation between some of the measurements and the computational method indicated that twice the plating thickness should be used in computing the factors.<sup>75</sup> Comparison of the two sets of values (listed in Table 17-5) shows that in the B section of the ship (where the compartments were larger), the majority of the computed values were less than 28% different from the experimental values, an agreement considered very good. In the A section of the ship, where there were many small compartments, the majority of computed values were more than 50% larger than the experimental values, and thus did not indicate as much attenuation of the radiations as the experimentally obtained factors revealed. The most divergent results occurred for the location on the main deck (22 ft from the centerline) where the computed factor was about 2.6 times larger than the experimental one. The divergence in values for the B section of the ship may indicate that use of twice the deck-plating thickness is not sufficient to account for all the shielding in certain portions of the ship. Shielding factors computed by the method described probably will overestimate the dose or dose rate at a given location; hence they provide a safety factor.

No data are available to indicate whether radiations from deposited activity will affect shipboard equipment. However, high doses (thousands of roentgens) or high dose rates (hundreds of thousands of r/hr) generally are required for such effects.

**BEST AVAILABLE COPY**

## 17.7 RADIATIONS FROM CONTAMINATED WATER

### 17.7.1 General Introduction

Water in the region of a nuclear water-surface or underwater burst will become contaminated by the radioactive particles produced by the detonation. These particles, suspended in the water, emit gamma radiations that may add to the nuclear-radiation exposures aboard a ship traversing the area or immobilized in it.

Determination of the interaction of a ship with the radiation field from the contaminated water, involves measuring or computing the exposure-point dose rate due to the water. This dose rate is dependent not only on the source strength (determined by the distribution of radioactive particles in the water), but also on the source gamma-ray spectral distribution, the source geometrical distribution, and the energy degradations that occur in the water and in penetrating the ship. The distribution of particles in the water will differ with burst conditions, as well as with water currents and weather conditions.

The mechanisms by which radioactivity is distributed in the water by surface and underwater bursts are briefly described in 17.7.2, followed by available water-contamination data gathered at test shots in 17.7.3, and by shipboard dose-rate data, due to the "hot" water, in 17.7.4. A summary of the section is given in 17.7.5.

### 17.7.2 Mechanisms of Water Contamination

Radioactive particles reach the water by several mechanisms. Some activity mixes with the water of the column or plume thrown up into the air, and a region of contaminated water results when the plume or column falls back to the surface. The water may also become contaminated from radioactive fallout, as well as from activity suspended in the base surge, which eventually deposits on water surface. Some of the radioactivity never is thrown into the air, but remains in the water near the burst point. For an underwater burst, some of this radioactivity is brought to the surface by the event, and some is trapped below the surface.

The nature of the radioactive particles formed will depend on the mass of water and any ship material engulfed by the fireball. The distribution of these particles in the water is governed by their size and density as well as by wind speed and direction and by ocean layering and currents. If the burst occurs on free water and the fireball engulfs no solid material, the radioactive particles will be so small that they will be colloidal in nature. Thus, they will slowly become distributed in the mixed layer, where they will remain for a long period of time. Lateral dispersion of the particles will occur, and the whole contaminated area will move with the ocean currents. If the burst is a hit or near-miss,

so that it disintegrates a ship, some of the activity will become associated with heavier particles (of the disintegrated ship) than are formed for a true free-water burst, and more rapid mixing of the radioactive particles with the water and their penetration to greater water depths will probably occur. Exact rates and depths of fallout penetration are difficult to predict, but estimates can be made by comparing results at tests in the Pacific, where the differences in rates and depths of fallout penetration resulting from barge and island shots were probably primarily due to differences in particles sizes.

All the waterborne radioactive particles resulting from a surface or shallow subsurface burst will be distributed initially in the upper water layer, often referred to as the "mixed layer," that may be from less than 30 meters to more than 150 meters thick, depending on the geographic location. The temperature of this layer is quite uniform from the sea surface to the bottom of the layer, or to the thermocline, below which the temperature decreases rapidly with depth. When a substance of soluble or colloidal nature, or one having about the same density as water, falls on the ocean surface, it becomes distributed into the mixed layer fairly rapidly, often within a few hours. However, because of the sharp increase in density below the mixed layer, little further downward penetration of particles of this type occurs.

For an underwater burst so deep that the bubble undergoes one or more pulsations before reaching the surface, some activity probably will be distributed along the path of bubble migration, particularly at bubble minima, some activity will be thrown into the air and mixed with the plumes and base surge, and some will remain in the water at the surface where the bubble breaks through, resulting in a region of contaminated water about surface zero. The distribution of the radioactive particles at later times, for such a shot, will be dependent on the burst depth, the water depth, the thickness of the mixed layer, and the prevailing winds and water currents.

### 17.7.3 Water-Contamination Data

Some references\* give water-contamination data obtained following (1) land and water-surface shots at Operations Castle and Redwing; (2) the shallow underwater shot, Bikini Baker at Operation Crossroads; (3) the shallow bottom shot, Umbrella at Operation Hardtack; (4) the moderately deep shot Wahoo at Operation Hardtack; and (5) Wigwam, the deep underwater shot. Data indicate that both the nature and distribution in water of the radioactive particles resulting from bursts over land surfaces are different from those of particles resulting from bursts over water surfaces, and that these characteristics are affected by the kind and mass of material engulfed by the fireball.

\*References 31, 32, 33, 40, 42, 64, 65, and 76 through 84.

### 1. Water-Surface Bursts

Operation Castle: At Operation Castle, in the Spring of 1954, fallout with very small particle size occurred from the over-water shots.\* As a result, the settling rate was slow, and it is estimated that the depth-of-penetration and below-surface activity measurements were reliable. Following Yankee, Shot 5 at Operation Castle<sup>76</sup> (13.5 MT over about 250 ft of water), between H + 6 hr and D + 4 days a fleet tug carrying improvised radiological and oceanographic gear cruised the ocean downwind of Bikini Atoll, taking samples of the water at the surface and to depths of 2400 ft. In addition, gamma-ray dose rates were measured above the sea surface, just below the sea surface, and occasionally to 80 meters (about 262 ft) depth. Measurements were made by three sealed Geiger-counter instruments that were either towed or lowered to various depths at definite points in the area, and by a standard ionization-chamber Radiac termed a "pot," set in a steel tank 6 ft above the sea, and used to monitor the radiation from the surface every 5 to 20 minutes. These measurements indicated that at about 23.5 nautical mi from surface zero and within 18 hr after shot, activity became so concentrated that all the towed Geiger instruments deflected off-scale (range not specified). However, the "pot" instrument set on a scale of 0 to 50 mr/hr continued to indicate gamma dose rates of about 20 mr/hr (after corrections for drift error). The first depth cast was made at about 50 naut mi from surface zero at about H + 34 hr. At that time, maximum dose rates (in situ) of about 17 mr/hr registered fairly uniformly from the surface to depths of about 160 ft. Dose rates then decreased with depth to about 2 mr/hr at a depth of about 260 ft. By H + 75 hr, at about 140 naut mi from surface zero, dose rates were uniformly between 1 and 2 mr/hr from the surface to depths of about 250 ft.

Operation Redwing: At Operation Redwing in 1956, a more elaborate program of radiological measurements of sea water was carried out. Measurements of early depths of fallout penetration were made<sup>77, 78</sup> within 15 naut mi of surface zero, and ship surveys after each event involved detailed radiological and oceanographic measurements, including surface-probe measurements, over the area of the fallout from both land and water-surface shots. The fallout from Shots Navajo (a barge shot of about

All the Flathead and Navajo fallout collected and examined consisted of slurry particles,<sup>42</sup> the inert components of which were water, sea salts, and a small amount of insoluble solids. Average densities of these particles were between about 1.15 and 1.5 gm/cm<sup>3</sup>. All the active fallout collected at Shot Zuni consisted of solid particles,<sup>42</sup> of average densities between 2.0 and 2.8 gm/cm<sup>3</sup>, and no slurry was observed. As would be expected by comparing the densities,

\* References 40, 64, and 76.

BEST AVAILABLE COPY



fallout from the barge shots settled in the water more slowly than that from the island shot. Probe measurements<sup>77</sup> of particle-penetration depth indicate that the rate of penetration of radioactive particles from Shot Zuni was about 11.0 meters/hr, whereas rates for Flathead and Navajo were about 3.5 meters/hr and 2.3 meters/hr, respectively. Shot Tewa was a 5-MT burst detonated on a barge over very shallow water (about 20-ft depth), and was considered more nearly a land-surface shot than a water-surface shot. However, Ref. 77 states that the thin film of water must have had a modifying effect on the fallout particles, as evidenced by the slow rate of penetration, only about 3.8 meters/hr, for relatively close-in fallout. At the same time, however, the region of fallout was extremely widespread, as in the case of a land-surface burst.

Comparisons of plots<sup>42</sup> of depth of penetration vs activity for Navajo and Tewa indicate dose rates of about 2 to 3 mr/hr at about 3 hr after Navajo, at ocean depths of between 10 and 20 meters (33 to 66 ft) whereas at the same depths at about 3.8 hr after Tewa, the activity levels were between 100 and 200 mr/hr. Reference 77 indicates that at about 2.5 hr after Tewa, saturation prevented the instruments from recording levels higher than 2.7 r/hr at depths of about 55 ft. This measurement was obtained by one of the Geiger-counter units which were moored to skiffs and suspended at various levels in the sea. The one unit that operated was located approximately 10 mi from surface zero, and was triggered by fallout at 18 min after burst. All other available water-probe contamination measurements for all the Operation Redwing shots were made from the survey ships at later times (7 to 10 hr after burst) and indicate very low activity levels, of the order of a few mr/hr.

The nature and behavior of activity from a surface burst at sea over deep water would probably resemble that from Shot Flathead or Navajo, particularly if the burst were a hit or near miss, such that the fireball engulfed a ship. The mass of a DD or DL may be from 6 to 11 million pounds, and that of a CVA may vary from 100 to 200 million pounds, whereas the total mass of the barges from Navajo and Flathead was only between 840,000 and 900,000 pounds. Ships would provide more insoluble solids to agglomerate with the fission products than did the test barges. However, some bottom material was probably also involved in the fallout from the test shots. Thus, it is estimated that following a nuclear burst on or near a ship at sea, fallout would consist of slurry particles of sizes and densities similar to those of the barge shots, and would be similarly distributed in the water.

## 2. Underwater Bursts

Operation Crossroads: The first nuclear underwater detonation on record, a shallow detonation, is Shot Baker of Operation Crossroads (23 KT at 90 ft in 180 ft of water in July 1946). According to Ref. 79, the radioactivity in the water was important, and between 10% and 50% of the

BEST AVAILABLE COPY

total amount of radioactive material produced by the explosion remained in the water. Fallout from the mushroom cloud caused a radioactive rain to fall in an area within the lagoon, and it was estimated that the largest part of the radioactive material was deposited on the surface of the water by that rain. In general, vertical diffusion of radioactive material in the lagoon was very slow. Gamma dose rates above the surface of the lagoon near surface zero went from about 400 r/24 hr ( $\sim 17$  r/hr) at H + 1 hr, to about 65 r/24 hr (2.7 r/hr) at H + 4 hr, and to less than 0.1 r/24 hr (0.004 r/hr) at 5 days after shot. However, at that time, the water was still sufficiently radioactive to seriously contaminate the evaporators and hulls of nontarget ships within the lagoon.<sup>65</sup>

Operation Hardtack: Some water-contamination records are available from the underwater shots of Operation Hardtack, in May and June 1958. Both, underwater and surface GTR dose rate data are available, as well as some water sample data.

At Shot Umbrella, a relatively shallow burst on the bottom (150 ft), ship records are available<sup>33</sup> from only one operating underwater GTR (gamma-intensity-time recorder). The GTR, suspended from a boom extending over the fantail of the DD 593, was located at about 11 ft underwater and 7900 ft from surface zero. Tabulated radiation data indicate by two peaks in the dose rate vs time curve that contaminants were in the water near the ship both at early times and at 6 hr after shot. However, during the period when the ship was enveloped by the base surge, the peak underwater dose rate registered was only 0.19 r/hr at 8 min after burst. Following this period, the underwater dose rates were very low until they again rose to the same peak rate at 6.4 hr after burst. The early peak was attributed to contaminants depositing in the water from the base surge, and possibly to some contaminants washed off the ship, which had washdown in operation. The late increase of underwater dose rate is attributed to a patch of contaminated water (detonation debris originally upwelling at surface zero) that drifted down on the ship. A few early-time surface-water and shallow underwater activity records from the coracles are also available for shots Umbrella and Wahoo, along with a comprehensive discussion of the significance of the records.<sup>32</sup> Seven early-time underwater GTR records were obtained for Wahoo, and four for Umbrella. The instruments were so mounted on the edges of the coracles that the passage of the shock wave triggered a mechanism to drop them into the water. It was planned that, after release, they would be suspended at approximately 6 ft below the water surface. Similarity of the underwater records to the above-water standard GTR records of corresponding coracles indicated that a number of the detectors may have been closer to the surface than the planned 6-ft depth.<sup>32</sup> Nevertheless, the close-in station records are of value, and show evidence of radiation due both to water directly contaminated by the bomb and to patches of radioactive foam. The closest-in record obtained was that of the underwater GTR (calculated to be almost at the surface) located at 1760 ft

**BEST AVAILABLE COPY**

upwind from Umbrella surface zero, which indicated a recorded 3-min dose of 604 r, while at 6740 ft downwind of surface zero, the detector (calculated to be 55 inches deep) recorded only a milliroentgen dose. No depth-penetration measurements are available for Shot Umbrella, and water sampling is mentioned only briefly. Analysis of sea water collected in the lagoon 75 min after burst<sup>80</sup> was carried out by separating the isotopes detected into two groups, particulate ( $>0.45\mu$ ) and either soluble or colloidal ( $<0.45\mu$ ). It was found that  $N_p^{239}$  was present in high amounts in both groups, and several other isotopes were present in lesser amounts.

For shot Wahoo (500 ft in deep water), contaminated-water dose rates at 11-ft depths near the ships are unavailable because the starting signals were not received on the instrumented ships. For Wahoo, on the underwater GTR's at 3900 ft and 4100 ft from surface zero, dose rates peaked briefly at over 2000 r/hr at about 8.5 min and 1400 r/hr at 6.3 min, respectively.<sup>32</sup> These dose rates are considered to have been due to waterborne radioactive material. The cumulative doses up to 3 min on the same GTR's, calculated to have been floating at about 12 and 18 inches below the surface, respectively, were about 16 r and 4 r. An experiment<sup>81</sup> whose objective was "investigating the dispersal in time and sea of the contamination resulting from Shot Wahoo" resulted in meager information. As the USS REHOBOTH cruised the area for several days after shot time, the sea-water intake of the ship was monitored for contamination, numerous depth-penetration measurements of activity were made, and Navy radiac survey-instrument readings were taken at the bow. Some information was obtained on the dimensions of the radioactive pool with time, and of the radiation levels measured by the bow survey meters, which "viewed a large solid angle but were shielded from the nearby water surfaces." These readings probably represent the field at the bow due to waterborne activity, and were used to indicate the size of the contaminated surface layer of water. The first post-shot dose-rate-vs-depth readings of the scintillation detectors, taken at about H + 3 hr at about 3 naut mi downwind of surface zero, indicated a maximum of about 4000 counts/sec at the surface, about 2400 counts/sec at depths from about 5 to 35 ft., and then decreased to about 250 counts/sec at a 60-ft depth. According to the radium-calibration curve given in Ref. 81, these measurements correspond to about 1 mr/hr, 0.6 mr/hr, and 0.06 mr/hr, respectively, if it is assumed that an error has been made in labeling the abscissa of the calibration curve. The maximum in-situ level encountered, about 16,000 counts/sec at depths of 90 to 130 ft (at H + 28 hr, about 5 naut mi downwind of surface zero), correspond to about 10 mr/hr on the calibration curve. The sea-water-monitor ionization-chamber results are presented in terms of amperes vs time, but no method of conversion to mr/hr is presented except for the statement that "current readings could be converted to mr/hr if certain assumptions are made." It was concluded that the base surge distributed a large amount of activity in the upper water layers, over an area of about 1 mi in radius, and prevailing winds carried the contaminated aerosol in a westerly direction to form an initial

elliptical contaminated surface area with the leading edge about 2.5 mi west of the shot point at H + 2 hr. The contamination extended to depths of 50 ft at early times. According to Ref. 80, the greatest amount of radioactivity in the water at surface zero at H + 48 hr was found in samples taken below the thermocline, which was located at 100 meters.

Doses due to the water recorded in the second hour after burst appear to be insignificant. Floating film packs dropped into the downwind array 120 min after Wahoo and 60 min after Umbrella "did not register any dose significantly above background; therefore the film-pack data indicate no contribution from radioactive material suspended in the water after those times." Reference 32 concludes that the passage of radioactive foam would represent a serious hazard to small boats between 5 to 15 min after burst, although waterborne radioactivity is of secondary importance aboard ships.\*

Investigation of the radioactive contamination of the water following Shot Wahoo<sup>80</sup> indicated that, at the end of 3.5 days, the boundaries of the radioactive water mass extended beyond the survey area, 50 mi to the west of Eniwetok Atoll, and to a depth of at least 300 meters. Analysis of water samples collected at 5.5 hr and 27 hr after detonation indicated activity present at all depths sampled (from the surface to 300 meters). The measured amounts of beta radioactivity in the water were the same at both times. At 48 hr after burst, at surface zero, the greatest amount of radioactivity was found in the samples taken below the thermocline.

Operation Wigwam: On 14 May 1955, Shot Wigwam (about 32 KT) was detonated at a depth of 2000 ft in very deep water. Reports of water-surface radioactivity from this operation are contradictory, and it is impossible to determine which of the primary documents<sup>31, 82</sup> is more reliable. Discussion of the depth-probe measurements<sup>82</sup> is also difficult to interpret.

Reference 83 states that "Project 2.1 arranged that samplers be dropped and towed through the area, but had no part in the sample recovery." Unfortunately, most of the samples were lost.

\*More recent data from the Sword Fish underwater shot, received too late for detailed inclusion in this report indicate that the early-time radioactive-pool hazard to larger ships can be of considerable significance during the first half hour after burst.

**BEST AVAILABLE COPY**

The final report, "Mechanism and Extent of the Early Dispersion of Radioactive Products in the Water,"<sup>82</sup> which was not issued until March 1962, states that it "is the result of painstaking analysis of measurements obtained," but "for a number of reasons the measurements left something to be desired." According to this analysis, 32% of the total activity in the water was found in the thermocline (at 110 meters) and above, and 68% at depths of 200 to 300 meters. The deep activity was found to be complexly distributed in laminae that moved more or less independently of the surface and other waters. It was concluded that the mechanism that gave rise to this distribution was an emergence of a deep column of water at early times following the detonation and a subsequent mixing of these deeper waters with the surface layers and their sinking to an intermediate depth as a result of instability. It is postulated that the emergence of the column gave rise to a mass of water moving from east to west on the surface, perhaps due to the earth's rotation.

Values given in Ref. 82 of early-time maximum radioactivity at the water surface, as determined by survey aircraft, are higher by factors of 3 to 7 than those given in Ref. 31. According to Ref. 82, the 27 min, 33 min, and 130 min maximum surface dose rates over the radioactive pool of 550 r/hr, 230 r/hr, and 8 r/hr, respectively, were derived by arbitrarily doubling aircraft results that had been corrected to 3 ft above water. This doubling was done to roughly reduce these measurements to in-situ measurements made by the probe. The area of surface activity at H + 30 min is tabulated as 5.5 sq. mi. According to Ref. 31, the earliest aerial survey at H + 19 min established that the principal contaminated zone of water was about 2.5 miles in diameter, with an area of about 5.3 square miles, and at that time dose rates varied between 32 and 70 r/hr at 3 ft above the water. Several sets of radac data-telemetering transmitters were dropped into the water by aircraft at various times from H + 26 min to D + 1 day. It was planned for these instruments to measure the dose rates in about the top 6 inches of water and transmit the information to the primary radar room aboard the CVL-49. Of the original 5 sets dropped, telemetering pulses were received from only four. Of these, two units were of too high a range to produce data, and one unit transmitted intermittently. One unit produced consistent and apparently reliable data (although no range and bearing information was obtainable) that compared satisfactorily with information obtained from another unit dropped at D + 5.3 hrs. Available telemetered data indicate that dose rates in the top few inches of water somewhere in the area of the original circular upwelling were about 40 r/hr at about 1 hr after burst, and decreased to about 1.5 r/hr at 6.67 hr (400 min).

**BEST AVAILABLE COPY**

It is difficult to obtain a coherent picture of the distribution of activity below the water surface, since available records do not agree well on this subject. According to Ref. 82, the maximum dose rate encountered by the depth probe on the first day was 27 mr/hr at 1.5 hr after burst, at a mean lamina depth of 60 meters. At D + 12.5 hr, about 21.5 mr/hr was recorded at a mean lamina depth of 122 meters, and at D + 70.2 hr, a level of 23.6 mr/hr was recorded at a mean lamina depth of 265 meters. According to Ref. 31, the GTR located at station 2 on the YAG-40 (about 30 ft below the water surface) provided another source of early in-situ dose-rate information from Shot Wigwam. The first pass through the contaminated area by the YAG-40 at 51 min after detonation took 25 min, and the unshielded keel station (station 2) accumulated a 3-r dose in that time and registered dose rates that peaked at more than 10 r/hr. The water-sampling and analysis portion of Project 2.4 obtained samples of contaminated water from beneath the keel of the YAG-40 at a depth of about 30 ft and from 18 inches below the water surface. Early radiochemical analyses of a number of samples were made, and results are presented in units of counts/sec vs time after burst, and in mc/ml vs time after burst. It was concluded that the specific activity of the contaminated area varied considerably from location to location, and the limited number of samples precluded any generalization regarding the total contaminated volume of water.

Late-time water analyses and depth probes of the area, described in Ref. 84, indicate that activity in the water was detectable as late as 3 weeks after the shot. The results of this late survey were meager because the radioactive water did not move in the predicted fashion, and was not located until late in the period allotted for the operation.

In May 1962, a nuclear device [REDACTED] was detonated at about 670 ft in very deep water. Reduction of the data from Operation Swordfish has not been completed, but aerial surveys were able to easily track the contaminated patch for 6 days after detonation, and the surface ship was tracking the patch at least through D + 12 days.

### 3. Summary

Water-contamination data from nuclear water-surface and underwater bursts are limited, as the preceding paragraphs illustrate. Observations of the penetration of activity from water-surface bursts at Operations Castle and Redwing indicate that most of the water-borne activity became well mixed and remained above the thermocline for periods of many days. It was also observed that radiation levels in the water were low, not in excess of 1 r/hr in situ. However, since few measurements were obtained earlier than H + 7 hr on any shot, mixing and decay probably

**BEST AVAILABLE COPY**

account for the low observed levels. Thus, it is possible that at early times, radiation levels in the water around surface zero could add to the radiation field aboard a ship traversing the area. However, it is concluded that available data from surface bursts do not provide a reasonable basis for predicting dose rates around surface zero at early times.

The underwater-burst data indicate that within 2000 ft of surface zero and within the first 15 min after burst, doses of several hundred roentgens could be accumulated from contact with the first few feet of surface water. However, after 1 hr after burst, activity in the water probably would be of no significance aboard ship, and by several hours after burst, activity levels in the water from either water-surface or underwater detonations would probably be lower than 1 r/hr.

#### 17.7.4 Shipboard Dose-Rate Data from Contaminated Water

Shipboard dose and dose-rate data have been obtained at various weapons tests. In compartments below the water line, the recorded gamma doses and dose rates that were considered to be due only to contaminated water surrounding the ship were negligible in all cases; in fact, they contributed less than 1% of the levels measured at exposed locations. Simultaneous measurements of dose rates in the water around a ship and dose rates aboard that ship are required for reliable estimates of the contribution of waterborne radiation. Such measurements are available for only a few shots. However, efforts have been made to distinguish the contribution of waterborne radioactivity from the contributions of other sources for several additional tests.

##### 1. Water-Surface Bursts

Operation Castle: For Operation Castle, two Liberty Ships (YAG's 39 and 40) were modified to have various parts of each ship simulate portions of Navy combatant ships. For instance, the recorder-room area on each ship simulated compartments below the waterline, adjacent to the shell, and was well-shielded from the weather surfaces by a 12-inch concrete slab. Doses and dose rates measured in these rooms were attributed only to radiation penetrating the ships' skins, and not to radiation from sources above, such as fallout. Dose rates in the recorder rooms after Shot 5 (Yankee) peaked at only 0.07 to 0.08 r/hr between 6 and 7 hr after burst, and the total doses measured to 12 hr were only about 0.5 r. During the same period, doses of over 100 r were recorded at unprotected topside stations on the same ships. It

was concluded that radiation from the water contributed significantly to the total radiation field at shipboard locations below the waterline, but the low absolute value of the measured dose rates and doses made the waterborne contribution unimportant.<sup>40</sup>

[REDACTED]

Operation Redwing: During Operation Redwing, the YAG's 39 and 40 were again used as test ships. As part of the ship-shielding studies,<sup>41</sup> estimates were made of the upper limits of contaminated-water contribution to total dose rates and doses in the test ships' holds. Gamma detectors were placed at several locations below the waterline, in the double bottom of the YAG 39, and below the keel of the YAG 40. Available data for Shot Navajo include estimates of 4-pi free-field gamma dose rates as functions of time in the water at 20- and 30-ft depths around the YAG 39. In addition, washed- and unwashed-deck area time-dose-rate histories are recorded. Also presented is a curve giving the ratio of the dose rate in the recorder room (which was unchanged from Operation Castle) to that on the washed-deck area. Comparison of the records indicates that peak dose rates in the water and on the deck areas occurred at the same time about 5 hr after burst. Peak water dose rates at 20- to 30-ft depths were about 0.05 to 0.08 r/hr, and free-field gamma doses in the water were estimated to be about 0.4 r by 10 hr, about 0.93 r by 30 hr, and about 1 r by 40 hr. The recorder-room dose rate, calculated from other information in Ref. 18, appeared to be about 0.002 r/hr by about 5 hr after burst, and the doses calculated to 10 and 30 hr appeared to be about 0.018 r and 0.04 r, respectively. The dose rate in the lower No. 2 hold, similarly calculated, was found to be about 0.06 r/hr by 5 hr, and the doses to 10 to 30 hr appear to have been about 0.27 r and 0.45 r, respectively. The dose rate on the unwashed weather deck at 5 hr was about 1.5 r/hr, and the accumulated doses by 10 and 30 hr were about 6 and 9.5 r. These data are tabulated in Table 17-6 for ease of comparison.

**BEST AVAILABLE COPY**



Table 17-6. Dose rate and dose data for Shot Navajo.

Station Location	Peak Dose Rate (r/hr)	Time (Hr)	Dose (r)	Time (Hr)
Water, 20- to 30-ft Depth	0.05 to 0.08	5	0.4	10
			0.93	30
			1.0	40
Recorder Room	0.002	5	0.018	10
			0.04	30
Lower No. 2 Hold	0.06	5	0.27	10
			0.45	30
Unwashed Weather Deck	1.5	5	6.	10
			9.5	30

It is apparent from these data that at locations well shielded from airborne and deposited activity, such as the recorder room, the dose rates and doses were extremely low, less than 6% of those recorded in the water. In the hold, the major portion of the recorded dose is estimated to have been due to backscattered radiation from airborne and deposited activity. According to Ref. 41, the highest estimates of water contribution were obtained during participation in Shot Tewa, which is classified as a land-surface, rather than a water-surface shot. At Tewa, water contribution to both dose and dose rate was estimated to have been less than 11% in the lower hold where the 10 hr recorded dose was about 1 r, while the 10-hr deck dose was about 25 r, and the 10-hr dose in the water was about 3 r. It was further estimated that radiation from the water contributed less than 1% of the total deck dose.

2. Underwater Bursts

Operation Hardtack: At Operation Hardtack, three destroyers utilized as target ships during the two underwater shots were instrumented with film badges and GTR's in many compartments. In addition, a GTR was suspended from a boom over each ship's fantail, and was to drop into the water after the passage of the underwater shock wave. After Shot Umbrella, GTR and film-badge data were obtained on all 3 ships, although not all GTR's operated. From gamma dose-histories tabulated in Appendix D of Ref. 33, it is possible to compare doses recorded by the GTR's at several shipboard stations located 3 to 6 ft below the waterline of the DD-593 with the doses recorded by the GTR suspended in the water over the fantail at station 15. Stations 11 and 18 were at the lower level in the forward and aft firerooms, respectively, and station 8 was located in the magazine. At station 15, doses measured were 0.01 r by 18 min, 0.03 r by 81 min, and 0.367 r by 8.5 hr. At stations 11 and 18, doses measured about 2.8 r by 9 min. They were about 3.24 r at station 11 by 93 min and 2.91 r at station 18 by 92 min. At station 8, doses were 13.2 r by 9 min and 13.4 r by 90 min. These doses are listed in Table 17-7.

Table 17-7. Dose data from DD-593 for Shot Umbrella.

Station	Location	Dose	Time
15	In water	0.01 r 0.03 r 0.367 r	18 min 81 min 8.5 hr
11	Lower level, fwd fireroom	2.8 r 3.24 r	9 min 93 min
18	Lower level, aft fireroom	2.85 r 2.91 r	9 min 91 min
8	Magazine	13.2 r 13.4 r	9 min 90 min

Comparison of the doses recorded in the water with the doses recorded aboard ship indicates that the former were only about 1% of the latter even at shipboard locations only partially shielded from airborne activity. Thus the contribution of waterborne contamination to shipboard doses must have been very small. Although shipboard doses were recorded at Shot Wahoo,

no shipboard radiation measurements due to contaminated water were obtained because the starting signals were not received on the instrumented target ships; thus, no comparison is possible between shipboard and water doses for a Wahoo-type shot. Reference 33 concluded that although radiation from the water may have contributed to compartment dose rates at later times, the contribution of contaminated water to the total dose observed aboard the target ships was of little significance.

Operation Wigwam: From Operation Wigwam, little data are available that permit estimation of the contribution of waterborne radiation to shipboard doses. One figure in Ref. 31 gives dose-rate histories at stations below the waterline during the first traverse of the contaminated area by the YAG 40 between 50 and 80 min after burst. Dose rates at the keel station (about 30 ft below the waterline) peaked at about 13 r/hr at about 75 min. At about the same time, dose rates (estimated to be due only to radiation from the water) at station 64 in the Recorder room, peaked at about 0.8 r/hr. This one plot indicates that, for the duration of the traversal of the area, the dose rates at station 64 were only about 6% of those recorded at the keel station.

#### 17.7.5 Summary

No contaminated-water dose or dose-rate histories are available at early times near surface zero for water-surface test shots. Available data indicate that at times of 4 hr and later, the contribution of waterborne radiation to shipboard doses is negligible, but it is possible that at early times contamination in the water around surface zero could add to the radiation field aboard a ship traversing the area.

Analysis<sup>32</sup> of records of underwater test shots leads to the conclusion that radiation from waterborne radioactive material is significant. There appear to be three major sources of waterborne radiation: (1) radiation from material deposited in the water from the base surge; (2) radiation due to water directly contaminated by the bomb (white water); and (3) radiation due to patches of radioactive foam generated during eruption and collapse of the column or plumes. Radioactive material deposited in the water from the base surge appears to dissipate rapidly after the passage of the base surge, whereas white water may be highly radioactive up to an hour after burst time. Radioactive foam, estimated to be the most important early-time waterborne source, is suspected of causing peak dose rates of 1000 to 2000 r/hr observed in the underwater dose-rate records for Shot Wahoo at times between 6 and 9 min after burst.<sup>32</sup> A direct observation of such foam was made by personnel who passed through a patch that read in excess of 50 r/hr at 2 hr after Shot Umbrella. Nevertheless, it was concluded<sup>80</sup> that combatant ships could safely traverse an Umbrella-type detonation area at about 25 min after burst, because the shielding provided by the ships structure and the height of decks above the water surface would result in sufficient attenuation of any gamma

radiation from the water. However, it is estimated that the contaminated water patches would still represent a real hazard to small craft as late as 1.5 hrs after burst, unless the patches were dissipated as a result of wind and wave action.

After the first half hour, the decrease in dose rates in the contaminated water results because the radioactive particles are not concentrated in a mass on a flat surface, but are distributed at different depths in the water and tend to disperse with the current, and because water is an extremely effective shield for gamma radiation. The half-value thickness of water (the thickness that will absorb half the gamma radiation incident upon it) for gamma energies characteristic of mixed fission products may be determined roughly by the equation

$$1/2 = e^{-\mu x_{1/2}}$$

then  $x_{1/2} = \frac{0.693}{\mu(E\gamma)} \text{ cm}$

$x_{1/2}$  = half-value thickness (in cm) of water

$E\gamma$  = gamma-ray energy, which may vary between 0.5 and 2.0 Mev

$\mu(E\gamma)$  = linear absorption coefficient, which lies between  $0.097 \text{ cm}^{-1}$  and  $0.049 \text{ cm}^{-1}$  for water, for 0.5 and 2.0 Mev respectively.

The value of  $x_{1/2}$  then lies between 7 and 14 cm, and thus, only a few ft of water will most effectively eliminate the gamma radiations of radioactive particles suspended in the water.

Theoretical calculations have also been carried out<sup>67</sup> to determine the shielding effectiveness of an aircraft carrier to waterborne radiation sources. These calculations indicate that not only is the ship shielding highly effective, but also that the radiation from the water is negligible compared to other sources of radiation, even at times as early as 70 sec after burst. Further calculations<sup>70</sup> indicate that consideration of radiation from waterborne activity is of academic interest only, because of the minor operational importance of the hazard from such activity aboard combatant ships. For example, computations were made of the percent of the in-situ water dose rate that would exist under worst conditions in a carrier. Results indicate that, assuming uniform activity distribution in a semi-infinite volume of water, this fraction would be only 8% of the in situ dose rate at a location next to the hull and just above the armor belt and waterline. Combining results of theoretical calculations with weapons-test data on dose rates from waterborne activity reaffirms the conclusion that negligible radiation from waterborne sources would penetrate combatant ships later than 1 hr after burst.

## 17.8 CONTAMINATION INGRESS

### 17.8.1 Introduction

If a ship were operating in the base-surge region or in the fallout zone resulting from a nuclear water-surface or underwater burst, airborne radioactive particles could gain access to the ship's interior through any breaks in the ship's weather envelope. The presence of radioactive particles would result in radiation fields within the ship, since the particles might deposit on ship surfaces or remain suspended in the air within the ship. In such cases, the means of ingress determines the amount of activity entering the ship, and the access paths affect the amount of deposition and the concentration of activity suspended in the air within the ship. The conditions under which such ingress of activity could occur and the interaction of the ship with the radioactive particles and with the radiations emitted by those particles have been studied at field tests, by the use of simulants, and by theoretical calculations. Results of these studies will be presented in 17.8.2 and 17.8.3.

The investigation of Ref. 88 has indicated three possible breaks in a ship's weather envelope that could provide means of ingress of contaminant to below-decks spaces: physical damage to a ship; the boiler-air system; and the ventilation-air system. Examination of available data indicated that the primary effects likely to cause physical damage to a ship operating in the region of a nuclear burst are airblast and underwater shock. Unless a ship were at a range close enough to be immobilized, the deckhouse structure and lightly-constructed nonwatertight doors appear to be the only topside items likely to be damaged by airblast, and such damage would probably not be of sufficient magnitude to permit significant ingress of activity belowdecks. Unless a ship is at such close range that underwater shock causes major hull damage, it is unlikely that breaks in the weather envelope will result from underwater shock. Therefore, means of contaminant ingress which could be of significance to operable ships were concluded to be the boiler-and ventilation-air systems. Results of theoretical calculations and field-test measurements of the radiation fields resulting from these two sources of shipboard contaminant ingress follow.

### 17.8.2 Theoretical Investigations

In an investigation<sup>89</sup> of gamma radiation dose due to contaminated boiler air, theoretical calculations were made of the dose to boiler-room personnel due to contaminated air that had leaked through boiler casings and idle burner ports into the boiler room of a destroyer. Bursts of the Shot Baker type, ranging in yield from 20 to 200 KT were considered. The investigation assumed that the ship was mobile and that all activity remained airborne. Only external-gamma and inhalation

hazards were considered. Results were calculated for two boilers operating at 120% of full power, and for ship entry times into the contaminated aerosol ranging from 1 to 10 min after burst, and for ship exit times ranging from 2 to 20 min. The exact concentration of fission-product activity in the aerosol produced by Shot Baker was not known, but was estimated to be between 0.1 and 4 curies/ft<sup>3</sup>. The external gamma dose to boiler-room personnel was then calculated to be from 2 to 88 r, respectively. The study pointed out that if activity were absorbed on surfaces in the combustion air ducts, much higher doses could result to personnel exposed to the ducts. The inhalation hazards to personnel are discussed in Chapter 18, which deals with personnel hazards.

A theoretical investigation<sup>88</sup> was carried out to estimate the significance of the doses due to contaminated ventilation air in below-decks spaces on a ship beyond the region of immobilization at the time of a shallow underwater burst. The investigation considered two cases: (1) all activity carried by the aerosol entering a below-decks space is deposited on the deck of the space; (2) all activity remains airborne and flows into and out of the space. It was assumed that no deposition of contaminant occurred in the ventilation ducts, and that the activity per unit volume of the aerosol entering the ship was the same as that surrounding the ship. Since the exact concentration of activity which would be produced in the aerosol by such a burst is unknown, the ventilation-air dose could not be computed directly, and instead was expressed as a fraction of the weather deck transit dose. Ratios were calculated for two ventilation conditions: (1) blowers OFF (ventilation by natural draft); (2) blowers ON (operating at rated capacity for various spaces). Ship entry times into the aerosol ranged from 0.3 min to 10 min; exit times, from 1 to 10 min. Results of the calculations indicated that, for the blowers OFF condition, the ventilation air dose was about 1.3% of the transit dose, and thus would be negligible. For the blowers ON condition, the ventilation air dose for 15 min (within the first half hour after burst) ranged from about 4% to 15% of the transit dose, and would be significant. The contact-beta and inhalation hazards to personnel, which also may be considerable, are discussed in Chapter 18. If deposition occurred along the ventilation ducts, the ratio of the vent dose to the transit dose would be reduced in proportion to the amount of contaminant deposited, but the ducts themselves would then become sources of radiation.

Theoretical analyses indicated that, under certain conditions, the combustion-air and ventilation-air systems of a ship could permit the ingress of contaminated aerosol to interior spaces of the ship, resulting in a complex radiological problem. Limited field-test experiments were carried out to determine the extent of the problem.

## 17.8.3 Weapons-Test Data

1. Water-Surface Bursts

Operation Castle: Measurements were made<sup>90</sup> in the ventilation systems of the test ships (YAGS 39 and 40) to obtain evidence on (1) the concentration of airborne activity entering them, (2) the effectiveness of ventilation countermeasures, and (3) the extent to which airborne material was deposited in the system. Small ventilation cubicles (16 x 25 x 10 ft) were built into the between-deck space of the No. 3 hold of each YAG. Each cubicle had its own duct system with a mushroom-head type of intake, and the system was built to provide adequate flow for measurements of activity per unit volume of air carried into the spaces for seven different conditions of ventilation. The conditions included the standard system, operation of the fan at low speed, use of a precipitron mounted in the duct near the intake, use of an openmesh (ACC) filter, etc. Some data were obtained following Shots 2, 4, and 5.

Attempts to accurately measure particle sizes of the radioactive material in below-decks spaces failed because of the low activity in the molecular filters at the time the analysis began, but it was estimated that the mean diameter of particles gaining entrance to the ship's interior was of the order of  $\mu$  or less.

Measurements in the ventilation systems for Shots 4 and 5 resulted in the following conclusions: (1) there was a gradual decrease in concentration of airborne activity between station 1, directly beneath the mushroom intake, and station 5, in the cubicle exhaust; (2) in the test systems where no particle-removing device was present, there was a marked uniformity of airborne-activity concentration, (3) in cubicles ventilated by unprotected duct systems, the average airborne-activity concentration was about 0.02% of the average weatherside concentration, and the particle concentration in the duct was not greatly influenced by the flow rate through the duct; (4) ventilation countermeasures (the ACC filter and the precipitron) effected a reduction of 94% to 98% in the airborne concentration; (5) gamma radiation from the ducts was about the same, or less than, the gamma radiation penetrating the decks from weather-surface deposits; (6) an increase in activity occurred near the region of the supply-duct Y branches.

Measurements in the boiler systems were obtained only from Shot 4, and indicated that airborne-activity concentrations in the fire room of the YAG-40 were negligible. Samplers located in the boiler systems showed higher deposition than those in the duct sections. However, significant comparisons could not be made between activity concentrations in boiler-air systems and either the weatherside area or the ventilation area.

No contamination-ingress measurements were made at Operation Redwing.

## 2. Underwater Bursts

Operation Crossroads, Shot Baker: All ventilation-system openings on target ships were sealed prior to Shot Baker. However, damage to the cover (an opening about 6 inches square) on the ventilation system for the after engine room of USS CRITTENDEN (1686 yd from surface zero) permitted entry of contaminant. Eighteen months after Shot Baker, the dust in the contaminated ventilation system was recovered and analysed.<sup>91</sup> Fission products equivalent to 115 microcuries of radioactivity were recovered from the dust at that time, and it was calculated, from radiochemical analysis and fission-product decay schemes that about 370 curies of radioactive aerosol entered the ventilation system from the base surge. The ship was, of course, rendered immobile by the burst, and was engulfed by the base surge for about 14 min. Thus, a significant amount of contaminant gained ingress through the small break in the weather envelope.

Operation Hardtack: At Operation Hardtack, several projects were concerned with shipboard ingress of contaminant,<sup>33,66</sup> and the effects at below-decks locations. Three ventilated compartments were instrumented on the moored and washed DD-592. Conditions simulated the operational condition of blowers OFF, but no closures were used in the ventilation system. Measurements were made of contaminant ingress in (1) the galley, (2) the after engine room, and (3) the after crew's quarters. In addition, fullpower airflow was maintained through an unfired boiler in the after fireroom, which was also instrumented. The destroyer was moored with its starboard side to surface zero, 3000 ft downwind during shot Umbrella, and 4900 ft downwind during Shot Wahoo. Two other destroyers (DD-474 and DD-593) were also moored downwind with their sterns to surface zero. The forward firerooms of all three destroyers were instrumented with film badges and recording radiation detectors, and one boiler was fired with an airflow of about half the fullpower airflow. The following table, taken from Ref. 33, summarizes the conclusions on the probable paths of activity ingress into instrumented compartments.

**BEST AVAILABLE COPY**



Table 17-9. Estimates of portion of external gamma dose due to ingress of contaminant, DD-592, Shot Umbrella.<sup>66</sup>

Compartment	GITR Total Dose (r)	Film Badge Dose (r)	Ingress Dose Estimate (r)	% Contribution Due to Ingress Dose
Galley	288 ± 43	290 ± 58	2 to 78	0.7 to 27
Forward Fireroom (upper level)	52 ± 8	58 ± 12	4 to 18	8 to 35
After Fireroom (upper level)	65 ± 10	65 ± 13	8 to 26	12 to 40
After Engineroom (upper level)	81 ± 12	95 ± 19	9 to 31	11 to 38
Forward Fireroom (lower level)	25 ± 4	26 ± 5.2	8 to 13	33 to 50
After Fireroom (lower level)	28 ± 4	28 ± 5.6	11 to 15	39 to 54
After Engineroom (lower level)	26 ± 4	32 ± 6.4	14 to 18	54 to 69
After Crew's Quarters	158 ± 24	184 ± 37	1.5 to 50	1 to 32

It was concluded<sup>66</sup> that full-power operation of both boilers with ventilation systems open would more than double the fireroom ingress dose estimated for the test conditions (1-boiler operation and sealed ventilation openings). In addition, use of regular boiler fuel (instead of the diesel oil used during the tests) would result in larger soot deposits and therefore probably further increase deposits of radioactive material in the boiler.

Estimates of total ingress dose (boiler air and ventilation air) from film-badge data for Shot Wahoo indicate that the doses in test compartments in DD-592 were comparable to those at Shot Umbrella, even though the ship was slightly further away from surface zero.<sup>66</sup> Estimates of external doses due to boiler air alone on all the ships were higher for Shot Wahoo than for Shot Umbrella by factors of 2 to 6.

**BEST AVAILABLE COPY**

It was found<sup>66</sup> at Shot Umbrella that 90% to 95% of air-sample activity collected in the test compartments was due to particles in the submicron size range. The particles were readily airborne, and were capable of being respired.

Operation Wigvam: There was no detectable contamination of the interior of YAG 39, except for the slight contamination indicated in various seawater cooling systems and in the main trunk and pipe lines of the washdown system.<sup>31</sup>

### 3. British Experiments

A mist was simulated at preliminary British trials, according to Ref. 92, and measurements were made of particulate deposited in the combustion-gas paths of the boilers. It was found that more than 95% of the particulate intake consisted of "large" size particles that were deposited in the plenum chamber and fans. About 15% to 20% of the total radioactivity that got past the fans deposited as small particles on the boiler brickwork, and about 20% of the small-particle intake deposited as soot in the boiler (10% in the main tube banks and 10% in the economizer).

#### 17.8.4 Summary

Previous studies have indicated that the combustion-and ventilation-air systems are the only means of contaminant ingress of significance aboard operable ships. For water-surface bursts, it is estimated that negligible amounts of contaminant would gain access to below-decks spaces via these systems. However, test data in verification of this estimate are meager, and no theoretical analyses of the situation have been performed.

For underwater bursts, theoretical analyses indicated that in ships traversing the base surge from a Shot Baker type of burst, the doses due to contaminated aerosol reaching below-decks spaces via ventilation or combustion-air ducts would be small in comparison to the weather-deck doses. However, it was pointed out that such doses could become significant to personnel who are well shielded from the weather-deck radiation. Also, the amount of deposition along the ducts, an unknown factor, would affect the total doses. Available test data from Shot Umbrella have, to an extent, verified the theoretical estimates. The weather deck transit dose on the DD-592 was slightly greater than 500 r in 30 min. In below-decks test compartments, doses due to ingress of contaminated ventilation air were estimated<sup>60</sup> to be between 1.5 and 78 r. The minimum estimated ingress dose in each compartment is within + 50% of the theoretical estimate of 1.3% of the transit dose, although some of the maximum estimated ingress doses are as much as a factor of 7 larger than the theoretical estimate of Ref. 88. The doses at Operation

[REDACTED]

Hardtack resulting from combustion air intakes were within the dose range estimated theoretically.<sup>89</sup> It should be noted that accurate estimates of ingress dose are still impossible. References 33 and 66 represent the best available information, but even in these studies, results could be presented only as a wide range of values due to uncertainties, assumptions, and approximations in the ingress-dose estimates.

For underwater bursts at shallow or moderate depths, such as Shots Umbrella and Wahoo, comparison of estimated ingress doses with total doses at below-decks locations reveals that the doses due to ingress of contaminant were in all cases secondary to the doses due to transit radiation. However, if shielding were provided to reduce the dose due to exterior transit radiation, then radiation due to interior contamination from bursts such as these two could require consideration.

For deep underwater bursts, such as Wigvam, there was no detectable contamination of ships traversing the path of the aerosol within 20 min after burst.

## REFERENCES

1. Shnider, R. W., Compilation and Empirical Analysis of Radiant Exposures From Nuclear Surface Bursts, USNRDL-TR-658, September 1963
2. Capabilities of Atomic Weapons, Armed Forces Special Weapons Project, TM 23-200, OPNAV INSTR 03400.1B, Rev. November 1957
3. Hillendahl, R. W., Characteristics of the Thermal Radiation From Nuclear Detonations, Vol. III, USNRDL TR-383, AFSWP-902, 30 June 1959
4. Sulit, R. A., Prediction of Shipboard Thermal Combat Ineffectives (U), USNRDL TR-427, 7 June 1960
5. Shurcliff, W. A., Bombs at Bikini, the Official Report of Operation Crossroads, Wm. H. Wise and Co., Inc., N.Y., 1957
6. Monahan, T. I., Derksen, W. L., Effects of Thermal Radiation on Materials, WT-772, Operation Upshot-Knothole, May 1954
7. Bruce, H. D., Incendiary Effects on Building and Interior Kindling Fuels, WT-774, Operation Upshot-Knothole, March 1954
8. Sauer, F., Arnold, K., Ignition and Persistent Fires Resulting From Atomic Explosions, WT-775, Operation Upshot-Knothole, January 1954
9. Laughlin, K. P., Thermal Ignition and Responses of Materials, WT-1198, Operation Teapot, July 1960
10. Effects of Thermal Radiation From a Nuclear Detonation, Operation BUFFALO, FWE-199, July 1958
11. A Summary of Thermal Radiation Measurements Made by the U. K. at the Monte Bello Totem I and Totem II Bursts, FWE-5
12. Butler, C. P., Martin, S. B., Char Depth Measurements at Operation Teapot, USNDL-TR-144, AFSWP-1010, 29 July 1957

13. Martin, S. B., On Predicting the Ignition Susceptibility of Typical Kindling Fuels to Ignition by the Thermal Radiation From Nuclear Detonations, USNRDL TR-367, AFSWP-1135, 21 April 1959
14. Thermal Data Handbook, AFSWP-700, 1954
15. Derksen, W. L., Carter, J. A., Effects on Materials of Thermal Radiation From Nuclear Detonations (U), WT-1647, Operation Hardtack, September 1960
16. S. Martin, USNRDL, Proposed Nomographs, USNRDL-TR in Preparation.
17. Ferguson, J. M., Early Time Gamma Radiation From Nuclear Weapons (U), USNRDL TR-600, June 1961
18. Goad, W. B., Allen, L., Jr., Vulnerability of Nuclear Weapons to Neutrons From a Nuclear Explosion, LA2246, September 1958
19. Glasstone, S., Effects of Nuclear Weapons, U. S. Atomic Energy Commission, 1957
20. Gibson, H. F., Miller, W., et al, Delayed Gamma-Ray Measurements Part I, Gamma-Ray Spectrum Measurements, (abridged), WT-76, Operation Greenhouse, April 1954
21. Gibson, H. F., Miller, W., et al, Delayed Gamma-Ray Measurements Part I, WT-107, Operation Greenhouse, February 1954
22. Malik, J. S., Summary of Information on Gamma Radiation From Atomic Weapons, LA-1620, January 1954
23. AFSWP Field Command, Technical Summary of Military Effects, Programs 1-9, Operation Hardtack Preliminary Report, ITR-1660, 23 September 1959

24. The Nuclear Radiation Handbook AFSWP 1100, Nuclear Development Corp. of America, White Plains, N. Y., 25 March 1957, [REDACTED]
25. Blaylock, John A., A Study of the Sulfur Neutrons From Fission Weapons [REDACTED] AFSWC-TN-59-16, June 1959 [REDACTED]
26. Brown P., Carp, G., Gamma Rate vs Time, WT-913, Operation Castle, February 1959 [REDACTED]
27. Brown, P., et al, Gamma Exposure vs Distance, WT-1310, Operation Redwing, February 1960 [REDACTED]
28. Rainey, S. C., Shnider, R. W., Weapons Effects Predictions for AEC Diagnostic Weapons [REDACTED] USNRDL-TR-552 [REDACTED]
29. Strobe, W. E., Investigation of Gamma Radiation Hazards Incident to an Underwater Atomic Explosion, Operation Crossroads (U), USNRDL-TR-687, November 1963 [REDACTED]
30. Tuck, J. L., Radiation Intensity vs Time Inside Target Ships, Crossroads Technical Instrumentation Report, Project V-II, LAMS-439, September 1946 [REDACTED]
31. Hawkins, M. B., et al, Determination of Radiological Hazard to Personnel, WT-1012, Operation Wigwam, July 1956 (OUO).
32. Evans, E. C., III, and Shirasawa, T. H., Characteristics of the Radioactive Cloud From Underwater Bursts [REDACTED] WT-1621, Operation Hardtack, January 1962 [REDACTED]
33. Bigger, M. M., Rinnert, H. R., Zagorites, H. A., Shipboard Radiation From Underwater Bursts [REDACTED] WT-1619, Operation Hardtack, March 1961 [REDACTED]
34. Williams, J. H., Ship Shielding [REDACTED] Tripartite Symposium at NRDL, 1960, Vol. II, R&L No. 103 [REDACTED]
35. Behrens, W. V., Shauli, J. M., The Effects of Short Duration Neutron Radiation on Semiconductor Devices; Proceedings of the I. R. E., Vol. 46, No. 3, March 1958 [REDACTED]

[REDACTED]

DNA 1240H-2

36. Haas, P.H., Shaull, J.M., Behrens, W.V., Effects of Nuclear Radiation on Semiconductor Devices, WT-1489, Operation Plumbbob, October 1960 [REDACTED]
37. Behrens, W.V., Shaull, J.M., Effects of Nuclear Radiation on Semiconductor Devices, WT-1742, Operation Hardtack, 5 May 1961 [REDACTED]
38. Conrad, E.E., Dobriansky, B.J., Siman A., et al, Effects of Nuclear Radiation on Electronic Fuze Components and Materials, WT-1637, Operation Hardtack, 30 June 1961 [REDACTED]
39. Miller, B., Industry Probes Nuclear Pulse Radiation, Aviation Week, 8 August 1960 [REDACTED]
40. Molumphy, G.G. and Bigger, M.M., Proof Testing of Atomic Weapons Ship Countermeasures, WT-927, Operation Castle, October 1957 [REDACTED]
41. Rinnert, H.R., Ship Shielding Studies, WT-1321, Operation Redwing, July 1959 [REDACTED]
42. Triffet, T., and LaRiviere, P.D., Characterization of Fallout, WT-1317, Operation Redwing, 15 March 1961 [REDACTED]
43. Laurino, R.K., Schultze, D.P. and Van Den Berghe, G.C., Decision Procedures and Information Requirements for Ship-board Radiological Defense, USNRDL TR-407, 15 March 1960 [REDACTED]
44. Coles, J.S. and Young, G.A., Investigations of Base Surge Phenomena, NAVORD 1744, 1 September 1950 [REDACTED]
45. Arons, A.B., Young, G.A. and Milligan, Mary L., Further Investigations of the Base Surge, NAVORD 2144, 1 June 1951 [REDACTED]
46. Burrows, W.L., An Evaluation of Base-Surge Radioactivity..., ARL/R.1/C.759, May 1954 [REDACTED]
47. Weapons Effects Predictions for Operation Willow Surface/ Subsurface Events, USNRDL TR-346, September 1959 [REDACTED]

48. Huebsch, I. O., A Model For Computing Base-Surge Dose-Rate Histories For Underwater Nuclear Bursts, USNRDL-TR-653, May 1963
49. Swift, E. Jr., Young, G. A., et al, Surface Phenomena From Underwater Bursts WT-1608, Operation Hardtack, March 1962
50. Ksanda, C. F. and Laumets, E., Computation of Early-Time Fission Product Dose Rate Spectrum and Air Attenuation, USNRDL TR-361, 14 September 1959
51. Zigman, P. E. and Mackin, J. L., Early Time Decay of Fission Product Mixtures II Gamma Energy Release and Ionization Rates Following Thermal Neutron Fission of U-235, USNRDL TR-400, 11 February 1960
52. Goldstein, H. and Wilkins, J. Ernest, Jr., Calculation of the Penetration of Gamma Rays, AEC Report-NYO-3075, 30 June 1954
53. Ksanda, C. F., Shapiro, E. S. and Laumets, E., Attenuation of Gamma Radiation From Different Source Configurations, Vol. I, Theoretical Basis, USNRDL-TR in preparation
54. Laumets, E., Attenuation of Gamma Radiation From Different Source Configuration, Vol. III, Graphs for Computing Steel-Slab Attenuation of Air or Water Volume-Source Radiation, USNRDL-TR in preparation
55. Ksanda, C. F., Ship Shielding Calculations, and Computational Results, Proceedings of Tripartite Symposium on Technical Status of Radiological Defense in the Fleets, Vol. 1, R&L, No. 103, May 1960
56. Dolan, P. J., Gamma Spectra of Uranium-235 Fission Products at Various Times After Fission, AFSWP 524, March 1959
57. Laumets, E., and Ksanda, C. F., Pseudospectra for Calculating Gamma-Ray Shielding Attenuation, USNRDL-TR in preparation



58. Zagorites, H., Carr, E. A., Lee, D. Y., The Effects of Nuclear Radiation Environment at Sea on Shipboard Electronic Equipment, USNRDL TR in preparation.
59. Tomoeda, S., Hastings, M. B. and Miller, W. G., Gamma-Ray Penetration Experiments for a Light Aircraft Carrier Using Distant Sources and Sources Simulating Contamination of the Hull, USNRDL-TR-533, October 1961 [REDACTED]
60. Adams, C. E., Farlow, N. H., Schell, W. R., The Composition, Structure, and Origins of Radioactive Fallout Particles, USNRDL TR-209, February 1958 [REDACTED]
61. Armstrong, W. J., Bigger, M. M., Curtis, H. B., LTJG USNR, Verification of Shipboard Countermeasures, WT-1324, Operation Redwing, February 1959 [REDACTED]
62. Wilsey, E. F., French, R. J., West, H. I., Jr., Fallout Studies, WT-916, Operation Castle, February 1956 [REDACTED] (DATA).
63. Tompkins, E. R., Werner, L. B., Chemical, Physical, and Radiochemical Characteristics of the Contaminant, WT-917, Operation Castle, September 1955 [REDACTED] (DATA).
64. Stetson, R. L., et al, Distribution and Intensity of Fallout, WT-915, Operation Castle, January 1956 [REDACTED]
65. Report of the Technical Director Operation Crossroads, Encl. J, XRD-209, 1946 [REDACTED]
66. Bigger, M. M., et al, Shipboard Contamination Ingress From Underwater Bursts, WT-1620, Operation Hardtack, December 1961 [REDACTED]
67. Anderson, A. D., A Theory for Close-In Fallout From Land-Surface Nuclear Bursts, Journal of Meteorology, Vol. 18, No. 4, pp. 431-442, August 1961 [REDACTED]
68. Ksanda, C. F., Shnider, R. W., Meggs, H., Weapons Effects Predictions for Operation Willow, Chapter 7, NRDL TR-346, September 1959 [REDACTED]

69. Ksanda, C. F., Minvielle, L., Moskin, A., Scaling of Contamination Patterns, Surface and Underground Detonations, USNRDL TR-1, September 1953
70. Laumets, E., A Method of Determining Ship-Shielding Factors for Fallout Gamma Radiations, USNRDL-TR to be published
71. Laumets, E., Attenuation of Gamma Radiation From Different Source Configurations, Vol. II, USNRDL-TR in review.
72. Shumway, B. W., Tomoeda, S., et al, The Dose Distribution Within an Aircraft Carrier Exposed to Uniform Co<sup>60</sup> Contamination on the Flight Deck, USNRDL-TR-466, September 1960
73. Tomoeda, S., Kreger, W. E., et al, Gamma-Ray Penetration Into the Compartments of a Light Aircraft Carrier, USNRDL-TR-343, July 1959
74. Haggmark, L. G., Ship-Shielding Factors - Computational Method Compared to Experimental Results, USNRDL-TR-514, June 1961
75. Waldorf, W. F., Jr., A Correlation Between Theory and Experiment in Ship Shielding Studies, USNRDL-TR-373, October 1959
76. Folsom, T. R., Werner, L. B., Distribution of Radioactive Fallout by Survey and Analysis of Sea Water, WT-935, Operation Castle, April 1959
77. Jennings, F. D., et al, Fallout Studies by Oceanographic Methods, WT-1316, Operation Redwing, November 1956
78. VanLint, V., Killion, L. E., Chiment, J. A., Campbell, D. C., Fallout Studies, During Operation Redwing, ITR-1354, October 1956
79. W. A. Shurcliff, Technical Report of Operation Crossroads, XRD-208, November 1946

80. Palumbo, R. F., Lowman, F. G., Welander, A. D., Weeks, D. R., Distribution of Radioactivity in Sea Water and Marine Organisms Following an Underwater Nuclear Detonation at the Eniwetok Test Site in 1958, UWFL-58, Laboratory of Radiation Biology, University of Washington, February 1959 [REDACTED]
81. Duckworth, J. W., et al, Sea Water Radiological Monitoring Methods (U), WT-1689, Operation Hardtack, June 1959 [REDACTED]
82. Isaacs, J. D., Mechanism and Extent of the Early Dispersion of Radioactive Products in the Water, WT-1014, Operation Wigwam, March 1962 [REDACTED]
83. Van Dorn, W. G., Collection of Early Water Samples for Radiochemical Analysis and Yield Determination, WT-1039, Operation Wigwam, March 1957 [REDACTED]
84. Folsom, T. R., Mechanism and Extent of the Dispersion of Fission Products by Oceanographic Processes, and Locating and Measuring Surface and Underwater Radioactive Contamination, WT-1015, Operation Wigwam, July 1956 [REDACTED]
85. Morgan, D. T. G., H. M. S. DIANA in Light Fallout, Operation Mosaic, Proceedings of Tripartite Symposium, USNRDL R&L No. 103, Vol. III, 16-20 May 1960 [REDACTED]
86. Evans, E. C., III, Some Observations and Speculations on Base Surge Phenomena, Proceedings of Tripartite Symposium, USNRDL R&L No. 103, Vol. II, 16-20 May 1960 [REDACTED]
87. Laumets, E., Ship-Shielding Factors for the USS RANGER, USNRDL-TR in preparation.
88. Shnider, R. W., Morris, C. E., Significance of Breaks in Integrity of Weather Envelopes of Ships Operating During an Underwater Atomic Attack, USNRDL-TR-51, April 1955 [REDACTED]
89. Teresi, J. D., Shnider, R. W., Rinnert, H. R., Personnel Radiation Hazards Incident to Ship Boiler Operation Following an Underwater Atomic Attack, USNRDL-TR-16, September 1954 [REDACTED]

90. Wallace, N. R., Kawahara, F. K., Sherwin, J. G., Zaccor, J. V., Shipboard Interior Contamination, Chapter 6 of WT-927, Proof Testing of Atomic Weapons Ship Countermeasures, October 1957 [REDACTED]
91. Holden, F. R., et al, Radioactive Contamination of Ventilation Supply System, U. S. S. CRITTENDEN, From Baker Explosion, Operation Crossroads, USNRDL-551, NS085-005, AD-200(x), February 1950 [REDACTED]
92. Hallifax, LCDR, J. C., Deposition of Mist in Combustion Gas Paths of Boilers, Evaluation of Preliminary Trails in H. M. Ships Battleaxe and Decoy, ARL/RI/C758, April 1956, Memorandum [REDACTED]

[REDACTED]

DNA 1240H-2

THIS PAGE IS INTENTIONALLY BLANK

17-122

[REDACTED]

[REDACTED]

Addendum No. 1

for

DNA 1240H-2, Part 2

HANDBOOK OF  
UNDERWATER NUCLEAR EXPLOSIONS

21 January 1974

The attached pages (18-25 through 18-34) are to be inserted in Chapter 18 of your copy of the above handbook per DNA letter of approval dated 2 January 1974.

M. J. Dudash  
DASLAC  
General Electric Company-TEMPO  
816 State Street  
Santa Barbara, CA 93102

[REDACTED]

*entered 12 June 74  
J. L. Ripon*

[REDACTED]



CONTENTS

CHAPTER	TITLE	PAGE
VOLUME 2 - PART 1		
11	INTRODUCTION	11-1
12	UNDERWATER EFFECTS ON SURFACE SHIPS	12-1
13	AIRBLAST EFFECTS ON SURFACE SHIPS	13-1
14	SURFACE SHIP STRUCTURAL RESPONSE AND DAMAGE DEVELOPMENT: THE EFFECTS OF SURFACE WAVES	14-1
15	SURFACE SHIP EQUIPMENT DAMAGE FROM UNDERWATER PHENOMENA	15-1
VOLUME 2 - PART 2		
16	THE EFFECTS OF AIR BLAST ON SURFACE SHIP EQUIPMENT	16-1
17	THE INTERACTION OF SURFACE SHIPS WITH THE THERMAL AND RADIOLOGICAL ENVIRONMENT	17-1
18	SURFACE SHIP PERSONNEL CASUALTIES: EFFECTS OF UNDERWATER SHOCK ON PERSONNEL	18-1
→ 19	SUBMARINE HULL RESPONSES AND DAMAGE DEVELOPMENT	19-1
20	SUBMARINE EQUIPMENT	20-1
21	UNDERWATER SHOCK EFFECTS ON SUBMARINE PERSONNEL	21-1
22	NAVAL MINE SWEEPING WITH NUCLEAR EXPLOSIONS	22-1

[REDACTED]

19 August 1973

CHAPTER 18

## 18.7 THERMAL AND NUCLEAR RADIATION EFFECTS ON SURFACE SHIP PERSONNEL

Section 18.7, Thermal and Nuclear Radiation Effects on Surface Ship Personnel, is a brief addendum to Chapter 18, which presently contains information only on effects of underwater shock. This addition points out possibilities of effects on those personnel exposed to thermal and nuclear radiation from water bursts, and presents the new risk and casualty criteria for combat troops. Differences are noted in environmental conditions and tasks of surface ship personnel from those encountered by ground combat troops.

In the following paragraphs, thermal and nuclear radiation risk and casualty criteria are specified for combat troops exposed to air or land-surface bursts. Brief note is made of certain water-burst phenomena producing thermal and nuclear radiation that may affect ship personnel in an environment differing markedly from that of combat troops.

### 18.7.1 Casualty and Risk Criteria

Effects of thermal and nuclear radiation on personnel are presented in a number of published documents and reports. Two recent documents present a summary of much of the information. The first is Personnel Risk and Casualty Criteria for Nuclear Weapons Effects, which specifies new criteria for militarily significant effects on ground troops, and also contains an extensive list of references. This reference defines "personnel risk criterion" as the level of exposure to a nuclear weapons effect such that specified incidences of casualties will occur, but neutralization of friendly troops will not occur. A "casualty criterion" is defined as the level of a particular weapons effect parameter at which permanent combat ineffectiveness (personnel unable to perform any task) will occur within 50% of the population exposed to that level. The specified new criteria for combat troops (termed CDC criteria in the remainder of this section) are given in Table 18-2.



Table 18-2  
 CDC NUCLEAR AND THERMAL RADIATION CRITERIA

		New Nuclear Radiation Criteria		
Risk	% Incidence	Mechanism	Mid Trunk Dose (rad)	Midline Dose (rad, free-in-air)
Negligible	2.5	• Vomiting	35	50
Moderate	5	• Vomiting • Combat	45	70
Emergency	5	Ineffective	100	150

		New Thermal Radiation Criteria		
Time to Ineffectiveness	Casualty	Mid-Head Dose (rad)	Mid-line Dose (rad, free-in-air)	
15 min		14,500	19,000	
1 hr		10,700	14,000	
4 hr		9,220	12,000	
8 hr		8,300	11,000	
24 hr		4,000	5,000	

Risk Criteria for Burns Under Summer Uniforms to Warned, Exposed Personnel					
% Incidence	Mechanism	Casualties due to 2nd Degree Burns			
		10KT cal/cm <sup>2</sup>	100KT cal/cm <sup>2</sup>	1000KT cal/cm <sup>2</sup>	10000KT cal/cm <sup>2</sup>
Negligible	1° burn	3.1	4.2	5.8	
Moderate	1° burn	3.7	5.0	6.8	
Emergency	2° burn	6.3	8.8	12	
Time to Ineffectiveness					
24. hr		50	38	53	73

[REDACTED]

19 August 1973

CHAPTER 18

Personnel casualties and expected incapacitation resulting from exposure to nuclear weapon effects parameters at a number of levels besides those specified in the CDC criteria are also discussed in Capabilities of Nuclear Weapons, referred to as EM-1 in the remainder of this section.

Both of the aforementioned documents discuss effects of air or land-surface bursts on troops, but do not consider the specific environmental conditions of shipboard personnel exposed to the thermal and radiological effects of a water-surface or underwater burst. For instance, the CDC risk criteria are based on low incidence of sickness among many soldiers, and are assumed to result in the non-neutralization of friendly troops. On board ship, however, only a few individuals may be trained in the performance of specific tasks, and even temporary ineffectiveness may significantly hamper operations.

The CDC radiation criteria are based on responses of monkeys, under controlled conditions, since most available information on effects on humans are derived from hospital patients. These subjects in many cases are not comparable, physically, with ships' personnel or combat troops. However, certain effects noted in human patients should not be ignored. Among a number of older patients (Saenger, et al., 1970), it was found that after whole-body exposure of as little as 100 rads, some individuals experienced nausea and vomiting of the same duration and severity as those receiving whole-body doses twice as great. After 150 rads exposure, over one-half the patients experienced severe nausea and vomiting. Among somewhat younger patients in better physical condition (Saenger, et al., 1971), four of seven patients who received 200 rads whole-body radiation were so ill (nausea and vomiting) immediately following irradiation as to markedly impair their ability to function. In another report, all patients (in good general condition) receiving 300 rad absorbed dose within about 15 min exhibited the same symptoms with little individual variation (Rider and Hasselback): after an asymptomatic interval of 45-60 min, projectile vomiting followed for 15-20 min, succeeded by deep sleep alternating with vomiting for 6-8 hr. Shipboard personnel so affected would be "temporary casualties", a category not included in the CDC criteria, which consider only permanent ineffectiveness.

19 August 1973

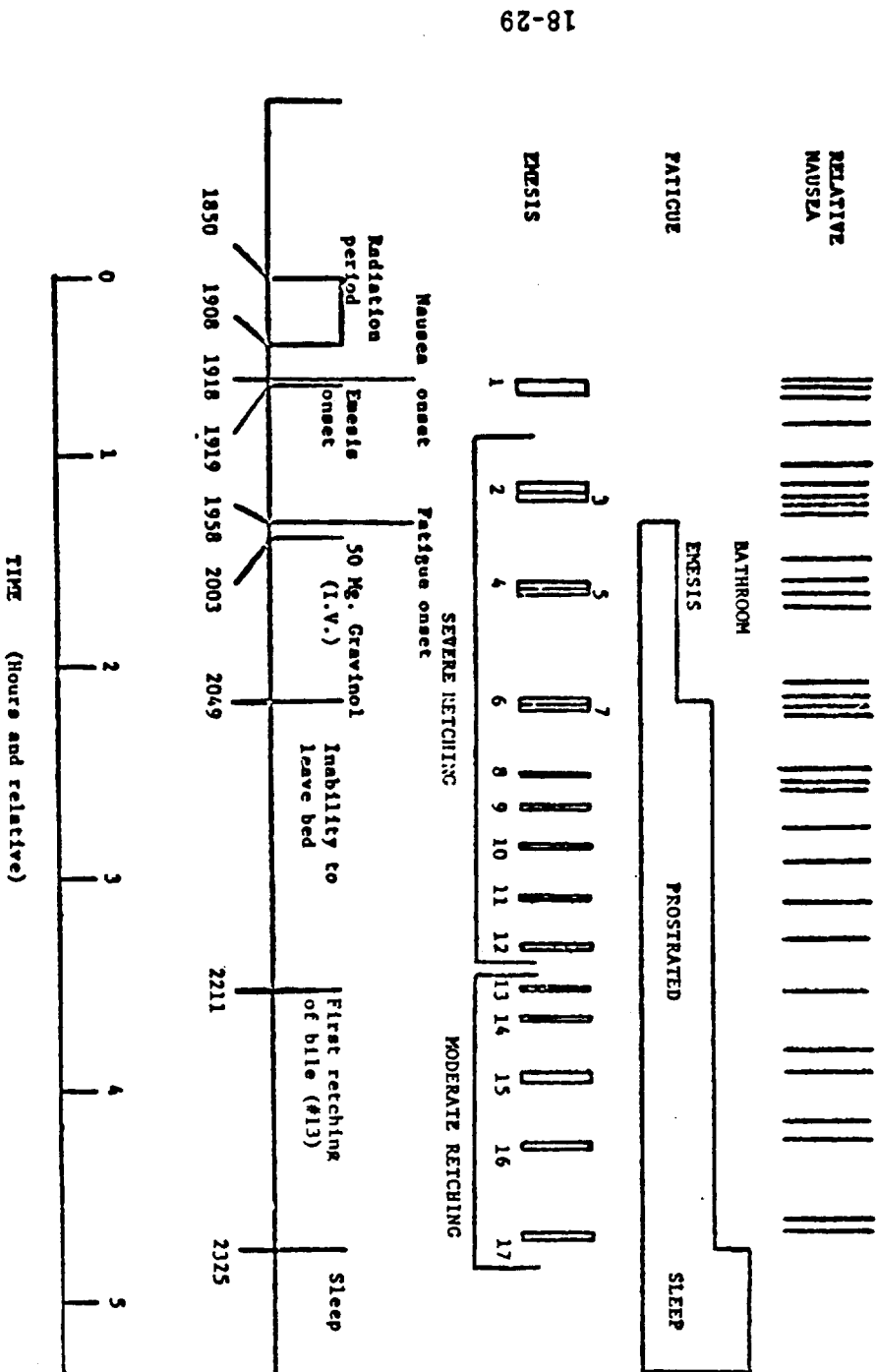
In some cases, the asymptomatic interval is even shorter than noted by Rider and Hasselback. Fig. 18-19 was prepared by Dr. Thomas Mobley of Air Force Weapons Laboratory, and will be published in a forthcoming Technical Report. The figure illustrates radiation effects on a young man (about 6 ft 4 in. tall, weighing about 180 lb), observed and documented by Dr. Mobley at the Ontario Tumor Clinic. The asymptomatic interval after irradiation in this case was only about 25 min, and for 5 hr after that, the patient was incapable of performing any task. Similar effects were noted, according to Dr. Mobley, in the treatment of patients at Naval Hospital, San Diego, California.

#### 18.7.2 Thermal Radiation

Thermal radiation from underwater bursts is either negligible or non-existent, and will cause no injuries or incapacitation to shipboard personnel. Thermal radiation from a surface burst will not affect below-decks personnel, but the eyesight and/or exposed or lightly covered skin areas of topside personnel may be affected.

Although no CDC casualty or risk criteria are given for either retinal burn or flashblindness, it should be noted that vision is vital to task performance of many topside personnel. Visual acuity is only slightly affected by a retinal burn (a permanent effect), unless an individual is looking directly at the fireball, a circumstance considered unlikely. However, vision may be immediately temporarily, partially, or totally impaired due to the bright flash of a nuclear burst, even though the burst is not directly in the visual field. Time for recovery from this condition, termed flashblindness, may be from several seconds to several hours, depending on exposure conditions. Such effects can occur at far greater distances from surface zero than are hazardous due to any other weapon effect, and the possibility that some topside personnel may be unable to perform their duties should be noted.

Fig. 18-19  
 CLINICAL RESULTS OF PATIENT WITH 264 RADS M/LT DOSE



The CDC thermal radiation criteria deal with times to ineffectiveness from burns of not less than 24 hr. The document states that data indicate that complete ineffectiveness within 8 hr or less may not be achieved by thermal burns, and notes that burns around the eyes or hands may cause local disability that may or may not be incapacitating within a day or so. EM-1 points out that any burn around the eyes that causes occluded vision because of resultant swelling of eyelids will be incapacitating, and burns of the hands will also cause ineffectiveness. Accurate vision and use of their hands are task requirements of many topside personnel, such as flight deck personnel on a carrier. Cheek or hand burns resulting from exposure to thermal radiation from a surface burst could produce temporary ineffectiveness for certain tasks within a very short time.

The CDC thermal emergency risk criteria (second degree burn) for warned, exposed personnel in summer uniform is  $12 \text{ cal/cm}^2$  from a 1 MT burst. Analysis of nuclear test data in the Pacific indicates that this level of exposure would occur at about 10,000 to 11,000 yd from surface zero, with the moderate risk level of  $6.8 \text{ cal/cm}^2$  at about 14,000 yd.

### 18.7.3 Nuclear Radiation

Sources of nuclear radiation resulting from water bursts differ in several respects from those of air or land-surface bursts. Furthermore, the nuclear radiation produced by water-surface bursts differs from that produced by underwater bursts due to phenomenological differences.

#### Water-Surface Bursts

Water-surface bursts produce primary neutron and gamma radiations (initial radiation) that are emitted by the fission products in the fireball and above surface formations. These radiations are similar to those emitted by the corresponding formations of a land-surface burst. It is

[REDACTED]

19 August 1973

CHAPTER 18

stated in EM-1 that the methodology for calculating total initial radiation exposure as a function of distance from land-surface bursts of several weapon types, given in Chapter 5, may also be used for water-surface bursts. Since a ship's structure forms effective shielding, only topside personnel could be affected by this radiation. However, since initial radiation attenuates rapidly with distance, in only rare instances would it have a dominant effect. For instance, it is estimated that topside personnel could be exposed to the CDC emergency personnel risk criteria of 150 rad midline dose at about 3000 yd from a 1 MT 100% fission burst. At such close-in range, other weapon effects are expected to dominate, as noted in the figures illustrating Governing Effects in the CDC document, as well as by Hansen and by Klingman.

Residual radiation is produced by radioactive particles in base surge, fallout, and in the water. A base surge due to a water surface burst has never been observed. However, it is probable that some radiological debris combines with the water particles that form the column wall during fireball rise and disintegration. As a result, a radioactive base surge should occur as the column walls return to the surface, although the walls may be so tenuous that the surge would be invisible. Neither data nor models exist to predict transit radiation from water-surface bursts. The fallout from water surface bursts has been observed to return to the surface very slowly, usually dispersed by the wind, and only low-level radiations are emitted by the time it reaches the surface (Huebsch). If it deposited in ship ventilation ducts or in unwashed locations on deck, a continuously-emitting source of low level radiation could form below decks. Such radiation could produce adverse effects such as fatigue and/or reduced ability in exposed personnel, but only after a considerable time had elapsed (Lushbaugh).

**BEST AVAILABLE COPY**

The water around surface zero is probably radioactive, particularly within the first hour or so after burst. Personnel in a small boat in the water for 1/2 hour or more could be exposed to levels of radiation meeting or exceeding personnel risk criteria.

18-31

[REDACTED]

  
Underwater Bursts

Initial radiation from underwater bursts is not considered a personnel hazard. Residual radiation is emitted at a high level from radioactive particles in the base surge, the water pool, and the foam produced by underwater bursts.\* A radioactive base surge rainout may also occur, depending on meteorological conditions. Topside personnel could receive exposures from above-surface formations that would be in the moderate or emergency risk categories of the CDC criteria, even though the ship itself was sufficiently far from surface zero to suffer no serious damage. The DAEDALUS computer program (Schuert, Killeen, et al.) will calculate exposure rates and total exposures from the base surge and the water pool, for times up to 30 min after burst. However, the yield range is limited to bursts between 0.01 and 150 kt.

If the base surge entered ventilation ducts or any break in a ship's weather envelope, radioactive particles could settle out and create a continuously emitting radioactive source below decks. Adverse effects on personnel would occur, but only after a period of time that would be long in relation to a particular tactical situation.

#### 18.7.4 Summary

**BEST AVAILABLE COPY**

Environmental conditions and tasks of shipboard personnel exposed to thermal and nuclear radiation from water bursts differ from those of

---

\* Young has categorized underwater bursts by burst depth for yields between 1 and 100 kt and has described differences in the phenomena produced in each category. Different above-surface formations result in differences in emitted nuclear radiation.

[REDACTED]

19 August 1973

CHAPTER 18

combat troops exposed to air or land-surface bursts. It is suggested that the temporary combat ineffectives that may occur among topside shipboard personnel could present problems of a different significance than is observed among ground combat troops, and that the long-term effects of radiation sources within the ship be considered.

18-33

[REDACTED]



19 August 1973

## REFERENCES

- Capabilities of Nuclear Weapons [redacted], Philip J. Dolan, Editor, DNA EM-1, Part II, July 1972 [redacted]
- Hansen, I. S., Airblast Effects on Surface Ships [redacted] Chapter 13, DNA 1240H-2, Vol. 2, Part 1, March 1972 [redacted].
- Huebsch, I. O., Fallout Predictions for Water-Surface Nuclear Bursts, USNRDL-TR-67-147, Nov. 1967.
- Huebsch, I. O., The Formation, Dispersion, and Deposition of Fallout Particles from Sea-Water-Surface Nuclear Explosions, USNRDL-TR-68-141 December 1968.
- Klingman, Sanford, Surface Ship Structural Response and Damage Development: The Effects of Surface Waves [redacted], Chapter 14, DNA 1240H-2, Vol. 2, Part 1, March 1972 [redacted]
- Langham, Wright H., Editor, Radiobiological Factors in Manned Space Flight, Report of the Space Radiation Study Panel of the Life Sciences Committee, National Academy of Sciences, National Research Council, 1967.
- Lushbaugh, C. C., Predicted Levels of Human Radiation Tolerance Extrapolated from Clinical Studies of Radiation Effects, Oak Ridge Associated Universities, 1971.
- Personnel Risk and Casualty Criteria for Nuclear Weapons Effects [redacted] ACN 4260, U. S. Army Combat Developments Command Institute of Nuclear Studies, August 1971 [redacted]
- Rider, W. D., and R. Hasselback, The Symptomatic and Haematological Disturbance Following Total Body Radiation of 300-Rad Gamma-Ray Irradiation, Guidelines to Radiological Health, August 1967.
- Saenger, Eugene L., E. B. Silberstein, H. Horwitz, et al., Radiation Effects in Man: Manifestations and Therapeutic Efforts, DASA 2428, October 1970.
- Saenger, Eugene L., E. B. Silberstein, B. S. Aron, et al., Radiation Effects in Man: Manifestations and Therapeutic Efforts, DNA 275IT, October 1971.
- Schuert, E. A., P. A. Killeen, J. W. Pritchett, and F. H. Young, DAEDALUS, A Gamma Exposure-Rate Prediction Code for Underwater Nuclear Explosions [redacted] USNRDL-TR-68-137, July 1968 [redacted]
- Young, George A., Surface Phenomena of Underwater Nuclear Explosions [redacted] Chapter 7, DNA 1240H-1, Vol. 1, Part 2, November 1971, [redacted]

Table 17-8. Compartments in which it is estimated that radiation fields were caused by ingress of radioactive contaminants.<sup>33</sup>

Compartment	Ship	Shot	Probable Ingress Path
Galley	DD 592	Umbrella	Ventilation air
Forward Fireroom	All Three	Umbrella and Wahoo	Boiler air (fired boiler)
Forward Engineerroom	DD 474 DD 592	Umbrella	Condenser water (?)
After Fireroom	DD 592	Umbrella	Boiler air (unfired boiler)
After Engineerroom	DD 592	Umbrella	Ventilation air
After Crew's Quarters	DD 592	Umbrella	Ventilation air

The film-badge doses in the forward fireroom varied with location, the highest doses being at stations closest to the blower room of the operating boiler. The following average dose values, summarized from a table in Ref. 66, indicate for Shot Umbrella the portion of the total gamma dose estimated to have been due to ingress at various locations aboard DD 592. "Film badge doses are 24-hr doses; GTR doses vary from approximately 1 to 2 hr doses. The ingress dose estimates are round figures, adequate to represent these estimates for 1 to 24 hr. The uncertainties inherent in the basic data and in the assumptions and approximations used in the estimating techniques have resulted in a wide range of values for the ingress dose estimates at each location."<sup>66</sup>

It should be noted that "between 17 and 50 minutes after Shot Wahoo (after passage of the base surge), the dose rates in the fireroom of DD 593 were on the order of ten times higher than on the washed weather decks, and about 100 times higher than the dose rates in the adjacent engineerroom. The fireroom dose rates...appear conclusively to be due to deposited radioactive material in the boiler or boiler-air system. The dose for this period, approximately 35 minutes, was 5 r. The dose for all other compartments in the ship for the same period was less than 1 r."<sup>66</sup>